Investigation of the Molecular Genetic Basis of Molybdenum Hydroxylase Deficiencies in Rats and Man

by

Joanne Jackson, B.Sc. (Hons)

A thesis submitted in partial fulfilment for the Degree of Doctor of Philosophy at the University of Huddersfield in collaboration with the Purine Research Laboratory Guy's Hospital, London

October 2003

CONTENTS

LIST OF TABLES AND FIGURES

A) TABLES

B) FIGURES

ACKNOWLEDGEMENTS

I would like to express my thanks to my supervisor, Dr Dougie Clarke for his advice, support and encouragement throughout the course of this research study and thesis write up.

I acknowledge the University of Huddersfield for financial support funding this work.

I would also like to express my thanks to Dr Anne Simmonds and Dr John Duley from the Purine Research Laboratory, Guy's Hospital, London, UK. for providing the xanthinuric blood sample and information upon request.

Finally I would like to thank my family and friends especially my husband Mark and my parents for their constant support and encouragement throughout this study.

SUMMARY

Aldehyde oxidase (AO) and xanthine oxidoreductase (XOR) are molybdenum hydroxylases involved in endogenous compound and drug metabolism. Molybdenum hydroxylase deficiencies have been observed in rat strains and humans. The absence of XOR activity is responsible for type I hereditary xanthinuria in humans. To date, only 6 families have been studied worldwide for the molecular genetic basis of hereditary xanthinuria, none of which were of European descent. Discontinuous variations of AO activity have been noted in the Sprague Dawley (SD) strain of rat but the molecular basis for this variation is unknown. Studies previously carried out in this laboratory have identified both an AO-active wild type rat strain (Wistar) and an AO-deficient rat strain (Fischer).

In this study all three strains of rat (Wistar, SD and Fischer) were phenotyped and the two AO-deficient strains were found to possess up to six-fold less AO activity towards dimethylaminocinnamaldehyde (DMAC) than the Wistar rat strain and had a complete lack of activity towards a N-heterocyclic AO substrate (phenanthridine).

Polymorphisms found previously in the SD rat by another laboratory were examined for cosegregation with the deficiency, however all three rat strains were found to be identical at these polymorphic sites. Cloning and DNA sequencing of the AO cDNA in the three strains of rat revealed two differences between the wild type and AO-deficient strains. Comparison of these two differences with an evolutionary diverse range of molybdenum hydroxylases, suggested that the G110S difference was most likely to cause the AO deficiency in the AO-deficient rat strains.

Cellulose acetate electrophoresis determined that there were two AO homologues in rat liver and the activity of the aldehyde oxidase homologue 1 (AOH1) responsible for N-heterocycle oxidase activity was absent in the AO-deficient rat strains. Cloning and DNA sequencing of this novel AOH1 cDNA from the three strains of rat revealed five codon differences between the strains. Comparison of these differences with an evolutionary diverse range of molybdenum hydroxylases suggested that the R39Q difference was most likely to be responsible for the AOH1 deficiency in the SD and Fischer rat strains.

In this study the XOR gene sequence of a British hereditary xanthinuric patient was studied to identify the mutation causing the disease. Cloning and DNA sequencing analysis of the patient's XOR gene determined a novel mutation (33T>G) in exon 1.

This was predicted to cause an asparagine to lysine substitution at amino acid positio
11 of the predicted protein sequence. Analysis of this difference with an evolutionar
diverse range of molybdenum hydroxylases from bacteria to man established that thi
asparagine residue was 100% conserved through evolution. This suggested that
positively charged lysine residue at this position in the mutant XOR protein is the caus
of hereditary xanthinuria in this patient.

ABBREVIATIONS

ADase	Adenosine deaminase
AO	Aldehyde oxidase
AOH	Aldehyde oxidase homologue (1, 2 and 3)
AOR	Aldehyde oxidoreductase
ARMS	Amplification refractory mutation system
BAC	Bacterial artificial chromosome
bp	Base pair
BSA	Bovine serum albumin
cDNA	Complementary deoxyribonucleic acid
Da	Dalton
DACA	N-[(2`-Dimethylamino)ethyl]acridine-4-carboxamide
DEPC	Diethylpyrocarbonate
D. gigas	*Desulfovibrio gigas*
DMAC	Dimethylaminocinnamaldehyde
DME	Drug metabolising enzyme
DNA	Deoxyribonucleic acid
dNTP	Deoxynucleotide triphosphate
EDTA	Ethylenediamineteracetic acid
EST	Expressed sequence tag
FAD	Flavine adenine dinucleotide
GDase	Guanine deaminase
GTP	Guanine triphosphate
HPLC	High pressure liquid chromatography
kb	Kilobase
ma-l	*Drosophila* molybdenum cofactor sulphurase gene (maroon like)
MCS	Molybdenum cofactor sulphurase
MoCo	Molybdenum cofactor
MOCS	Molybdenum cofactor synthesis step (1, 2 and 3)
mRNA	Messenger ribonucleic acid
NAD	Nicotine adenine dinucleotide
NAT	Arylamine N-acetyltransferase
NCBI	National Centre for Biotechnology Information

PCR	Polymerase chain reaction
PhIP	2-amino-1-methyl-6-phenylimidazo[4,5-*b*]pyridine
PNPase	Purine nucleotide phosphorylase
RACE	Rapid amplification of cDNA ends
R. capsulatus	*Rhodobacter capsulatus*
RFLP	Restriction fragment length polymorphism
RNA	Ribonucleic acid
ROS	Reactive oxygen species
RT-PCR	Reverse transcribed polymerase chain reaction
SD	Sprague Dawley
SO	Sulphite oxidase
SNP	Single nucleotide polymorphism
SSCP	Single-stranded conformation polymorphism
Taq	*Thermus aquaticus*
TBE	Tris borate EDTA
TE	Tris EDTA
UGT	UDP-glucuronosyltransferase
XD	Xanthine dehydrogenase
XO	Xanthine oxidase
XOR	Xanthine oxidoreductase

1. INTRODUCTION

1 Introduction.

1.1 Overview of molybdenum hydroxylase catalysis and distribution.

In mammals there are three enzymes present which contain a molybdenum cofactor, aldehyde oxidase (AO) (E.C.1.2.3.1), sulphite oxidase (SO) (E.C.1.8.3.1) and xanthine oxidoreductase (XOR). AO and XOR are referred to as molybdenum hydroxylases due to the reaction they catalyse (Beedham., 1987). Molybdenum hydroxylases catalyse the oxidation of substrates via a complex internal electron transfer pathway (Hille & Nishino, 1995). These enzymes are homodimeric with two subunits of approximately 150,000 Da each. Each subunit contains one molybdenum-pterin cofactor (MoCo), one flavin adenine dinucleotide (FAD) and two different iron sulphur ($2Fe_2S_2$) clusters as prosthetic groups (Garattini *et al.*, 2003; Rajagopalan, 1997).

The molybdenum hydroxylases are capable of catalysing 2 reactions at once as the molybdenum redox group oxidises one compound while the FAD site is capable of simultaneously reducing another (Figure 1) (Beedham., 1987). The iron-sulphur centres act to transfer electrons from the oxidised compound at the molybdenum site to the FAD site where a reduction can take place. AO and XOR catalyse the oxidation of a number of aldehydes and nitrogenous heterocyclic compounds (Beedham., 1985; Beedham., 1997). The presence of an electron donor mediates reduction of a number of compounds (Beedham., 1985; Krenitsky *et al.*, 1972). The proposed electron transfer pathway and reactive sites of molybdenum hydroxylases are summarised in figure 1.

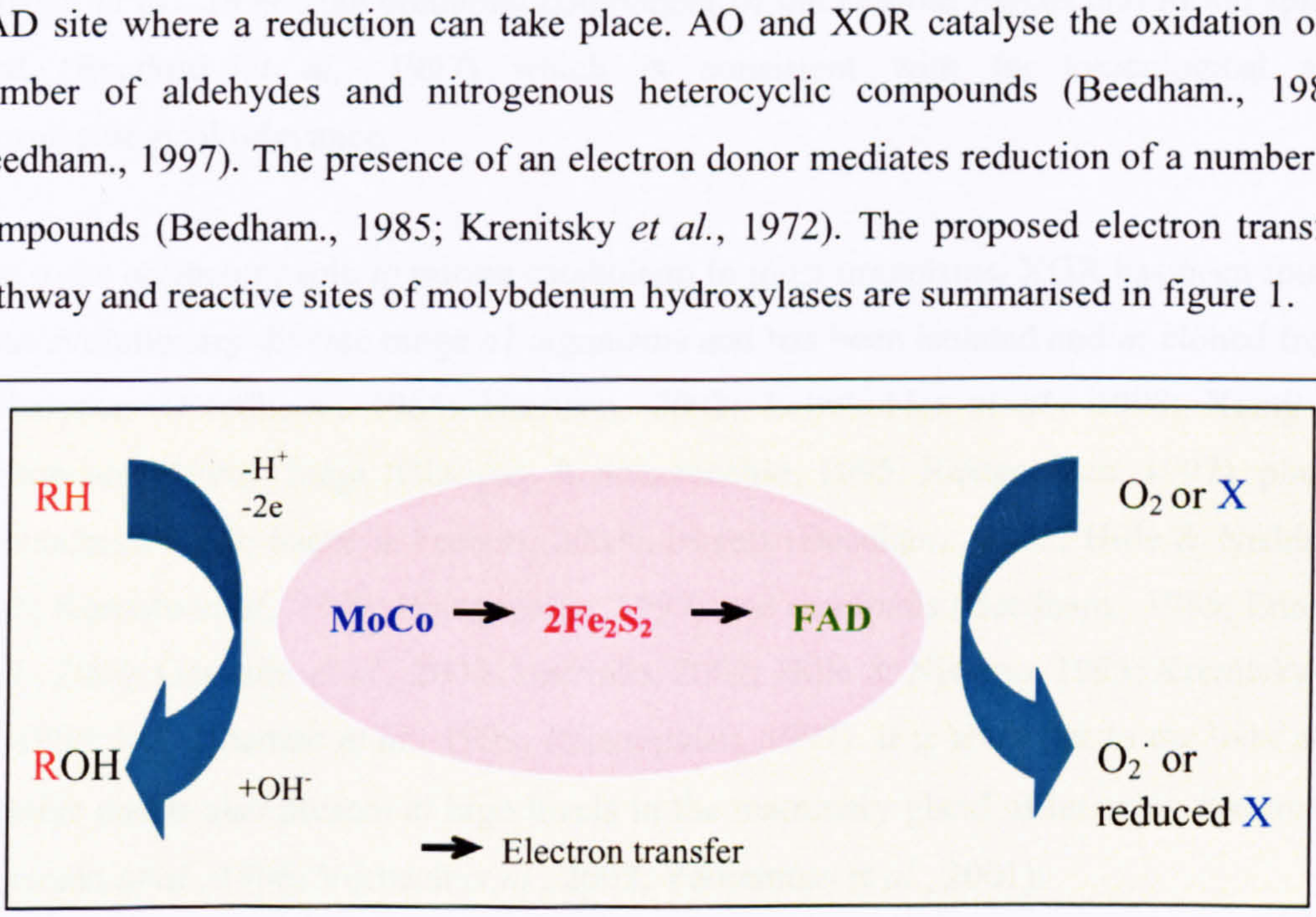

Figure 1 – Illustration of the catalytic capabilities of molybdenum hydroxylases.

A schematic diagram showing at which cofactor sites reactions occur and the proposed path of electrons through the enzyme based on Iwasaki *et al.*, 2000, Enroth *et al.*, 2000, Beedham., 1987.

RH = Aldehyde or N-Heterocycle (electron donor).

X = Electron Acceptor e.g. NAD (with XOR only) or xenobiotic electron acceptor (XOR and AO).

The general catalytic reaction of molybdenum hydroxylases takes the form of a hydroxyl transfer from water to an aldehyde forming the carboxylic acid or to an N-heterocycle forming the hydroxylated N-heterocycle (Beedham., 1987). The catalytic properties of these enzymes such as substrate specificity and susceptibility to inhibitors are very different although the substrate specificities overlap (Krenitsky *et al.*, 1972). For example, menadione is an inhibitor of AO but not XOR, while oxipurinol inhibits XOR but not AO (Beedham., 1987).

AO is present in a wide range of species and is found in almost all animals, several insects and some plants (Beedham., 1985). Several groups have studied the location of AO in various species. It is found mainly in the liver of animals, (Moriwaki *et al.*, 1998; Wright *et al.*, 1999; Yoshihara & Tatsumi, 1997) although it has been observed in other tissues such as the lung (Beedham *et al.*, 1987; Calzi *et al.*, 1995; Moriwaki *et al.*, 1998; Wright *et al.*, 1999), the spleen (Beedham *et al.*, 1987; Calzi *et al.*, 1995; Wright *et al.*, 1999), the kidney (Beedham *et al.*, 1987; Calzi *et al.*, 1995; Wright *et al.*, 1999), the epithelium of the tongue (Moriwaki *et al.*, 1998), the eye (Calzi *et al.*, 1995), the heart (Wright *et al.*, 1999), the epithelial component of the choroid plexus and in the spinal cord (Bendotti *et al.*, 1997) which is consistent with its toxicological and pharmacological relevance.

Due to its obligatory role in purine catabolism in most organisms, XOR has been found in an evolutionary diverse range of organisms and has been isolated and/or cloned from prokaryotes (Beedham., 1985; Harrison, 2002; Leimkuhler *et al.*, 1998; Xiang & Edmondson, 1996), fungi (Glatigny & Scazzocchio, 1995; Rajagopalan, 1997), plants (Montalbini, 2000; Sauer & Frebort, 2003), insects (Beedham., 1985; Hille & Nishino, 1995; Komoto *et al.*, 1999; Rajagopalan, 1997) and mammals (Beedham., 1985; Enroth *et al.*, 2000; Garattini *et al.*, 2003; Harrison, 2002; Hille & Nishino, 1995; Krenitsky *et al.*, 1986; McManaman *et al.*, 1999; Rajagopalan, 1997). It is abundant in the liver and intestine and is also present at high levels in the mammary gland of lactating mammals (Kurosaki *et al.*, 1996; Vorbach *et al.*, 2002; Yamamoto *et al.*, 2001).

1.2 Role of aldehyde oxidase in endogenous and exogenous compound metabolism.

With regards to the substrate specificity of AO the name aldehyde oxidase is misleading as it implies that it only oxidises aldehydes, when its actual substrate specificity is much wider than this and includes N-heterocycles as substrates. Alternative names that have been proposed such as quinine oxidase or methotrexate oxidase imply an even smaller specificity for the enzyme, while the broader term molybdenum hydroxylase may also be used to describe XOR as well. As it was historically known as aldehyde oxidase, this nomenclature has been kept to the present day (Beedham., 1987; Garattini *et al.*, 2003). Whereas the role of AO in endogenous compound metabolism has not yet been unequivocally identified its role as a enzyme involved in xenobiotic metabolism has been well established (Beedham., 1985). It serves as a detoxification enzyme whose substrates include exogenously derived compounds of wide structural diversity (Beedham., 1985; Krenitsky *et al.*, 1972)

1.2.1 Role of aldehyde oxidase in endogenous compound metabolism.

One physiological role of AO that has been proposed is that it could be a regulator of vitamin B_6 (nicotinamide) concentration, due to the formation of pyridones from the vitamin catabolism product, N^1-methylnicotinamide, by AO (Stanulovic & Chaykin, 1971a; Stanulovic & Chaykin, 1971b).

AO is also known to metabolise endogenous substrates such as retinaldehyde (Terao *et al.*, 1998), which is the main component of the visual pigments and is a potential precursor of the active metabolite of vitamin A, retinoic acid (Ambroziak *et al.*, 1999). It has been speculated that AO may also play a role in visual processes due to its ability to metabolise retinaldehyde. AO has been shown to be the same enzyme as retinal oxidase (Tomita *et al.*, 1993) which catalyses the oxidation of retinaldehyde to retinoic acid (Huang & Ichikawa, 1994). Retinoic acid has multiple functions in the body, for example it is responsible for the formation of limb buds and plays a part in cellular differentiation and morphogenesis. A major role of aldehyde oxidase therefore could be the synthesis of retinoic acid from retinaldehyde (Tomita *et al.*, 1993).

Studies by Berger *et al.* (Berger *et al.*, 1995) have demonstrated that AO is also expressed in the human ventral horn glial cells, which form approximately 90% of the cells within the nervous system. These cells support the environment around nerve cells and are responsible for removing and inactivating neurotransmitter molecules (Berger *et al.*, 1995). In addition, it has also been suggested that AO may metabolise dihydroxymandelaldehyde, a product of the catabolic pathway of adrenaline and noradrenaline, which could indicate another possible physiological role for AO (Terao *et al.*, 1998).

1.2.2 Role of aldehyde oxidase in exogenous compound metabolism.

Although AO's role in endogenous compound metabolism has not been unequivocally proven the main reason for the interest in AO is as a xenobiotic/drug metabolising enzyme. AO catalyses phase one drug metabolism with a complementary substrate specificity to the microsomal cytochrome P450 monooxygenases (Beedham., 1985; Beedham., 1987). Phase one drug metabolism reactions are usually oxidation, reduction or hydrolysis reactions, which introduce or expose a functional group. As mentioned in section 1.1 AO oxidises a multitude of substrates including N-heterocycles such as phenanthridine and aldehydes such as benzaldehyde. It also oxidises many N-heterocyclic drugs including several anticancer and anti-viral agents such as those described in more detail below.

As there are many xenobiotics and drugs that are substrates for this enzyme only a few are described in more detail here. Several different types of drugs are substrates for AO these include anti-viral agents such as famciclovir (2-[2-(2-amino-9H-purin-9-yl) ethyl]-1,3-propanediol diacetate (ester)), which undergoes rapid hydrolysis and oxidation in man to yield the active anti-herpes agent penciclovir by AO (figure 2a) (Clarke *et al.*, 1995; Rashidi *et al.*, 1997). Penciclovir is active against herpes simplex virus types 1 and 2 (causing herpes), varicella zoster virus (causing chicken pox), Epstein-Barr virus and hepatitis B (Rashidi *et al.*, 1997). Various anti-cancer drugs are also substrates for AO examples of these include

N-[(2`-Dimethylamino)ethyl]acridine-4-carboxamide (DACA) which is undergoing phase II clinical trials and shows high activity against various solid murine tumours and various multidrug resistant human tumour cell lines (Schofield *et al.*, 2000). DACA is

metabolised to acridone metabolites by AO, which appears to play a major role in its elimination in patients and rodents (figure 2b) (Robertson *et al.*, 1993; Schlemper *et al.*, 1993; Schofield *et al.*, 2000). Another drug metabolised by AO is methotrexate (4-amino-N^{10}-methylpteroglutamic acid), which is widely used to treat acute lymphocytic leukaemia in children, osteosarcomas, lymphomas and various other malignancies in both adults and children (Kitamura *et al.*, 1999a; Kitamura *et al.*, 1999b). Methotrexate has also become a standard therapy for the treatment of rheumatoid arthritis (Grosflam & Weinblatt, 1991). The metabolism of methotrexate to 7-hydroxymethotrexate occurs due to the activity of AO (figure 2c) (Kitamura *et al.*, 1999a). Another example of an anti-cancer agent is thioguanine, (a thiopurine antimetabolite), which is used for the treatment of acute leukaemia. The thiopurines are prodrugs, which are converted to nucleotides intracellularly before they are able to exert their cytotoxic effect. Thioguanine is oxidised by AO to form 8-hydroxy-thioguanine which is in turn deaminated by guanine deaminase to thiouric acid (figure 2e) (Kitchen *et al.*, 1999). The last example is zaleplon (*N*-[3-(3-cyanopyrazdo[1,5-*a*]pyrimidine-7-yl)phenyl]-*N*-ethyl-acetamide), a nonbenzodiazepine compound being developed as a ultra-short acting sleep inducer with a prompt onset of action (Kitamura *et al.*, 1999b). Zaleplon is oxidised to 5-oxo-zaleplon by AO (figure 2d) (Kawashima *et al.*, 1999).

As well as hydroxylation of compounds AO also catalyses the reduction of many compounds such as sulphoxides, N-oxides, nitrosamines, hydroxamic acids, azo compounds, oximes, epoxides and aromatic nitrocompounds (Beedham., 1985; Krenitsky *et al.*, 1972).

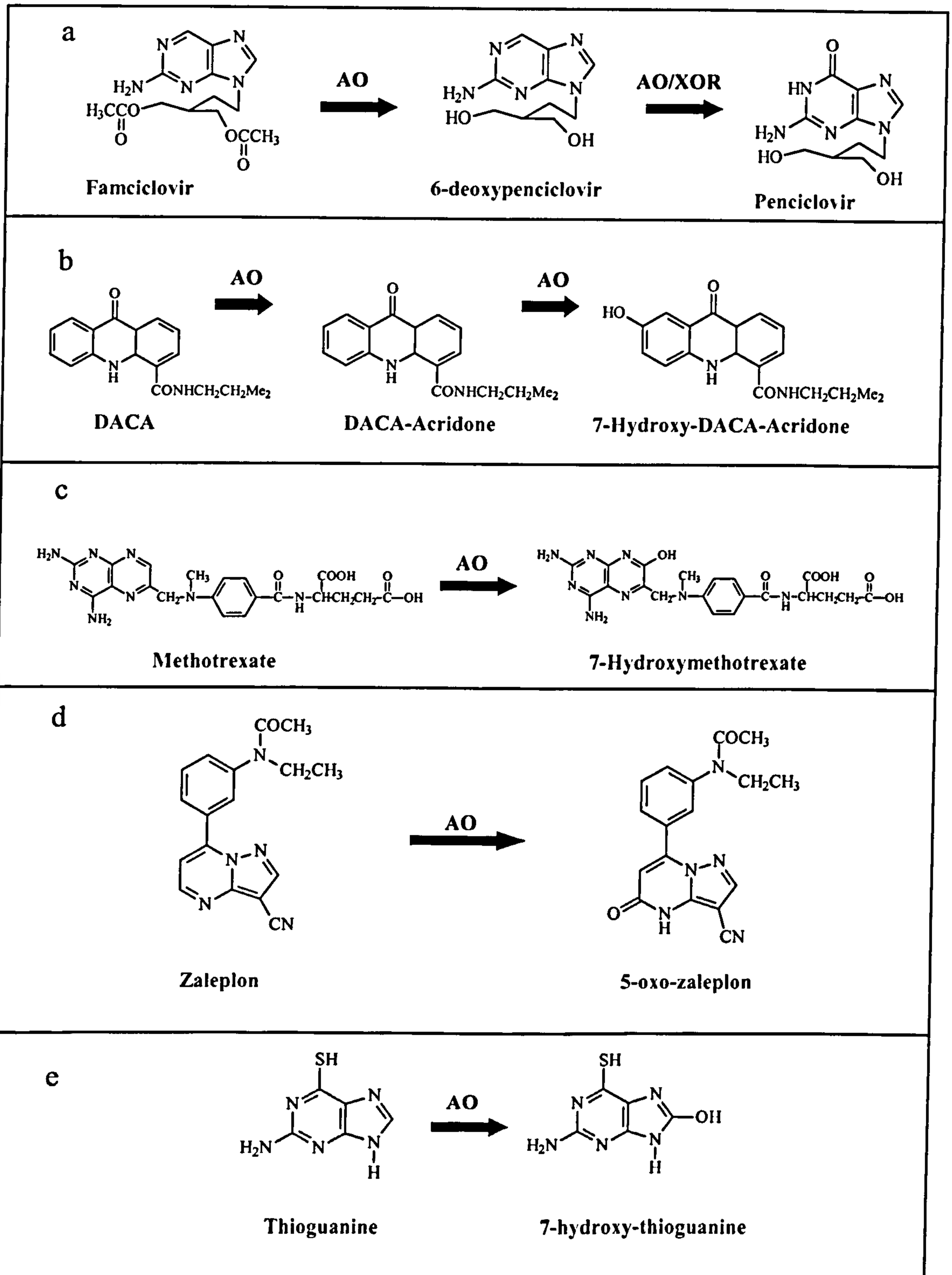

Figure 2 – Examples of the role of aldehyde oxidase in N-heterocyclic drug metabolism.

a, b, c, d & e shows the role of AO in the metabolism of famciclovir, DACA, methotrexate, zaleplon and thioguanine respectively.

1.3 Role of xanthine oxidoreductase in endogenous and exogenous compound metabolism.

Like AO, XOR has roles in both endogenous and exogenous metabolism but unlike AO, XORs role in endogenous compound metabolism is definitively proven. Also unlike AO the name xanthine oxidoreductase accurately describes the enzyme but it should be pointed out that XOR can exist in two forms, which has important implications in disease processes (section 1.6). The two forms that are found naturally are a dehydrogenase form (XD) (E.C.1.1.1.204) and an oxidase form (XO) (E.C.1.1.3.22). The oxidase form is formed from the dehydrogenase form by two mechanisms, reversible oxidation of thiol groups and irreversible partial proteolytic cleavage, which occurs rapidly when atmospheric oxygen is introduced to the dehydrogenase form (Marti *et al.*, 2001). Whereas all the mammalian XORs so far studied undergo conversion (Amaya *et al.*, 1990; Enroth *et al.*, 2000), XOR in the prokaryote *Rhodobacter capsulatus* (*R. capsulatus)* (Truglio *et al.*, 2002) and the chicken XOR (Sato *et al.*, 1995) are examples of species that have no capability to undergo conversion and exists as XD only.

1.3.1 Role of xanthine oxidoreductase in endogenous purine metabolism.

XOR is an obligatory enzyme in the endogenous purine degradation pathway. It is responsible for converting xanthine and hypoxanthine to uric acid, which is the final product of purine degradation in humans (Voet *et al.*, 1999) (figure 3). Loss of function of this enzyme results in a condition known as xanthinuria where a build up of xanthine and to a lesser extent hypoxanthine in the body occurs (Simmonds *et al.*, 1995). Xanthinuria is described in more detail in section 1.6.3.

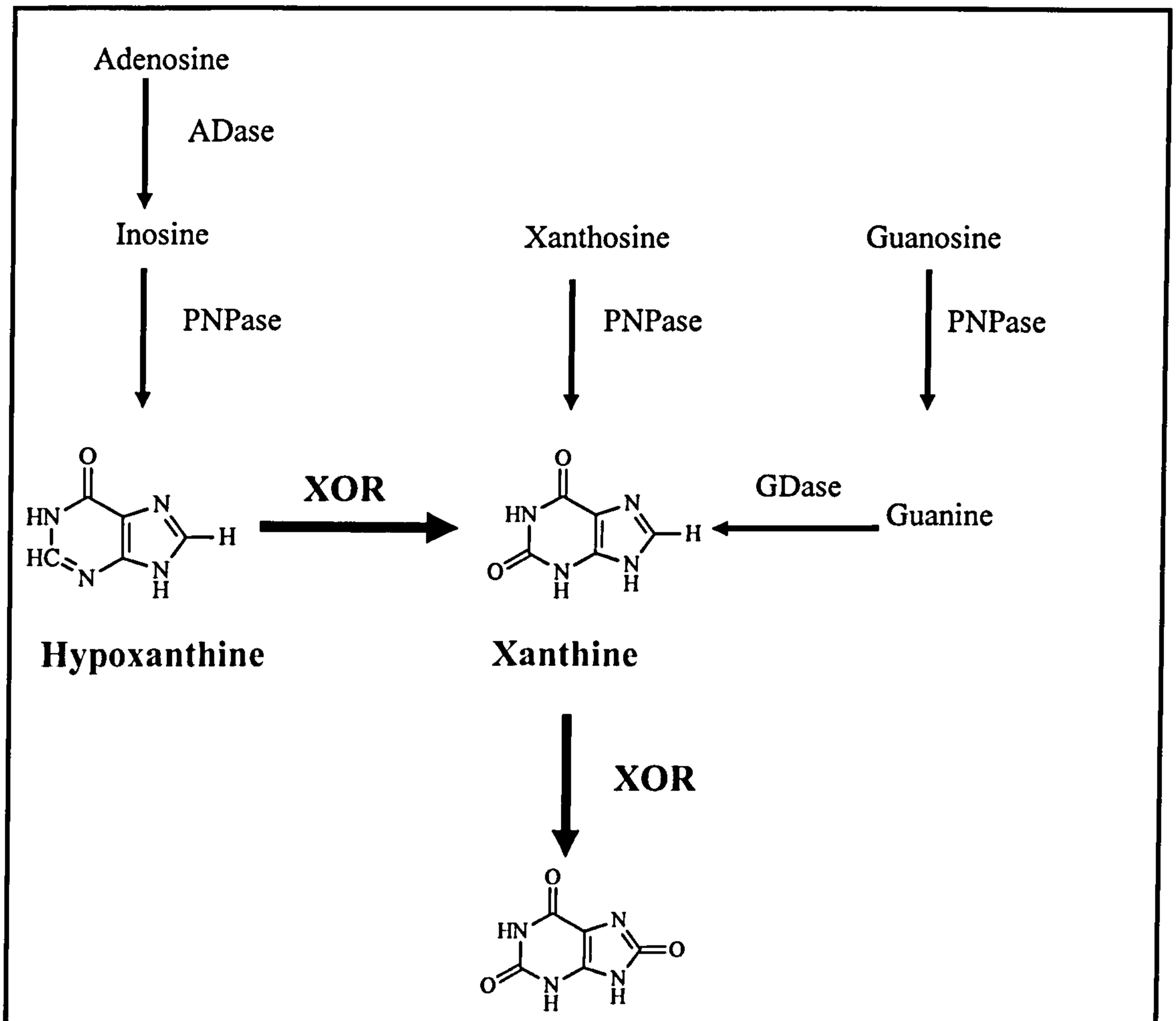

Figure 3 -The role of xanthine oxidoreductase in purine catabolism in man (based on Voet *et al.* 1999).

ADase – adenosine deaminase, PNPase – purine nucleoside phosphorylase, GDase – guanine deaminase

1.3.2 Role of xanthine oxidoreductase in exogenous compound metabolism.

As well as endogenous compound metabolism, XOR is also important as a xenobiotic drug metabolism enzyme. Like AO, it also has complementary substrate specificities to the cytochrome P450s and catalyses phase one drug metabolism. Aciclovir is an antiviral drug effective against herpes simplex virus and varicella zoster virus, however high doses need to be given due to the ineffective oral absorption of the drug. The prodrug 6-deoxyaciclovir was developed which is activated to aciclovir by XOR (figure

4b), unfortunately high toxicity problems highlighted in animal studies resulted in further development being terminated (Beedham., 1997). An example of a cancer chemotherapeutic agent oxidised by XOR is 6-mercaptopurine (Van Scoik *et al.*, 1985) (figure 4b). XOR also plays a role in the breakdown of caffeine, which undergoes 3-demethylation by a cytochrome P450 to form paraxanthine which is then 7-demethylated to 1-methylxanthine which is then 8-hydroxylated by XOR resulting in the formation of 1-methylurate (Kalow & Tang, 1991) (figure 4c).

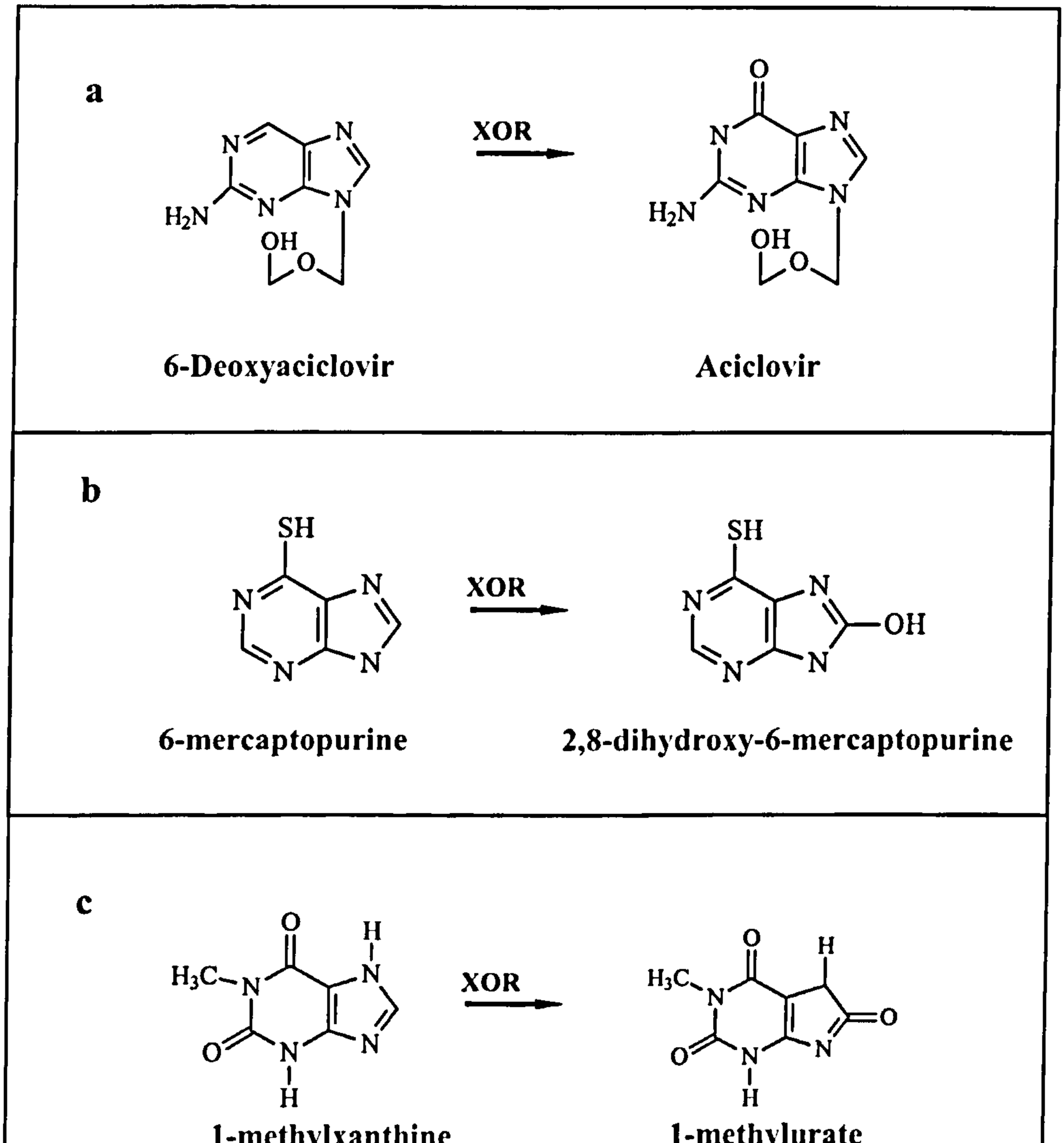

Figure 4 – Examples of the role of xanthine oxidoreductase in N-heterocyclic drug metabolism.

a, b and c shows the role of XOR in the metabolism of 6-deoxyaciclovir, 6-mercaptopurine, and 1-methylxanthine respectively.

1.4 Structural features of molybdenum hydroxylases.

As summarised in section 1.1 AO and XOR contain one FAD, one MoCo and two iron-sulphur centres per subunit. Insight into the domain structure of molybdenum hydroxylases have recently been provided by the successful crystallization of three molybdenum hydroxylases from a mammalian (Enroth *et al.*, 2000) and two bacterial species (Romao *et al.*, 1995; Truglio *et al.*, 2002). X-ray crystallography data has determined that each subunit of the bovine XOR enzyme may be divided into three subdomains. The first subdomain (residues 1-165) at the N-terminus contains both the iron-sulphur cofactors. It is connected to the FAD-binding domain (residues 226-531) by a long segment of amino acids (residues 166-225). Another linker segment (residues 532-861), connects this subdomain to the molybdenum cofactor binding domain (residues 590-1,332), which is spatially positioned close to the interfaces of the iron sulphur and FAD binding domains (Enroth *et al.*, 2000). Interestingly the XOR enzyme from the prokaryote *R. capsulatus* contains a $(\alpha\beta)_2$ heterotetramic structure with the cofactors located on two different polypeptide chains. The two iron sulphur cofactors and the FAD cofactor bind to the XD subunit A and the molybdenum cofactor binds to the XD subunit B. Each subunit of the bovine enzyme is equal to one heterodimer of *R. capsulatus* (Truglio *et al.*, 2002). Another interesting point is that aldehyde oxidoreductase (AOR), a related bacterial enzyme from *Desulfovibrio gigas* (*D. gigas*), only possesses the molybdopterin cofactor and the two iron-sulphur binding domains as the protein domain associated with FAD binding is missing, which results in a smaller enzyme (Romao *et al.*, 1995). This *D. Gigas* enzyme was the first of the three crystal structures to be determined (Romao *et al.*, 1995). Three-dimensional structural analysis of this molybdoenzyme identified that the first iron sulphur domain chain fold was very similar to that of the plant and cyanobacterial iron-sulphur ferredoxins but the second iron sulphur domain had a previously undescribed iron sulphur ferredoxin type fold. Further work by Enroth *et al.* using X-ray crystallography data obtained from bovine milk XOR also noted the two distinct binding sites and found that the plant ferredoxin-like N-terminal iron-sulphur centre was spatially situated close to the FAD cofactor and that the C-terminal unique iron-sulphur centre was spatially situated close to the MoCo site (Enroth *et al.*, 2000). Iwasaki *et al.* studied these iron sulphur clusters in more detail. By comparing the primary amino acid sequence of XOR and AO with other iron-sulphur proteins they identified that the N-terminal iron-sulphur centre was plant

ferredoxin-like following the same binding motif as found in plant ferredoxins (figure 5) (Iwasaki *et al.*, 2000), but the C-terminal iron-sulphur centre was unique to the molybdenum hydroxylases exhibiting an unusual binding motif as illustrated in figure 5 (Iwasaki *et al.*, 2000).

N-terminal plant ferredoxin-like motif	C-terminal unusual motif
Rat xanthine oxidoreductase:	
-^{43}Cys-X-^{48}Cys-X-^{51}Cys-//-^{73}Cys-	-^{112}Cys-X-^{115}Cys-//-^{147}Cys-X-^{149}Cys-
***D. gigas* aldehyde oxidoreductase:**	
-^{40}Cys-X-^{45}Cys-X-^{48}Cys-//-^{60}Cys-	-^{100}Cys-X-^{103}Cys-//-^{137}Cys-X-^{139}Cys-
***Anabaena* 7120 vegetative ferredoxin:**	
-^{41}Cys-X-^{46}Cys-X-^{49}Cys-//-^{79}Cys-	

Figure 5 – The iron-sulphur binding domains of molybdenum hydroxylases.

Schematic diagram of the two iron sulphur binding motifs in the iron sulphur domain of rat XOR, *D. gigas* AOR and the plant-type ferredoxin motif of *Anabaena* 7120 vegetative ferredoxin. Based on (Iwasaki *et al.*, 2000). The N-terminal plant ferredoxin-like motif is highlighted in pink and the C-terminal unusual motif is highlighted in green.

Enroth *et al.* also found that the FAD molecule binds within a deep cleft of the bovine XOR enzyme allowing space for interaction with the NAD molecule. This cofactor is situated between the iron-sulphur centres and the MoCo binding domains (Enroth *et al.*, 2000). In their structural analysis of XOR from *R. capsulatus* Truglio *et al.* noted several residues that form hydrogen bonding with the FAD molecule that were conserved in all the XORs they studied. The corresponding residues in the human XOR protein are Asn349, Asp358 and Lys424 (Truglio *et al.*, 2002). In addition to FAD binding residues five binding sites have been identified with regard to MoCo binding situated towards the C-terminus of the protein. MoCo I spans residues 797-804 in the mouse XOR protein sequence, MoCo II spans residues 913-921 in the mouse XOR protein sequence, MoCo III spans residues 1041-1044 in the mouse XOR protein sequence, MoCo IV spans residues 1080-1083 in the mouse XOR protein sequence and

MoCo V spans residues 2262-2267 in the mouse XOR protein sequence (Terao *et al.*, 2000). In their thorough analysis Enroth *et al.* propose that as there are no obvious "through bond" pathways connecting the two iron-sulphur domains and the FAD domain, that tunnelling is the most probable mechanism for electron transport between the cofactors. The geometrical arrangements and redox potentials of the cofactors also provide support for the theory that the electrons are transferred from MoCo to the two iron-sulphur centres to the FAD cofactor proposed by Iwasaki *et al* (Enroth *et al.*, 2000; Iwasaki *et al.*, 2000).

These crystal structures reveal a wealth of information previously unknown about these enzymes. With knowledge of these structures effects of misense mutations found in other species might be predicted, as has been done for human dihydropyrimidine dehydrogenase gene mutations (Kuilenburg *et al.*, 2002). As time progresses more crystal structures will probably be elucidated which will reveal even more information about this group of enzymes.

1.5 Genes involved in molybdenum hydroxylase biosynthesis.

In the past decade there have been several genes identified involved in molybdenum hydroxylase biosynthesis. These include genes that encode the apoenzymes and several genes that are involved in the synthesis of the molybdenum cofactor (Garattini *et al.*, 2003; Reiss & Johnson, 2003). A summary of what is known about these genes is outlined in this section with special emphasis on XOR and AO apoprotein genes, which were the focus of the research project described in this thesis.

1.5.1 The xanthine oxidoreductase gene.

Xanthine oxidoreductase is well characterised from a wide range of species. It has been cloned from many species from bacteria to humans (Glatigny & Scazzocchio, 1995; Komoto *et al.*, 1999; Saksela & Raivio, 1996; Sato *et al.*, 1995; Terao *et al.*, 1992; Tsuchida *et al.*, 2001). The first XOR cDNA sequence to be cloned was rat liver XOR by Amaya *et al.* in 1990 (Amaya *et al.*, 1990) which subsequently enabled the mouse and human XOR cDNA to be cloned (Ichida *et al.*, 1993; Saksela & Raivio, 1996; Terao *et al.*, 1992; Wright *et al.*, 1993; Xu *et al.*, 1994a). Interestingly there have been four separate sequences published for human XOR cDNA (Ichida *et al.*, 1993; Saksela & Raivio, 1996; Wright *et al.*, 1993; Xu *et al.*, 1994a). There was confusion about which of the published sequences were correct. In July 1993 Ichida *et al.* published the first cDNA sequence and detailed differences found between individual clones (Ichida *et al.*, 1993). Wright *et al.* (1993) published another cDNA sequence in November 1993, which they claimed was human XOR, however it contained no coding information for a NAD binding site and was only 60% identical to rat XOR and Ichida *et al*'s cDNA sequences (Wright *et al.*, 1993). This was later suggested to be AO (Glatigny & Scazzocchio, 1995). Xu *et al.* also published a sequence for human XOR cDNA (Xu *et al.*, 1994a) which was different again to the previous two however in 1995 they revealed several corrections to their sequence in a published erratum (Xu *et al.*, 1995), after Stratagene reported that the oligo(dT)-primed human liver cDNA library which Xu *et al.* had used was in fact not human. As three different sequences for human XOR had been published Saksela and Raivio also cloned human XOR in 1996 to try and determine which sequence was correct. They found that their sequence was over 99% identical to Ichida's sequence but only 60% identical to Wright's sequence

supporting the theory that this sequence was not XOR. Xu's original sequence showed 94% identity but the revised sequence showed 99.65% identity with Saksela's (Saksela & Raivio, 1996). It is now recognised that Saksela's sequence is the correct one. Following the cloning of the XOR cDNA this enabled Ichida *et al.* to map the chromosomal location of human XOR to chromosome 2 (Ichida *et al.*, 1993) and Xu *et al.* later published the subchromosomal location of XOR to chromosome 2p22 (Xu *et al.*, 1994b) which was independently confirmed (Rytkonen *et al.*, 1995). The intron/exon structure of the XOR gene was also determined by Xu *et al* (Xu *et al.*, 1996).

Analysis of both the cDNA and gene has revealed several important structural features of human XOR. The cDNA sequence of human XOR contains an open reading frame of 3999 nucleotides, which encodes a protein of 1333 amino acids. The gene spans a region of at least 60 kb (Xu *et al.*, 1996). This is over twice the size of the average human gene which only spans approximately 27 kb (Venter *et al.*, 2001). The coding sequence of XOR is split into 36 exons which vary in size from 53 bp to 279 bp. Interestingly the number of exons in the XOR gene is considerably greater than the average human gene which is split into approximately 7 exons (Venter *et al.*, 2001). In addition to the large number of exons the intron sizes of XOR are up to 5 kb which makes working with this gene tedious (Xu *et al.*, 1996).

1.5.2 The aldehyde oxidase gene.

As previously mentioned the cDNA encoding human AO was first reported to be XOR (Wright *et al.*, 1993). Subsequently the mRNA encoding AO has been cloned in several species including bovine (Calzi *et al.*, 1995), mouse (Demontis *et al.*, 1999; Huang *et al.*, 1999), rabbit (Huang *et al.*, 1999), rat (Wright *et al.*, 1999) and several plants (Barabas *et al.*, 2000; Min *et al.*, 2000). There is a high degree of similarity between species (greater than 80% in mammals) with several highly conserved regions, which have been found in all AO mRNAs cloned so far. Following the cloning of these cDNAs the gene was subsequently cloned in humans (Wright *et al.*, 1997) and mice (Demontis *et al.*, 1999). Mammalian AO is a single copy gene, which covers approximately 85 kb of DNA containing 35 exons (Terao *et al.*, 1998). Like the XOR

gene the AO gene has an open reading frame, 3999 nucleotides long, which encodes for a polypeptide chain of 1333 amino acids.

1.5.3 Similarity of aldehyde oxidase and xanthine oxidoreductase proteins and genes.

Comparison of the deduced AO and XOR primary amino acid sequences reveal that they are approximately 50% identical but have a high degree of sequence identity at certain regions allowing a consensus eukaryotic protein map to be proposed (Garattini *et al.*, 2003) (figure 6a). Comparison of the genes of AO and XOR reveal that they are very similar in structure. 34 out of 36 of the intron boundaries are exactly conserved between the two genes. Intron 26 in XOR is suppressed in AO and the sum of exons 26 and 27 in XOR are exactly the same size as exon 26 in AO (Terao *et al.*, 1998). This is illustrated in figure 6. All these similarities between the two genes have led to the conclusion that they probably arose from a gene duplication event despite the fact that they are located at opposite ends of chromosome 2 which is the second largest chromosome in humans (Terao *et al.*, 1998).

Figure 6 – Diagram showing the human xanthine oxidoreductase and aldehyde oxidase protein map and gene structure.

Schematic diagrams of the intron/exon structure of the human XOR and AO genes and molybdenum hydroxylase protein map. a is a molybdenum hydroxylase protein map illustrating the binding domains of the four cofactors, b is the human XOR gene and c is the human AO gene. The two iron sulphur binding domains are depicted in red, the FAD binding domain is depicted in blue and the MoCo binding domain is depicted in green.

1.5.4 Aldehyde oxidase gene homologues.

Although prior to the initiation of the project detailed in this thesis, it was widely accepted that a single AO enzyme carried out all AO activity in mammals. A study by Holmes in 1978 suggested that there may be two AO enzymes in mice based on cellulose acetate zymograms (Holmes, 1978). It was not until over two decades later that irrefutable proof of more than one AO enzyme existed. In September 2000 a paper was published detailing the discovery of two aldehyde oxidase mRNA homologues in mice (Terao *et al.*, 2000), this was followed by a sister paper in December of 2001 detailing more information on the genes and characteristics of the homologues (Terao *et al.*, 2001). Aldehyde oxidase homologue 1 (AOH1) is expressed in the hepatocytes of the liver and in spermatogonia while aldehyde oxidase homologue 2 (AOH2) expression

is limited to keratinized epithelia and the basal layer of the epidermis and hair folliculi (Terao *et al.*, 2001; Terao *et al.*, 2000). The mouse AOH1 and AOH2 cDNAs were found to code for polypeptides of 1335 and 1336 amino acids respectively. As they were more similar to AO than XOR and showed phenanthridine but not hypoxanthine oxidising activity they were presumed to be AO homologues rather than XOR homologues. Further evidence for the enzymes being AO homologues as opposed to XOR homologues was that the AOH1 and AOH2 sequences lacked the typical NAD binding consensus sequence, which is found in all XOR's. Like AO the AOH1 and AOH2 proteins also showed benzaldehyde oxidising activity when stained on a cellulose acetate plate (Terao *et al.*, 2001; Terao *et al.*, 2000).

Very recently a review on molybdenum hydroxylases in mammals reported the presence of a third AO homologue in mice (Garattini *et al.*, 2003). They reported that aldehyde oxidase homologue 3 (AOH3) was located approximately 9 kb downstream of the AOH2 locus summarised in figure 7. They have also carried out work on the human AO locus using various cDNA libraries and have found that the human genome is likely to contain only one functional AO gene and three tandem gene duplications homologueous to AOH1, AOH2 and AOH3. They propose that these duplications are pseudogenes which have replaced the AO homologues present in mice (Garattini *et al.*, 2003).

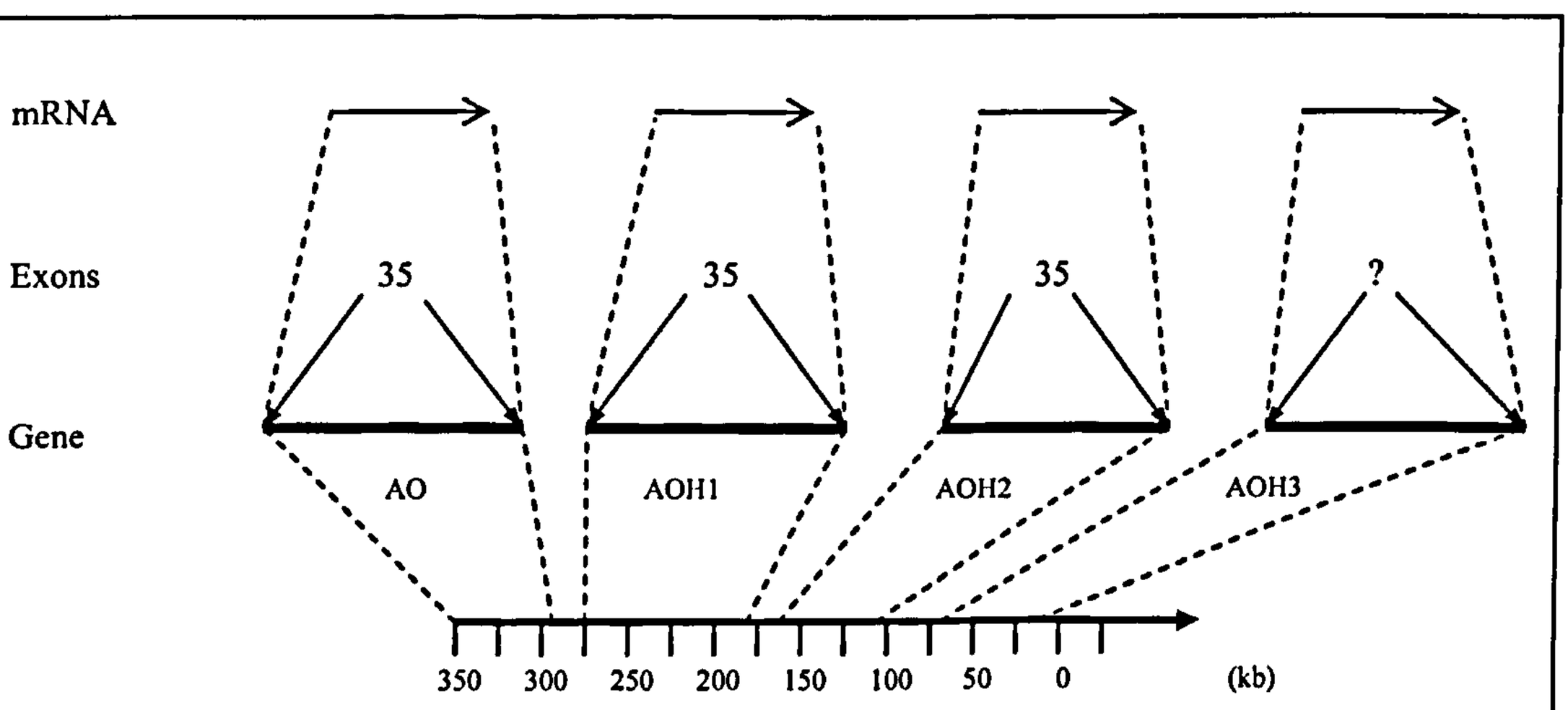

Figure 7 - Schematic diagram of the aldehyde oxidase gene cluster on mouse chromosome 1.

The arrows show the direction of transcript. The number of exons where known is shown above the gene. ? = unknown.

Interestingly around the same time that the murine AO homologues were reported it was also discovered that plants contain several AO genes (Barabas *et al.*, 2000; Min *et al.*, 2000).

1.5.5 Molybdenum cofactor synthesis.

As well as the structural genes that encode AO and XOR there are also several genes involved in the biosynthesis of the molybdenum cofactor that are essential for the formation of functionally active molybdenum hydroxylase holoenzymes.

The molybdenum cofactor synthesis step 1 (MOCS1) gene product catalyses the formation of precursor Z from the guanine triphosphate (GTP). The molybdenum cofactor synthesis step 2 (MOCS2) gene product, activated by the molybdenum cofactor synthesis step 3 (MOCS3) gene product, synthase sulphotransferase, then catalyses the formation of molybdopterin from precursor Z. Gephyrin then catalyses the insertion of the molybdenum atom into the molybdopterin to create an active molybdenum cofactor suitable for use in sulphite oxidase (Reiss, 2000). However a sulphur atom needs to be added in order for AO and XOR to utilise the cofactor. This is achieved by a recently cloned enzyme, molybdenum cofactor sulphurase (MCS) (Ichida *et al.*, 2001). Figure 8 summarises the steps involved in the biosynthesis of the molybdenum cofactor.

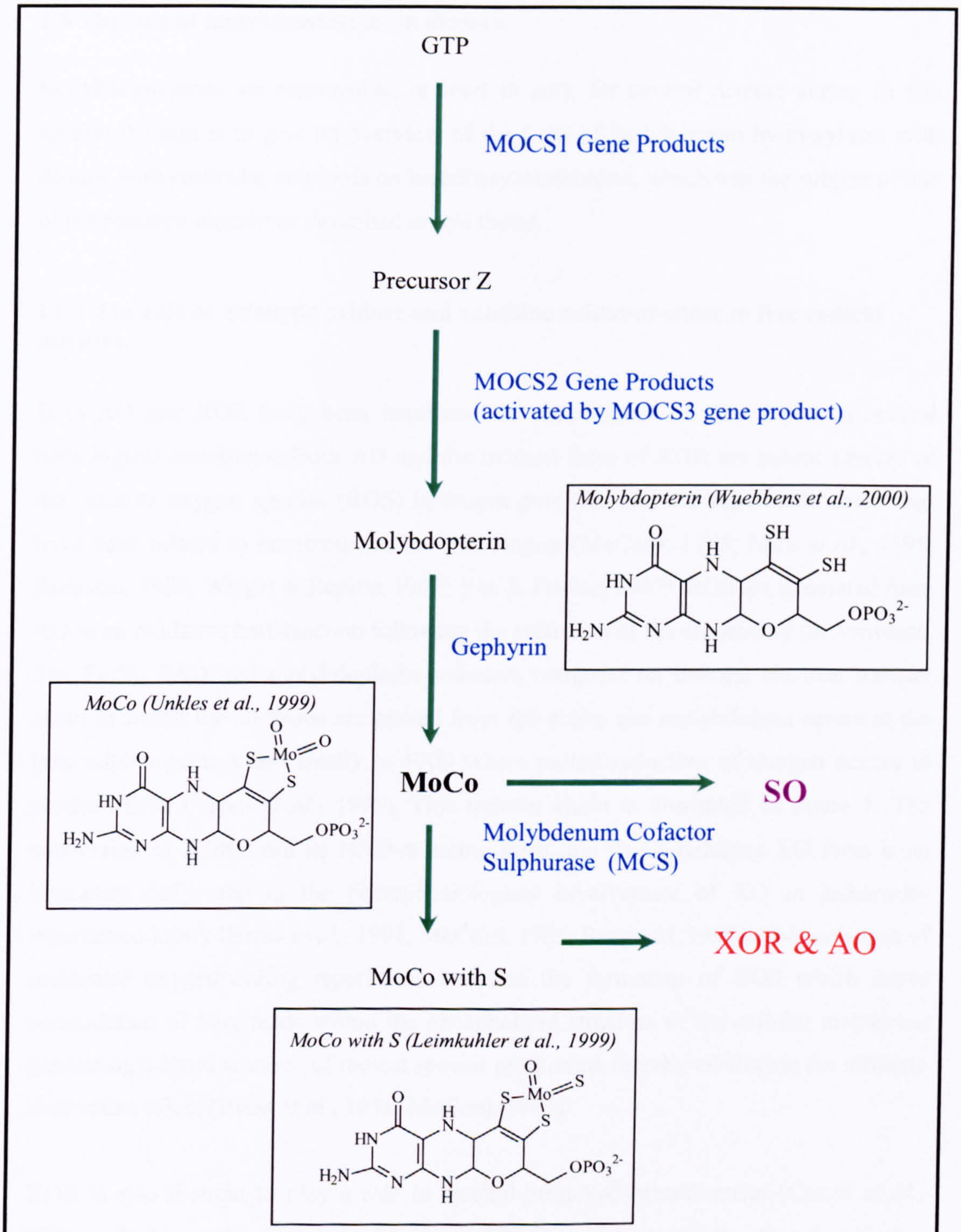

Figure 8 – Summary of molybdenum cofactor synthesis based on Reiss, 2000.

This schematic diagram shows the structure of the molybdenum cofactor illustrating where and at what step the sulphur is added to enable the cofactor to function in AO and XOR, MOCSx - molybdenum cofactor synthesis step x is1, 2 and 3 respectively. GTP is guanine triphosphate.

1.6 The role of molybdoenzymes in disease.

Molybdoenzymes are responsible, at least in part, for several disease states. In this section the aim is to give an overview of the links of molybdenum hydroxylases with disease with particular emphasis on hereditary xanthinuria, which was the subject of one of the research objectives described in this thesis.

1.6.1 The role of aldehyde oxidase and xanthine oxidoreductase in free radical diseases.

Both AO and XOR have been implicated to either cause or play a part in several pathological conditions. Both AO and the oxidase form of XOR are potent sources of the reactive oxygen species (ROS) hydrogen peroxide and the superoxide anion that have been related to numerous human pathologies (McCord, 1985; Mira *et al.*, 1995; Saugstad, 1996; Wright & Repine, 1997; Yee & Pritsos, 1997). ROS are generated from AO in an oxidative half-reaction following the reduction of the enzyme by the substrate. The Fe_2S_2, FAD and molybdopterin cofactors comprise an internal electron transfer chain in which the electrons are passed from the active site molybdenum centre to the iron-sulphur centres and finally to FAD where partial reduction of oxygen occurs to produce ROS (Terao *et al.*, 1998). This transfer chain is illustrated in figure 1. The conversion of XOR from its NAD-reducing form into its O_2-reducing XO form is an important early step in the pathophysiological involvement of XO in ischaemia-reperfusion injury (Brass *et al.*, 1991; McCord, 1985; Saugstad, 1996). The induction of molecular oxygen during reperfusion leads to the formation of ROS which cause peroxidation of fatty acids within the phospholipid structure of the cellular membrane generating a chain reaction of radical species production thereby enhancing the ultimate destructive effect (Brass *et al.*, 1991; McCord, 1985).

XOR is also thought to play a role in alcohol-promoted breast cancer (Castro *et al.*, 2001). It has been shown that the XO form of XOR participates in the ethanol oxidation to acetaldehyde in breast cytosol thereby producing ROS (Castro *et al.*, 2001). Acetaldehyde is a known mutagenic and carcinogenic chemical and ROS are thought to be involved in the initiation and promotion stages of ethanol-induced cancers in various different tissues (Castro *et al.*, 2001). During acute alcohol intake there is an increase in purine degradation resulting in higher levels of xanthine and hypoxanthine in the blood

and serum. This coupled with intakes of caffeine such as coffee or certain soft drinks may significantly increase the formation of acetaldehyde in breast tissue (Castro *et al.*, 2001).

AO has also been shown to produce free radicals during ethanol metabolism (Mira *et al.*, 1995; Shaw & Jayatilleke, 1990), during which there is an increase in the $NADH/NAD^+$ ratio resulting from ethanol oxidation into acetaldehyde by alcohol dehydrogenase and from acetaldehyde oxidation into acetate by aldehyde dehydrogenase. As acetaldehyde is a substrate for AO these processes contribute to a higher amount of ROS being produced which initiates lipid peroxidation of the liver XOR also contributes to the ROS production. (Mira *et al.*, 1995; Shaw & Jayatilleke, 1990).

1.6.2 Role of xanthine oxidoreductase in defence against pathogenic organisms.

It has been shown that XOR activity increases in mice after infection with the influenza virus (Oda *et al.*, 1989). Treatment of these mice with superoxide dismutase (a superoxide scavenger) conjugated with a pyran copolymer protected mice against a potentially lethal influenza virus infection if administered 5-8 days after infection. This illustrates that oxygen radicals of which XOR is a source are important in the pathogenesis of influenza virus infection (Oda *et al.*, 1989).

XOR expression is also induced by the presence of interferons and it appears to mediate some of the toxic effects produced by interferons and their inducers such as bacterial lipopolysaccharides (Terao *et al.*, 1992). Terao *et al.* proposed that the increased production of superoxides derived from the XOR system may be related to the antiproliferative or antiviral activity of interferons (Terao *et al.*, 1992).

In a study of infant rats that were infected with *Streptococcus pneumoniae* (type 3), which causes bacterial meningitis in these rats XOR activity also increased (Christen *et al.*, 2001). However it is thought that rather than aggravating the disease, the formation of urate due to this activation exerts a protective effect. Further evidence of XOR's protective role is provided by the $p47^{phox-/-}$ mouse model, in which the relative contributions of the NADPH oxidase and XOR to superoxide generation have been

evaluated. Following infection of the p47$^{phox-/-}$ mice with *Burkholderia cepacia,* which are sensitive to superoxide-derived reactive oxidants, the superoxides produced by XOR aided clearance of the pathogenic bacteria as shown by inhibition experiments by pre-treatment of the mice by the specific XOR inhibitor allopurinol (Segal *et al.*, 2000). Studies carried out on mice infected with *Salmonella typhimurium,* which is responsible for the symptoms of typhoid fever, and administered allopurinol, a specific XOR inhibitor, have established that XOR activity plays an important role in the antimicrobial mechanism against this bacterium in mice (Umezawa *et al.*, 1997).

1.6.3 Molybdenum cofactor deficiencies.

Molybdenum cofactor deficiency leads to a combined deficiency of all three molybdenum cofactor containing enzymes AO, XOR and SO. This rare disease is characterised by neonatal seizures and other neurological symptoms identical to those found in isolated SO deficiency. It is a rare disease with only about 100 cases known worldwide, in all ethnic groups, although the actual figure is likely to be higher due to its similarity to isolated SO deficiency resulting in misdiagnosis (Reiss, 2000; Reiss & Johnson, 2003; Rhoden *et al.*, 2000). No therapy is known for this disease, which leads to death in early childhood. MoCo deficiency can be divided into two groups with identical phenotypes. Type A is the most common (two-thirds of patients) with the mutation occurring in the MOCS1 gene. Type B is less common (one-third of patients) with the mutation occurring in the MOCS2 gene (Reiss, 2000). Approximately 50 unrelated families worldwide have been studied at the molecular level with 16 different mutations identified in the MOCS1 gene and 15 different mutations identified in the MOCS2 gene (Reiss & Johnson, 2003). Figure 8 illustrates where each of these genes fit into the pathway of MoCo synthesis.

1.6.4 Hereditary xanthinuria.

Xanthinuria is an inherited deficiency of XOR, which results in the inability to convert xanthine and hypoxanthine to uric acid (Dent & Philpot, 1954; Holmes & Wyngaarden, 1989). The exact incidence is not known but is thought to be approximately 1 in 6000 although this is likely to be an underestimation as many sufferers go undiagnosed (Simmonds *et al.*, 1995). The main clinical manifestation in xanthinuria is the formation

of urinary xanthine calculi due to the extreme insolubility of xanthine, which in extreme cases can lead to renal failure. Other symptoms can include arthropathy, irritability, hematuria, urinary tract infection, renal colic, myopathy and duodenal ulcers (Simmonds *et al.*, 1995). However classical xanthinuria is often benign and not always diagnosed and most often discovered while the patient is undergoing investigation for an unrelated disorder (Holmes & Wyngaarden, 1989; Simmonds *et al.*, 1995).

Hereditary xanthinuria can be subdivided into two types. Hereditary xanthinuria type I is caused by a defect in the structural gene for XOR so only XOR is absent (Simmonds *et al.*, 1995). Hereditary xanthinuria type II is distinguished from hereditary xanthinuria type I by the oral administration of the AO substrates allopurinol, nicotinamide or pyrazinamide. Hereditary xanthinuria type I patients show a normal ability to oxidise these compounds whereas patients with hereditary xanthinuria type II show a defective ability to oxidise these compounds indicating a dual deficiency of both AO and XOR (Levartovsky *et al.*, 2000) (caused by a defect in the molybdenum cofactor sulphurase (MCS) gene (Ichida *et al.*, 2001)). To date only 6 families have been studied for the mutations that causes hereditary xanthinuria type I. Ichida *et al.* found two mutations one of which R682X was present in two unrelated subjects (Ichida *et al.*, 1997). Levartovsky *et al* used genomic DNA from blood to screen the gene using single-strand conformation polymorphism (SSCP) analysis and PCR sequencing in an Iranian-Jewish patient (Levartovsky *et al.*, 2000), while the disease causing mutations in all Japanese patients were determined by sequencing XOR cDNA prepared from duodenal mucosal biopsy RNA (Ichida *et al.*, 1997; Sakamoto *et al.*, 2001; Yamamoto *et al.*, 2001). Mutations have been found in the XOR gene in 5 unrelated hereditary xanthinuric type I patients (summarised in table 1).

Nucleotide – site	Base change	Amino acid site	Amino acid change	Nationality	Reference
445	C>T	149	Arg-Cys	Japanese	(Sakamoto *et al.*, 2001)
682	C>T	228	Arg-Ter	Japanese *	(Ichida *et al.*, 1997)
1660	Ins C		Frameshift	Iranian-Jewish	(Levartovsky *et al.*, 2000)
2567	Del C		Frameshift	Japanese	(Ichida *et al.*, 1997)

Table 1 – Mutations characterised in hereditary xanthinuria type I.

Table showing the mutations found so far in hereditary xanthinuric type 1 patients. * found in two brothers and another, unrelated xanthinuric patient. The other mutations were only found in one patient.

In addition to the patients indicated in table 1 another Japanese patient's XOR cDNA has been cloned, but no mutation was found in the coding region, however severely reduced XOR mRNA levels were noted (Yamamoto *et al.*, 2001).

Although it had been speculated for many years that hereditary xanthinuria type II was due to a deficiency of a proposed MCS it was not until 2000 that a gene encoding a putative sulphurase was found in mammals (Watanabe *et al.*, 2000). The gene was identified by the study of a herd of cattle in Japan affected by xanthinuria type II (July 2000). Pedigree analysis indicated that the condition was inherited as an autosomal recessive trait (Watanabe *et al.*, 2000). As the gene involved was unknown, genotyping and linkage analysis was used to link the putative xanthinuria type II locus to the centromeric region of bovine chromosome 24. A mouse EST homologueous to a putative *Drosophila* MCS gene (called *ma-l)* was used for primer design which cloned a 110 bp product. FISH analysis was then used to physically map the position of the homologue to the centromeric region of bovine chromosome 24 (Watanabe *et al.*, 2000). This subsequently led to the bovine MCS gene being cloned and sequenced. The bovine MCS gene has an open reading frame of 2547 nucleotides, which encodes a protein of 849 amino acids. This amino acid sequence was 40% identical to the *Drosophila ma-1* protein (Watanabe *et al.*, 2000). When compared to the sequence obtained from the affected offspring in the herd a three base pair deletion from nucleotides 769-771 resulting in the loss of tyrosine 257 was discovered (Watanabe *et al.*, 2000).

Following the studies in cattle the human MCS gene has recently been cloned and the mutation that causes hereditary xanthinuria type II in two independent xanthinuric patients from the Kanto region of Japan identified (Ichida *et al.*, 2001). Both patients possessed a base change from a C to a T at nucleotide 1255 that resulted in an arginine 419 becoming a stop codon that is predicted to lead to the formation of an inactive truncated protein (Ichida *et al.*, 2001).

1.7 Animal models for drug metabolising enzyme and molybdenum hydroxylase deficiencies.

1.7.1 Animal models for drug metabolising enzyme deficiencies.

Pharmacogenetics is the study of the hereditary basis of interindividual differences in drug metabolism (Bertilsson *et al.*, 1995). Single nucleotide polymorphisms (SNPs) in drug metabolising genes have been demonstrated to be responsible for many pharmacogenetic based aberrations in drug metabolism. These include rapid and slow metabolisers that may result in a drug having no beneficial effect or high toxicity respectively.

Obviously the applied aspect of such studies pertains to humans however the use of animal models to study deficiencies in drug metabolising enzymes (DME) is invaluable for ethical and safety reasons. Review of the literature reveals that there are many laboratory strains of rodent that have been discovered that are models for DME deficiencies some of which are described here as examples.

The Gunn rat strain has a nonsense mutation in a shared exon that encodes the C-terminus of several UDP-glucuronosyltransferases (UGT) isoenzymes. This strain has been used to assess the role of these UGT isoenzymes play in the detoxification of the food derived carcinogen 2-amino-1-methyl-6-phenylimidazo[4,5-*b*]pyridine (PhIP) (Dietrich *et al.*, 2001) and the analgesic acetaminophen (paracetamol) (de Morais & Wells, 1988). Gunn rats are also used as an animal model for the study of the human genetic disease Crigler-Najjar syndrome (Li *et al.*, 1998).

A study was carried out on arylamine N-acetyltransferase (NAT) which had been shown to have repercussions on the susceptibility to drug toxicity and cancer in humans (Boukouvala *et al.*, 2002). C57BL/6J mice are representative of the rapid acetylator phenotype and A/J mice are a representative strain of the slow acetylator phenotype. While the *NAT1* protein is identical in both rapid and slow acetylator mice *NAT2* has been shown to be polymorphic with a single nucleotide substitution causing a D99I codon substitution that results in the slow acetylator phenotype in the A/J strain of

mouse (Boukouvala *et al.*, 2002; Levy *et al.*, 1992). This strain of mouse has been invaluable in assessing the role of NAT in toxicology studies.

As well as naturally occurring variants the first gene knockout mice have been created to evaluate cytochrome P450s role in detoxification (Buters *et al.*, 1999; Gonzalez & Kimura, 2001; Otto *et al.*, 2003; Pineau *et al.*, 1998). This group of enzymes are responsible for the oxidation of a wide range of xenobiotics the lack of which could have serious consequences on drug metabolism (Gonzalez & Kimura, 2001). Several mice have been genetically engineered to lack activity in one or more of these enzymes to examine the role of some of the cytochrome P450 enzymes in drug metabolism in more detail and identify similarities between the human and mouse systems with a view to using mouse models in drug toxicity testing and establishing the effects of deficiencies in one or more of these enzymes on drug metabolism in humans (Buters *et al.*, 1999; Gonzalez & Kimura, 2001; Pineau *et al.*, 1998). Recently studies done in mice which lack all the cytochrome P450's died in early to middle gestation indicating that these enzymes are essential for the development of the embryo (Otto *et al.*, 2003).

1.7.2 Animal models for molybdenum hydroxylase deficiencies.

As described in the introduction both AO and XOR are involved in drug and exogenous compound metabolism so laboratory animals that have deficiencies in these enzymes would be invaluable in studies of the relationship between the pharmacological action of a drug and its rate of metabolism catalysed by these enzymes.

Interestingly studies have recently been carried on mice which are deficient in XOR using mice which had undergone targeted gene disruption to create the XOR deficient animals (Vorbach *et al.*, 2002). They found that mice homozygous (-/-) for the mutation in XOR are runted and do not survive beyond 6 weeks postpartum, however XOR heterozygous (+/-) mice are viable and show normal fertility, litter size and maternal behaviour but all pups from XOR +/- females, regardless of genotype, die of starvation at around 12 days postpartum. Fostering experiments showed that pups from +/- female mice may be raised normally by wild type mothers indicating that the +/- female mice have a problem with milk production (Vorbach *et al.*, 2002). The association of XOR in milk lipid production has begun to be characterized (Berglund *et al.*, 1996; Kurosaki *et*

al., 1996; McManaman *et al.*, 1999; Vorbach *et al.*, 2002) and is thought to play a structural role, as a membrane-associated protein, in the secretion of milk fat droplets (Vorbach *et al.*, 2002). However lactation problems in xanthinuric patients have not been reported, one potential explanation for this difference between humans and mice is the difference in milk fat content between the two species as human milk is only approximately 4% fat compared with a milk fat content of between 20-30% in mice. Therefore a mutation in the XOR gene resulting in a defect in milk fat droplet secretion may have a stronger impact on murine lactation than human.

As far as rats are concerned there have been several studies that show natural AO activity variations between rat strains and within a strain. There have been several studies done on the AO activity in rats which have found not only differences in AO activity between different strains of rat but also variations in AO activity within a single strain. Sugihara *et al* studied AO activity between twelve different rat strains using benzaldehyde, 2-hydroxypyrimidine and phthalazine as substrates. They found that between the highest AO activity rat strain tested (Sea:SD) and the lowest AO activity rat strain tested (WKA:Sea) there was a 63.5-fold difference. They also tested XOR activity in these strains and found no significant differences in this activity between the strains (Sugihara *et al.*, 1995). Kitamura *et al* followed up this work testing eight of the twelve strains using methotrexate as substrate and found a 104-fold difference between the above strains (Kitamura *et al.*, 1999a).

Of relevance to the study reported in this thesis are two reports that describe AO deficiency in Sprague Dawley (SD) rats. In 1971 Stanulovic and Chaykin (Stanulovic & Chaykin, 1971a) detailed an investigation into the genetics of AO in mice and rats demonstrating that the SD strain of rat in their institute exhibited a discontinuous variation in AO activity. They established that the activity was inherited in an autosomal recessive fashion and that the presence of activity was dominant over the absence of activity. They grouped the rats into three categories, with approximately equal numbers of animals, high activity animals, intermediate activity animals and deficient animals using the N-heterocycle, N^1-methylnicotinamide as substrate. In a more recent study Rashidi *et al.* had also found an AO variation in the SD strain using three different AO substrates (Rashidi *et al.*, 1997). They found that their colony of SD rats fell into two groups each containing approximately equal numbers of animals.

Group A rats were active towards the AO N-heterocyclic substrates famciclovir, phenanthridine, phthalazine and the XOR substrate xanthine while group B rats were devoid of famciclovir, phenanthridine and phthalazine activity but retained activity towards xanthine. No significant differences were found in aldehyde oxidase activity between male and female animals of either group (Rashidi *et al.*, 1997).

Unpublished studies in my supervisor's (Dr. Dougie Clarke) laboratories at Dundee and Huddersfield Universities have shown that the colonies of SD and Fischer rats studied in this laboratory have low activity towards aldehydes and a complete inability to oxidise various N-heterocycles including phenanthridine and various anti-cancer drugs (Clarke, D.J., Marshall, L., and Meehan, W., unpublished results). In contrast the Wistar rat strain exhibited AO activity typical of mammalian species as it had high AO activity towards N-heterocycles and aldehydes. (Clarke, D.J., Marshall, L., and Meehan, W., unpublished results). The fact that both these AO-deficient rat strains are normal phenotypically suggests that as with other drug metabolising enzyme null-mutants (de Morais & Wells, 1988; Levy *et al.*, 1992; Otto *et al.*, 2003) the lack of the N-heterocyclic AO enzyme activity would only be noticed in unusual circumstances of a high intake of xenobiotics that are substrates for this enzyme.

Interestingly when an American group cloned AO from the SD strain of rat in 1999 they found 10 differences between rat AO cDNAs, 5 of which result in a predicted amino acid change as detailed in table 2 (Wright *et al.*, 1999).

No.	Nucleotide - site	Base Change	Amino acid change	Amino acid site
1	356	C > G	A > G	119
2	359	G > T	R > M	120
3	1,945	A > G	T > A	649
4	3,826	C > T	L > F	1,276
5	3,944	G > C	R > T	1,315

Table 2 – Nucleotide and predicted amino acid differences found in Sprague Dawley rats by Wright and co-workers (Wright *et al.*, 1999).

Wright and co-workers (1999) did not detail the functional significance of the SNPs that they found in rat AO cDNA or their incidence (Wright *et al.*, 1999). Although these SNPs might explain the AO deficiencies found in the SD strain by Stanulovic and Chaykin (Stanulovic & Chaykin, 1971a) or by Rashidi *et al* (Rashidi et al., 1997) no link was made. At present the molecular basis for the differences in AO activity are unknown however possible codon changes in the SD rat strain described by Wrights' group (1999) could be the cause.

1.8 Aims of this study.

The general aim of this study was to study the molecular genetic basis of molybdenum hydroxylase deficiency in laboratory rat strains and in humans.

Specifically the purpose of the study with laboratory rats was to determine the molecular basis for the deficiency of AO activity in SD and Fischer rats by comparing the nucleotide sequence of their genes/cDNAs with that of the Wistar rat strain. In the first instance this would be done by determining if the polymorphisms found by Wright *et al* (1999) (section 1.7, table 2), correlated with the AO deficiencies in our rat strains. If this did not reveal the reason for the genetic deficiency then the entire rat AO cDNAs would be cloned from Wistar, Fischer and SD rats and the sequences obtained compared to determine the probable genetic basis of the deficiency.

With regard to the study of the human molybdenum hydroxylase deficiency the aim was to determine the molecular genetic basis of hereditary xanthinuria in a British patient. This would be the first time a xanthinuric patient of European descent has been studied (see section 1.6.3. for background information).

2. MATERIALS AND METHODS

2. Materials and Methods.

2.1 Animals and chemicals.

Chemicals were obtained from Merck Ltd, Poole UK; Sigma Chemical Company, Poole, UK; Roche Molecular Biochemicals, Penzburg, Germany; Invitrogen Ltd, Paisley, UK; Promega corporation, Southampton, UK; ID labs, Ontario, Canada or Qiagen, Crawley, UK.

All strains of rat were obtained from the Biomedical Services Unit, Ninewells Hospital, Dundee. They were housed in groups and maintained on standard rat chow *ad libtum* under standard conditions and weighed between 200 and 250 g.

2.2 Preparation of cytosol.

Wistar, Fischer 344 and Sprague Dawley rats were aged matched, stunned and sacrificed by cervical dislocation between 9am and 12noon. The livers of the rats were quickly excised, placed in ice cold 0.25 M sucrose, blotted dry then frozen in liquid nitrogen and stored at -80°C until use. For the preparation of cytosol all steps were carried out at 0-4°C. Approximately 2.5g of each liver were weighed out and finely chopped using scissors and homogenised in 4 volumes of buffer (0.25 M sucrose, 10 mM Tris HCl pH 7.4) using a Teflon™/glass homogeniser to produce a 20% w/v homogenate. The homogenates were then centrifuged at 10,000 x g for 15 minutes at 4°C. The supernatant was collected and centrifuged for a further 60 minutes at 105,000 x g at 4°C to obtain the cytosolic fraction which was aliquoted into 1.6ml tubes and stored at -80°C.

2.3 Gel filtration of cytosol.

In order to remove endogenous substrates and inhibitors prior to the xanthine oxidoreductase assay, cytosols were gel filtered. This was required because endogenous substrates and inhibitors present in unfiltered cytosol interfere with the assay. This was carried out according to the manufacturers instructions as follows: PD10 G25 Sephadex columns (Amersham Biosciences, Bucks, UK.) were equilibrated with 50 mM Tris HCl

pH 7.4. 2.5 ml of cytosol was applied to the column and eluted with 50 mM Tris HCl pH 7.4 and the red coloured protein-containing fraction collected. This fraction was aliquoted into 1.6 ml tubes and stored at -80°C.

2.4 Protein determination.

The amount of protein in each sample was calculated using a modification of the method described by Lowry *et al.* using bovine serum albumin (BSA) as standard (Lowry *et al.*, 1951). A standard curve (appendix 1) was prepared using known amounts of BSA following the protocol as described below.

2.4.1 Lowry stock solutions.

Copper/tartrate/carbonate solution.

To make the copper/tartrate/carbonate solution 10 g of Na_2CO_3 was dissolved in 500 ml distilled water. 0.5 g of $CuSO_45H_2O$ and 1g Na tartrate was then dissolved in 500 ml distilled water. The sodium carbonate solution was then slowly added to the copper tartrate solution.

5% (w/v) Sodium dodecyle sulphate (SDS)
0.8 M (w/v) Sodium hydroxide (NaOH)
10 % (w/v) Trichloracetic acid (TCA)

These stock solutions were stored at 4°C until use. Reagent A was prepared fresh as required by mixing one volume of the copper/tartrate/carbonate solution with two volumes 5% (w/v) SDS and one volume 0.8 M NaOH. Reagent B was also freshly prepared by mixing one volume of 2N Folin-Ciocalteau's phenol reagent with 5 volumes of distilled water.

2.4.2 Lowry methodology.

All assays were carried out in duplicate and at two different dilutions to ensure that they contained a protein content within the effective range of the assay (10 to 40 µg protein).

500 µl of 10% (w/v) trichloroacetic acid was added to 500 µl of each diluted sample. Following mixing this was then centrifuged for 5 minutes at 12,000 x g in a bench top microcentrifuge and the supernatant discarded. 500 µl of reagent A was then added to each sample, vortex mixed and incubated at room temperature for 10 minutes. 250 µl of reagent B was added and the sample mixed. The sample was then incubated at room temperature for 30 minutes, and diluted with 500 µl distilled water. The absorbance at 750 nm was measured on a spectrophotometer.

2.5 Spectrophotometric determination of molybdenum hydroxylase activity.

Molybdenum hydroxylase assays were conducted using a robotic centrifugal spectrophotometer analyser (Cobas Fara II, Roche Molecular Biochemicals, Penzburg, Germany) at 37°C. All assays were carried out in duplicate in 1 ml reaction volumes. All samples were frozen and thawed only once.

2.5.1 Spectrophotometric determination of dimethylaminocinnamaldehyde oxidase activity.

The oxidation of dimethylaminocinnamaldehyde (DMAC) was assayed by monitoring the decrease in absorbance at 398 nm (Kurth & Kubicel, 1984). The reaction was carried out with 100 µl of cytosol in a final concentration of 0.125 mM DMAC and 50 mM Tris HCl pH 7.4 in the Wistar rat strain. As the SD and Fischer rat strains had a much lower activity the cytosol volume was increased to 300 µl in these assays. The DMAC concentration and Tris HCl pH 7.4 concentration was kept the same throughout. The specific activity was calculated using the molar extinction coefficient for DMAC which is 9600 $M^{-1}cm^{-1}$.

2.5.2 Spectrophotometric determination of phenanthridine oxidase activity.

The oxidation of phenanthridine was assayed by monitoring the increase in absorbance at 322 nm (Johnson *et al.*, 1984). The reaction was carried out with 100 µl of cytosol in a final concentration 0.05 mM phenanthridine and 50 mM Tris HCl pH 7.4 with the Wistar rat samples. As a lower level of DMAC oxidase activity was found in the SD and Fischer rat strains the cytosol was increased to 300 µl in both strains. The phenanthridine and Tris HCl pH 7.4 concentrations were kept the same throughout. The specific activity was calculated using the molar extinction coefficient for phenanthridine, which is 6,400 $M^{-1}cm^{-1}$.

2.5.3 Spectrophotometric determination of xanthine oxidoreductase activity.

The oxidation of xanthine was assayed by monitoring the increase in absorbance at 295 nm (Waud & Rajagopalan, 1976). The reaction was carried out with 400 µl of gel-filtered cytosol in a final concentration of 0.15 mM xanthine and 100 mM Tris HCl pH 8. This standard assay was used for all the rat strains studied. The specific activity was calculated using the molar extinction coefficient for xanthine, which is 30,500 $M^{-1}cm^{-1}$.

2.6 Cellulose acetate electrophoresis.

Cellulose acetate electrophoresis was carried out using a Zip Zone® chamber from Helena Laboratories (Sunderland, UK.) according to the manufacturers instructions with modifications. The cytosols were loaded onto a cellulose acetate (Titan III) plate that had been pre-soaked for 30 minutes in 25 mM Tris, 192 mM glycine pH 8.5 buffer and electrophoresed in a negative to positive direction in 25 mM Tris, 192 mM glycine pH 8.5 buffer for 30 minutes. The plates were developed for enzyme activity by overlaying a 1.5% (w/v) agarose solution containing 0.9 mM (3-,(4,5-dimethylthiazol–2-y)-2,5-diphenyl tetrazolium bromide, 0.3 mM phenazine methosulphate and 5 mM benzaldehyde or 0.5 mM phenanthridine and incubating for 30 minutes at 37°C.

2.7 Bioinformatics.

Alignment of sequences and primer design was performed using Genejockey™ (Biosoft, Cambridge). In some cases primers had to be manually designed and checked for primer dimer and hairpin loop formation using Amplify©, a freeware program obtained from Bill Engles, Department of Genetics, University of Wisconsin, USA. Both programs were run on an Apple Macintosh computer with operating system 8.6 installed. Published sequences were obtained from the National Center for Bioinformatics website (NCBI) situated at http://www.ncbi.nlm.nih.gov/. The accession numbers for each sequence are listed in appendix 2.

After the primers were designed a BLAST alignment was carried out online at http://www.ncbi.nlm.nih.gov/, this program aligns the inputted sequences with all of the sequences found on the NCBI database. Primers were discarded if they were found to bind to the target gene in more than one place, or if they bound to other genes found within the organism of interest.

The sequences were translated using the genetic code as shown in appendix 3. The one letter and three letter amino acid codes are also listed in appendix 4.

2.8 Isolation of DNA and RNA from rat liver.

DNA and RNA were isolated from rat liver using Sigma® Tri Reagent™, which simultaneously isolates DNA, RNA and proteins. The livers of the rats were quickly excised, washed in ice cold 0.25 M sucrose, blotted dry then frozen in liquid nitrogen and stored at -80°C until use. The following method was carried out as detailed in the manufacturers instructions.

All plasticware except for the pellet pestles were purchased as guaranteed RNase free (Sigma, Poole, UK.). Water was rendered RNase free by treating with 0.2% (v/v) diethylpyrocarbonate (DEPC) for 16 hours prior to autoclaving. The pellet pestles (Sigma, Poole, UK.) were treated with RNase away (Merck Ltd, Poole, UK.) and rinsed with DEPC treated water before use.

50-100 mg of frozen tissue was homogenized with 1 ml of Tri Reagent™ in a 1.6 ml tube using a polypropylene disposable pellet pestle homogeniser (Sigma, Poole, UK.). The homogenate was then centrifuged at 12,000 x g for 10 minutes at 4°C to remove the insoluble material. The supernatant was transferred into a clean 1.6 ml tube for RNA isolation and the pellet was stored at 4°C for DNA isolation.

2.8.1 Isolation of rat liver RNA.

The supernatant was incubated for 5 minutes at room temperature. 0.2 ml of chloroform was then added and the sample vigorously shaken for 15 seconds. After another 15 minute incubation at room temperature the sample was centrifuged at 12,000 x g for 15 minutes at 4°C. The colourless upper aqueous phase was carefully transferred into a fresh 1.6 ml tube with care being taken not to remove any of the interphase layer, which would result in DNA contamination. 0.5 ml of isopropanol was then added and the sample was mixed and incubated at room temperature for 5 minutes. The sample was then centrifuged at 7,500 x g for 5 minutes at 4°C to precipitate the RNA. The pellet was then washed by adding 1.2 ml 75% (v/v) ethanol, vortex mixed and centrifuged at 7,500 x g for 5 minutes at 4°C. The pellet was then left to air-dry for 10 minutes after which the RNA was then dissolved in 200 µl RNase free water.

2.8.2 Isolation of rat liver DNA.

1.5 ml of 0.1 M sodium citrate, 10% (v/v) ethanol solution was added to the pellet (section 2.8) containing the high molecular weight DNA. The pellet was then incubated at room temperature for 30 to 90 minutes then centrifuged at 12,000 x g for 5 minutes at 4°C. The washing with 0.1 M sodium citrate, 10% (v/v) ethanol solution was repeated three times then the pellet was resuspended in 75% (v/v) ethanol and centrifuged at 12,000 x g for five minutes at 4°C. The supernatant was discarded and the pellet was then allowed to air dry for 10-20 minutes at room temperature. The DNA pellet was then resuspended in 300 µl TE buffer (10 mM Tris, 1 mM EDTA pH 8.0).

2.9 The xanthinuric patient.

A 52 year old British female was diagnosed with hereditary xanthinuria after persistently low plasma urate levels were noted over a period of several years while undergoing investigation for a variety of clinical problems resulting in the diagnosis of idiopathic thrombocytopenic purpura. She was on appropriate medications, prednisole, nalidoxic acid, atenolol and nifedipine for the latter disease at the time of diagnosis. Her creatinine clearance was normal 95.6 ml/min, which is within the normal range (85-130 ml/min) indicating that she had no renal impairment. The daily excretion of uric acid was undetectable, whilst excretion levels of xanthine and hypoxanthine were 1.46 and 0.37 mmol/24 hrs respectively (normal 0.05 and 0.05 mmol/24 hrs respectively).

2.10 Extraction of DNA from blood.

The xanthinuric patient's DNA was extracted from a blood sample provided with ethical approval from the Purine Research Laboratory, Guy's Hospital, London, UK. using the QIAamp DNA blood midi kit from Qiagen Ltd (Crawley, UK.). This was stored at –80°C until use. All steps were carried out using 15 ml polypropylene tubes and carried out as detailed in the manufacturers instructions

200 µl Qiagen protease stock solution and 2.4 ml buffer AL was added to 2 ml of the blood sample and incubated at 70 °C for 10 minutes. 2 mls of 100% ethanol was added to the sample and this was vortex mixed. Half of the sample was then applied to the QIAamp column. This was centrifuged for 3 minutes at 1850 x g. The filtrate was then discarded and the remainder of the sample applied to the column and centrifuged as before. The filtrate was then discarded and 2 mls of buffer AW1 added to the column which was the centrifuged at 4500 x g for 1 minute. Without discarding the filtrate another 2 mls of buffer AW1 was applied to the column and centrifuged as before. The filtrate was discarded and the column was placed into a clean 15 ml tube. 300 µl of buffer AE was placed onto the QIAamp membrane and incubated at room temperature for 5 minutes. This step was repeated in order to acquire the maximum DNA yield from the blood sample. The sample was then centrifuged at 4500 x g for 5 minutes and the filtrate aliquoted into 1.6 ml tubes and stored in the fridge until required.

2.11 DNA and RNA quantitation.

DNA or RNA yield may be determined by measuring the absorbance of a DNA/RNA sample at 260 nm as detailed in (Maniatis *et al.*, 1982).

5 µl of DNA or RNA sample was added to 1 ml distilled water and the absorbance at 260 nm was measured on a spectrophotometer. If the absorbance did not fall between 0.1 and 1.0 then the amount of DNA/RNA was adjusted accordingly as values outside this range do not give an accurate determination of the concentration. The amount of DNA/RNA was calculated using the following calculations.

DNA	50 µg/ml x A_{260} x dilution factor = amount of DNA in µg/ml
RNA	40 µg/ml x A_{260} x dilution factor = amount of RNA in µg/ml

Also the absorbance at 280 nm was recorded. To give the purity of the DNA/RNA the A_{260} is divided by the A_{280}. Pure DNA gives a ratio of 1.7-2.0, pure RNA gives a ratio of 1.9-2.1.

2.12 Reverse transcription of RNA.

First strand cDNA synthesis was carried out using the Omniscript™ reverse transcriptase kit from Qiagen Ltd (Crawley, UK.) following the instructions provided with the kit. The reaction was carried out in RNase free 1.6 ml tubes. The reverse primer designed for each clone was used to synthesize the cDNA.

RNase inhibitor (purchased from ID labs, Ontario, Canada) was diluted to a final concentration of 10 units/µl in 1x Buffer RT. All other reagents except for the primers were supplied with the kit. 2µl 10x buffer RT, 2 µl dNTP mix, 0.5 µL of 100 pmol/µl primer, 1 µl RNase inhibitor, 1 µl Omniscript reverse transcriptase, 1 µg RNA and RNase free water to a volume of 20 µl was mixed on ice in a 1.6 ml RNase free tube. This was briefly centrifuged in a benchtop microcentrifuge to ensure the reaction is mixed and to bring the reaction to the bottom of the tube. The reaction was then incubated at 37°C for 60 minutes. 2 µl of this reaction was then added in place of DNA into the PCR reaction, which was carried out as described in section 2.13.

2.13 Polymerase chain reaction amplification of DNA.

The polymerase chain reaction (PCR) was carried out with modifications to the manufacturers instructions.

The basic components for the PCR are a final concentration of 1 X PCR buffer (ID Labs, Ontario, Canada.), 0.2 mM of each of the dNTPs, 0.5 pM of each primer (forward and reverse) (MWG Biotech, Ebersberg, Germany), 1.5 mM $MgCl_2$ (ID labs, Ontario, Canada), 1.25 U *Taq* DNA polymerase (ID labs, Ontario, Canada) and 0.5 µg template DNA.

The components that may be varied in the optimisation process are primer, $MgCl_2$ and the annealing temperature.

A typical PCR reaction was carried out using the following conditions.

Cycle 1

1. Denature 94°C for 3 minutes
2. Anneal 45-67°C for 1 minute
3. Extend 72°C for 30 seconds – 2 minutes

Cycles 2-35

1. Denature 94°C for 1 minute
2. Anneal 45-67°C for 1 minute
3. Extend 72°C for 30 seconds – 2 minutes (variable depending on size of product)

On Cycle 35 an extra extension was carried out for 10 minutes.

Although once the primers were optimised as described in the results they would occasionally need to be repeated when changes were made to reagents.

2.14 Agarose gel electrophoresis.

Agarose gel electrophoresis was carried out according to the methods described by Maniatis *et al.*, 1982 with modifications.

Products larger than 300 bp were visualised on a 1% (w/v) agarose gel, while smaller products were visualised using a 2.5% (w/v) agarose gel.

For a 1% (w/v) agarose gel, 1 g of agarose was added to 100 ml 0.5 X TBE (44.5 mM Tris, 44.5 mM boric acid, 1 mM EDTA pH 8). This mixture was then heated in a microwave oven until all the agarose was dissolved. The heated mixture was allowed to cool to 60°C and 10 µg of ethidium bromide added. This was poured into a 11 x 14 cm gel tray, a 2 mm wide well former inserted and the gel allowed to set for approximately 30 minutes. The gel was then placed into a horizontal gel electrophoresis apparatus with the wells at the anode side. 0.5 X TBE was then poured into the tank until the gel was submerged to a depth of 2-3 mm.

For the analysis of PCR products 10 µl of PCR product was mixed with 1 µl loading dye. In order to approximate the size of the PCR products 5 µl of 1 kb DNA ladder purchased from Promega (Southampton, UK.) was mixed with 0.5 µl loading dye. This 1 kb ladder produced 13 fragments of 250 bp, 253 bp, 500 bp, 750 bp, 1,000 bp, 2,000 bp, 2,500bp, 3,000 bp, 4,000 bp, 5,000 bp, 6,000 bp, 8,000 bp and 10,000 bp.

The PCR products or size markers were loaded into individual wells of the gel and electrophoresed for 1 hr at 100 V. The gels were then visualised on an UV transilluminator and photographs taken when required.

2.15 Preparation of PCR samples for sequencing.

The PCR samples were prepared for sequencing using the QIAquick™ purification kit. All centrifugation steps were carried out in a benchtop microcentrifuge at 12,000 x g. The method followed manufacturers instructions as follows 500 µl of buffer PB were added to 100 µl PCR product and mixed. This was then applied to the QIAquick™ column and centrifuged for 60 seconds. The flow through was discarded and 750 µl of buffer PE added to the column. This was centrifuged for 60 seconds and the flow through discarded then centrifuged again for another 60 seconds. Finally the

QIAquick™ column was placed into a clean tube and 50 µl buffer EB applied to the centre of the membrane and centrifuged for 60 seconds to elute the DNA.

2.16 Sequencing of the PCR samples.

The purified PCR samples were sent either to the University Of Dundee for sequencing analysis on an ABI automated sequencer or at the University of Huddersfield on a Beckman CEQ8000 automated sequencer using dideoxy dye terminator methodologies.

RT-PCR products encoding rat AO or AOH1 cDNAs were sequenced in both forward and reverse directions using the primers designed for the PCR reaction and the sequencing repeated until the PCR product contig contained no ambiguities in the sequence obtained.

PCR products encoding the human XOR gene were sequenced in the forward direction only unless a difference was noted between the patient's and a normal individual's nucleotide sequence. If a difference was observed the PCR product was sequenced in the reverse direction. The sequencing was repeated until the whole of the exon and the intron/exon splice sites contained no ambiguities.

3. RESULTS

3. Results.

This results section is split into 5 main sections as follows. Firstly in section 3.1 the phenotyping of aldehyde oxidase activity in the various strains of rat with particular emphasis on the SD strain is described. The differences found between clones in the SD strain by Wright *et al.* (Wright *et al.*, 1999) are then compared with our SD, Fischer and Wistar strains (section 3.2). The cloning and DNA sequencing of rat liver AO and AOH1 from the AO-active and AO-deficient strains are subsequently described in sections 3.3 and 3.4. Finally in section 3.5 an investigation into the genetic cause of hereditary xanthinuria in a British patient is described.

3.1 Molybdenum hydroxylase activities in rat strains.

As mentioned in the introduction (section 1.7.2) Stanulovic and Chaykin had described a discontinuous variation in N-heterocyclic AO activity towards the substrate N^1-methylnicotinamide in the SD strain of rat (Stanulovic & Chaykin, 1971a). More recently Rashidi *et al* also found that in their colony of SD rats two groups existed that were AO-active and AO-null towards three N-heterocycles (phenanthridine, phthalazine and famciclovir) (Rashidi *et al.*, 1997), therefore our colony of SD rats were screened to determine if a discontinuous variation in AO-activity was present. A detailed study previously completed in our laboratory had established that the Fischer strain exhibited a low level of activity towards aldehydes and a complete absence of activity towards N-heterocycles in comparison to Wistar rats, which had typical mammalian activity towards both N-heterocyclic and aldehyde AO substrates (Clarke, D.J., Marshall, L., and Meehan, W., unpublished results). As the Wistar and Fischer strains had previously been extensively studied enzymologically only a few rats of these strains were assayed in this study as a comparison with the SD strain.

In order to determine if there was any AO activity towards N-heterocycles present in the three different rat strains, assays were carried out with the AO substrate phenanthridine. The results are shown in table 3.

Rat strain	Phenanthridine oxidase activity (nmol/min/mg protein)
Male Wistar rats (N=4)	12.12 ± 1.43
Male Fischer rats (N=4)	N.D.*
Male Sprague Dawley rats (N=24)	N.D.*
Female Sprague Dawley rats (N=35)	N.D.*

Table 3 - Phenanthridine oxidase activity in liver cytosol of different strains of rat.

Activities were determined as described in materials and methods (section .3.5.1) The activities are shown as nmol phenanthridine hydroxylated / min / mg protein and are expressed as means ± s.d. of N animals
*N.D. – not detectable. As a large number of male and female rats had already been studied in the Fischer and Wistar rat strains and as no gender differences were observed only male Wistar and Fischer animals are shown here.

No phenanthridine oxidase activity was detected in the Fischer or SD rats in contrast to the Wistar rats. In order to determine if aldehyde oxidase activity was present in the three rat strains, liver cytosols were phenotyped using DMAC oxidase assays (table 4).

Rat Strain	Dimethylaminocinnamaldehyde oxidase activity (nmol/min/mg protein)
Male Wistar rats (N=4)	10.86 ± 1.06
Male Fischer rats (N=4)	1.65 ± 0.53
Male Sprague Dawley rats (N=24)	3.03 ± 1.44
Female Sprague Dawley rats (N=35)	3.11 ± 1.67

Table 4 - Dimethylaminocinnamaldehyde oxidase activity in liver cytosol of different strains of rat.

Activities were determined as described in materials and methods (section 2.5.2). The activities are shown as nmol dimethylaminocinnamaldehyde hydroxylated/min/mg protein and are expressed as means ± s.d. of N animals.
As a large number of male and female rats had already been studied in the Fischer and Wistar strains and no gender differences were observed only male Wistar and Fischer animals were analysed in this study.

Reduced DMAC oxidase activity was observed in the SD and Fischer rats and no gender differences were found in the SD rat strain.

These assays demonstrated that the strains of SD and Fischer rats used in this study had low AO activity animals towards an aldehyde substrate compared to the Wistar rat strain and a complete absence of phenanthridine oxidase activity. No discontinuous variation in phenanthridine oxidase activity was present in the SD rat as previously reported (Rashidi *et al.*, 1997; Stanulovic & Chaykin, 1971a).

Rat liver cytosols were also tested for XOR activity to determine whether the deficiencies were due to a deficiency in the molybdenum cofactor (table 5), which can result in a dual AO and XOR deficiencies as described in the introduction sections 1.6.2 and 1.6.3.

Rat Strain	**Xanthine oxidoreductase activity (nmol/min/mg protein)**
Male Wistar rats (N=4)	6.48 ± 0.53
Male Fischer rats (N=4)	6.24 ± 0.42
Male Sprague Dawley rats (N=4)	6.13 ± 0.37
Female Sprague Dawley rats (N=4)	6.36 ± 0.48

Table 5 - Xanthine oxidoreductase activity in liver cytosol of different strains of rat.

Activities were determined as described in materials and methods (section 2.5.3). The activities are shown as nmol uric acid formed per min per mg protein and are expressed as means ± s.d. of N animals. As a large number of male and female rats had already been studied in the Fischer and Wistar strains and no gender differences were observed only male Wistar and Fischer animals are shown here.

The presence of XOR activity at similar levels in all the rat strains, indicates that the AO deficiencies are due to a defect in the AO gene and not a deficiency in the synthesis of the molybdenum cofactor. For the same reasons it also excludes the lack of the other two molybdenum hydroxylase cofactors (Fe_2S_2 and FAD) as the cause of the deficiency.

As the studies described in this thesis were ongoing this laboratory also developed HPLC assays for N-heterocycle xenobiotics and drugs that are AO substrates. These more sensitive assays definitely confirmed that the SD and Fischer rat strains were deficient in the oxidation of N-heterocycle substrates such as phenanthridine, DACA and methotrexate (Clarke, D. J. and Meehan W., 2003, unpublished results)

3.2 Are known single nucleotide polymorphisms the cause of the aldehyde oxidase deficiencies in rat strains?

As Wright *et al.* (1999) had already identified several deduced amino acid changes in the AO cDNA occurring in the SD strain of rat (Wright *et al.*, 1999), but did not mention or measure the activity of the well-documented AO deficiency in these rats it was decided to clone these regions to determine if they correlated with the AO deficiencies in the SD and Fischer rat strains.

3.2.1 Design of PCR primers for amplification of the polymorphic areas of the aldehyde oxidase gene in rats.

As PCR from genomic DNA is simpler, quicker and not as expensive as RT-PCR from RNA, it was decided to use this method for the amplification of the specific positions in the rat AO gene. The initial step in cloning of these regions of the rat AO gene was to deduce all the intron/exon boundaries in the rat AO cDNA sequence as the rat AO gene had not been published and was not available on any publicly accessible database (December 1999). When this work was initiated the only published intron/exon information was for the human AO gene (Terao *et al.*, 1998) (see figure 8 in introduction). In addition, although the details were unpublished the individual exons of the mouse AO sequence were available on the NCBI database. By using a pairwise alignment program (BLAST) the individual mouse AO exons were aligned with the mouse AO cDNA and the splice donor/splice acceptor sites identified in the mouse AO cDNA sequence. The mouse cDNA was then aligned with the human cDNA and the exon boundaries compared to identify the degree of conservation. This revealed that all of the exon boundaries between the species were 100% conserved therefore it was reasonable to postulate that the intron/exon boundaries would be conserved in another closely related mammalian cDNA. Following mapping of the likely exons in the rat AO cDNA each exon in the rat was then separated from the complete cDNA and primers designed using computer programs as described the materials and methods (section 2.7).

The first two amino acid differences observed by Wright *et al* (1999) (A119G & R120M) were encoded by exon 5, however the nucleotide sequence of this exon prevented suitable primer pairs being designed. It was therefore decided to ligate exons

4 and 5 *in silico* to provide a larger template for primers to be designed from. A similar strategy was employed for the R1315T polymorphism encoded by exon 34 as the change was situated 8 bp from the end of the exon. On this occasion, predicted exons 34 and 35 were spliced together to enable primers to be designed. The L1276F polymorphic codon is encoded by exon 34 and in contrast to the other regions primers were easily designed. Unfortunately it proved impossible to design primers to examine the T649A polymorphic site in exon 18 using these methodologies for primer design, due to its small size and the fact that adjacent introns are predicted to be >3 kb in genomic DNA. Table 6 lists the primers designed for amplification of the polymorphic areas of the rat AO gene.

Primer Code	Primer Sequence*	Polymorphism Detected	Expected Product Size	Notes
RAO4/5F	ATAGGCAACACCAGGACC	A119G R120M	~2 kb*	Includes intron 4
RAO4/5R	GTGGTTCCTGAGCAGAGCATAC			
RAO34F	GGAGAGTCTGGGGTGTTCCTGGG	L1276F	153 bp	
RAO34R	GAACTTATCTTCACAAGCCATTC			
RAO34/35F	CTCCAGAGAAAATCAGAATGGC	R1315T	~950 bp*	Includes intron 34
RAO34/35R	GTGCGTTCTGTAGTTGTTGAGC			

Table 6 – Summary of the primers designed for the PCR amplification of polymorphic areas of the rat aldehyde oxidase gene described by Wright et al (1999).

The table shows the primers used, the sequence of the primers *reading 5'-3', the polymorphism each primer pair is designed to detect and the expected size of the product. The notes column indicates the introns (if applicable) that the primer pair spans. * Estimate based on human intron 4 being ~1.9 kb. * Estimate based on human intron 34 being ~0.8 kb. F and R signify sense and antisense primers respectively

3.2.2 Optimisation of the PCR conditions for amplification of the polymorphic areas of the aldehyde oxidase gene in rats.

PCR optimisation was achieved by using the basic components as listed in materials and methods (section 2.11), varying one component at a time. The basic variable components were the temperature the PCR was carried out at, the concentration of the primers and the concentration of the $MgCl_2$. Also a PCR additive, Q solution™ (Qiagen Ltd) was occasionally used, this modifies the melting behaviour of DNA to facilitate the amplification of difficult templates.

As the hundreds of agarose gel images are too numerous to include in this thesis only a few examples of gels displaying examples of the PCR optimisation process are shown.

The agarose gel image shown in figure 9a demonstrates the effect that temperature and magnesium concentration can have on the performance of the PCR reaction. Lanes 1-6 contained 1.5 mM $MgCl_2$ and lanes 7-12 contained 3 mM $MgCl_2$. As illustrated in figure 9a this primer pair works more efficiently with the lower concentration of $MgCl_2$. It also illustrates the effect of temperature with the temperature increasing from left to right along the gel. It demonstrates that this primer pair works more effectively at the higher temperatures with one fragment present at 62°C but several fragments are present at 52°C (figure 9a, lanes 7-12). Figure 9b illustrates the effect that primer concentration can have on the performance of the PCR reaction. Lanes 1-5 contain 0.25 pM primer and lanes 6-10 contain 1 pM primer. This gel shows that too high a primer concentration can lower the amount of product formed and alter the range of temperatures that a primer pair works over.

Table 7 shows a summary of the conditions used and the results obtained using SD rat genomic DNA. The optimal conditions for each primer pair are highlighted in yellow.

a

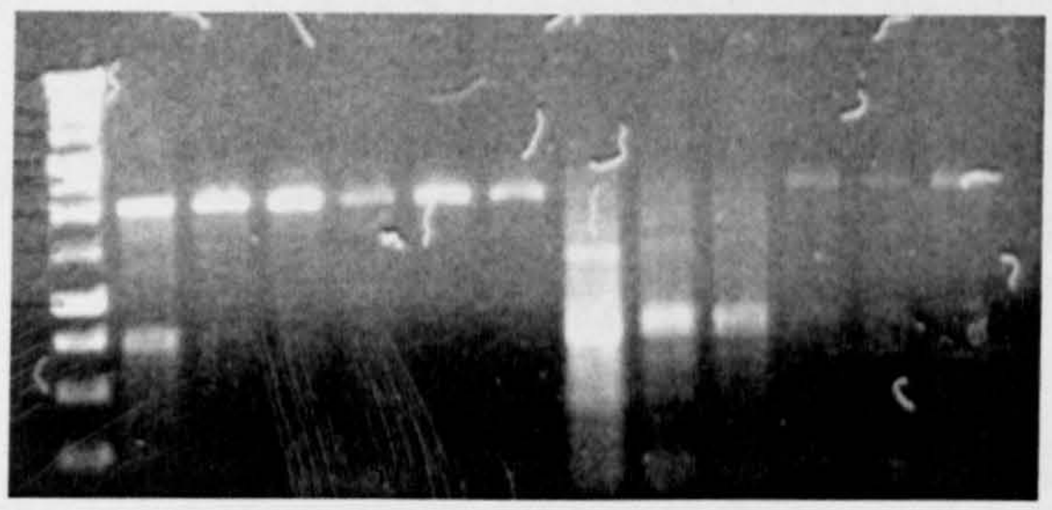

b

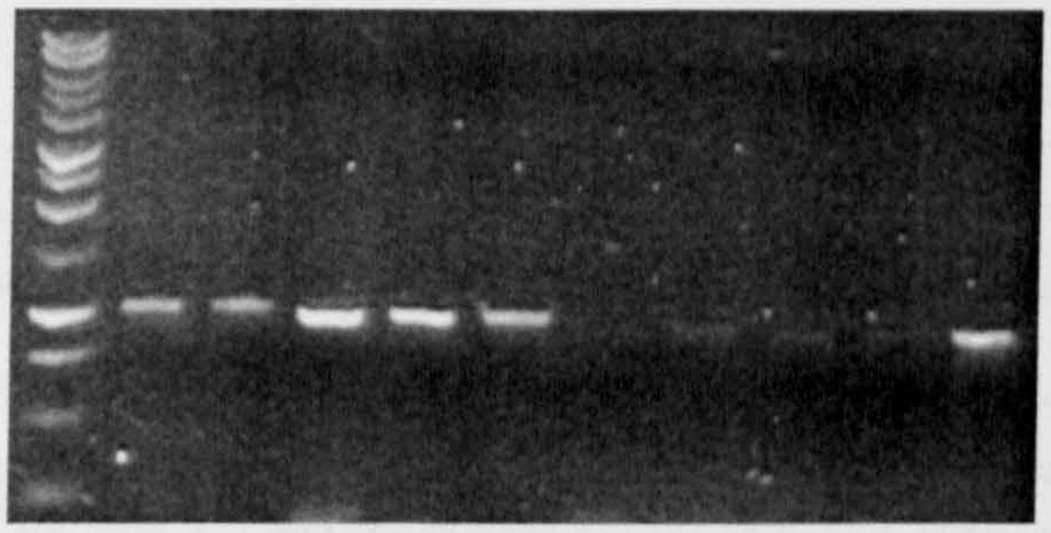

Figure 9 – Agarose gel images showing the optimised conditions for the PCR of rat aldehyde oxidase gene regions.

a- Agarose gel image showing the products formed using primer set RAO4/5. Lanes 1-6 were carried out using 0.5 pM primer and 1.5 mM $MgCl_2$. The annealing temperatures of lanes 1-6 are at 52°C, 54°C, 56°C, 58°C, 60°C and 62°C respectively. Lanes 7-12 were carried out using 0.5 pM primer and 3 mM $MgCl_2$. The annealing temperatures of lanes 7-12 are at 52°C, 54°C, 56°C, 58°C, 60°C and 62°C respectively. Lane M is 1 kb DNA marker purchased from Promega.

b- Agarose gel image showing the products formed using primer set RAO34/35. Lanes 1-5 were carried out using 0.25 pM primer and 3 mM $MgCl_2$. The annealing temperatures of lanes 1-5 are at 52°C, 53°C, 54°C, 55°C and 56°C respectively. Lanes 6-10 were carried out at 0.5 pM primer and 3 mM $MgCl_2$. The annealing temperatures of lanes 6-10 are at 51°C, 52°C, 53°C, 54°C and 55°C respectively. Lane M is 1 kb DNA marker purchased from Promega.

Primers used	Q solution*	Annealing temperatures °C	Primer conc.**	$MgCl_2$ conc.**	Fragments Generated
RAO4/5F /RAO4/5R		48,50,52,54,56,58	0.5 pM	1.5 mM	Several fragments
		48,50,52,54,56,58,60,62	0.5 pM	3 mM	Several fragments
		60,62	0.5 pM	1.5 mM	~2 kb fragment
RAO34/35F/RAO34/35R		47,49,51,53,55,57,60,62	0.5 pM	1.5 mM	No fragments
		48,50,52,54,56,58,60,62	0.5 pM	3 mM	Several fragments
		47,49,51,53,55,57	0.5 pM	2 mM	Several fragments
		47,49,51,53,55,57,60,62	0.5 pM	2.5 mM	Several fragments
		57,58,59,60,61,62	0.5 pM	3.5 mM	Several fragments
	$^1/_{10}$	52,53,54,55,56	0.5 pM	1.5 mM	Several fragments
	$^1/_{20}$	47,49,51,53,55,57	0.5 pM	1.5 mM	Several fragments
	$^1/_{20}$	47,49,51,53,55,57	0.5 pM	3 mM	~1 kb fragment faint
	$^1/_{20}$	51,52,53,54,55	0.25 pM	3 mM	~1 kb fragment
RAO34F/ RAO34R		47,49,51,53,55,57	0.5 pM	1.5 mM	~150 bp fragment

Table 7 – Summary of the experimental conditions and outcomes of the PCR of the rat aldehyde oxidase gene spanning the single nucleotide polymorphisms as listed in table 6.

This table shows the optimisation process for primer sets RAO4/5, RAO34/35 and RAO34. It illustrates the temperatures used with each set of conditions and the outcomes from each set of conditions used. *Q solution is a PCR additive $^1/_{10}$ and $^1/_{20}$ indicates $^1/_{10}$th or $^1/_{20}$th volume of PCR reaction is Q solution respectively. ** concentration

To confirm that the correct products had been amplified the three PCR products obtained were sequenced as described in materials and methods (section 2.11). The DNA sequencing confirmed that all the PCR products were to the required regions of the rat AO.

Unfortunately the ~2 kb product produced with primers designed to exon 4 and 5 did not sequence over the SNPs, as the changes were too close (10 bp) to the start of the reverse primer. The ~950 bp product obtained with the primers designed to exon 34 and 35 also did not sequence over the SNP, as it was only 18 bp from the end of the forward primer (figure 10). As the sequencing chromatogram only provided approximately 700 bp of usable sequence from the fragments 5`and 3` termini, the opposite ends of the intron from each primer were not obtained. Unfortunately the first 60 bp of each termini of the fragment was ambiguous so the SNP could not be determined from the primer

closest to the change. Figure 10 shows a sequencing chromatogram of the product obtained showing some of the novel intronic sequence obtained for intron 34.

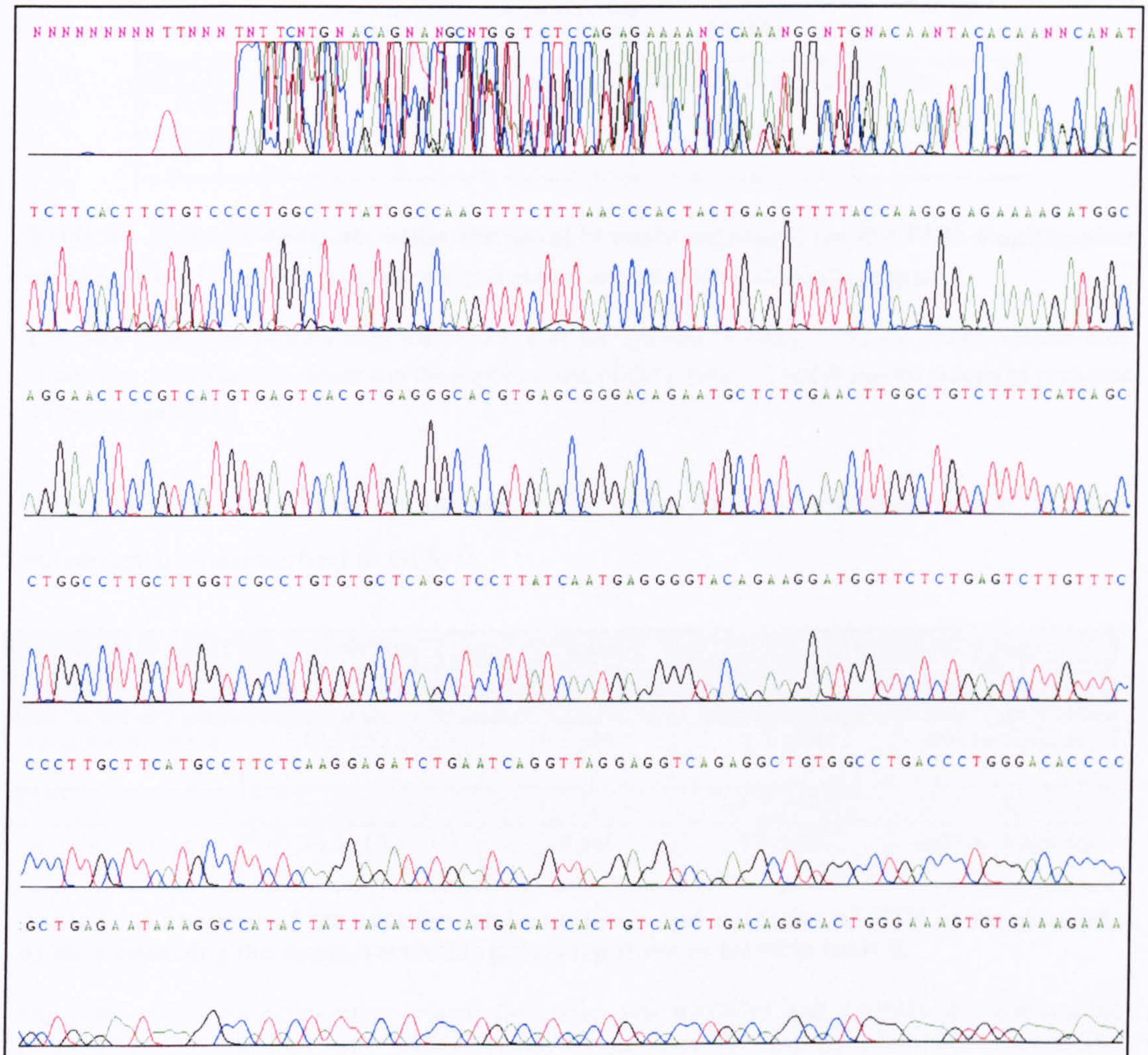

Figure 10 – Chromatogram of the novel sequence obtained for intron 34.

Chromatogram illustrating a portion of the novel intronic sequence, which was obtained when the PCR product of primers RAO34/35F and RAO34/35R was sequenced using RAO34/35F as the sequencing primer.

In order to obtain new sequence data for these areas new primers were designed using the novel intronic sequence obtained to produce a smaller product enabling clear sequence to be obtained over the polymorphic region of codons 119, 120 and 1315 (table 8). The novel intron 4 sequence used to design primers, which amplify over the polymorphic region of codons 119 and 120 is shown in appendix 5.

Primer code	Primer sequence*	Polymorphism detected	Expected product size
RAOEX5F	CTGCTTGGAACTTGCTCTGTCC	A119G R120M	543 bp
RAOEX5R	GGTTCCTGAGCAGAGCATTACAT		
RAO34aF	GCAGGAGAGAGGCATCT	R1315T	474 bp
RAO34aR	CCACAGCCTCTGACCTCCTAACC		

Table 8 – Primers designed, using the novel intronic sequence, for the PCR amplification of Wright et al's (1999) polymorphic areas of the rat aldehyde oxidase gene.

The table shows the primers used the sequence of the primers *reading 5'-3', the polymorphism each primer pair is designed to detect and the expected size of the product. F and R signify sense and antisense primers respectively

These primers were then optimised in the same way as described above and the outcomes are summarised in table 9.

Primers used	Annealing temperatures °C	Primer conc.**	$MgCl_2$ Conc.**	Fragments Generated
RAOEX5F/ RAOEX5R	47,49,51,53,55,57	0.5 pM	1.5 mM	~500 bp fragment
RAO34aF/ RAO34aR	47,49,51,53,55,57	0.5 pM	1.5 mM	~500 bp fragment

Table 9 – Summary of the experimental conditions and outcomes of PCR of rat aldehyde oxidase spanning the single nucleotide polymorphisms as listed in table 8.

This table shows the optimisation process for primer sets RAOEX5 and RAO34a. It illustrates the temperatures used with each set of conditions and the outcomes from each set of conditions used. The optimal conditions for each primer pair are highlighted. ** Concentration.

Following the successful amplification of all of the PCR products, these exonic regions were amplified in eight animals (four of each gender) from the Wistar, SD and Fischer 344 strains. The products were then sequenced and the codon changes observed by Wright *et al* scrutinised. No differences were found between the AO sequences from different strains or genders of rat. For each of Wright *et al*'s polymorphic areas representative chromatograms and a summary of the results are shown in figure 11 and table 10 respectively.

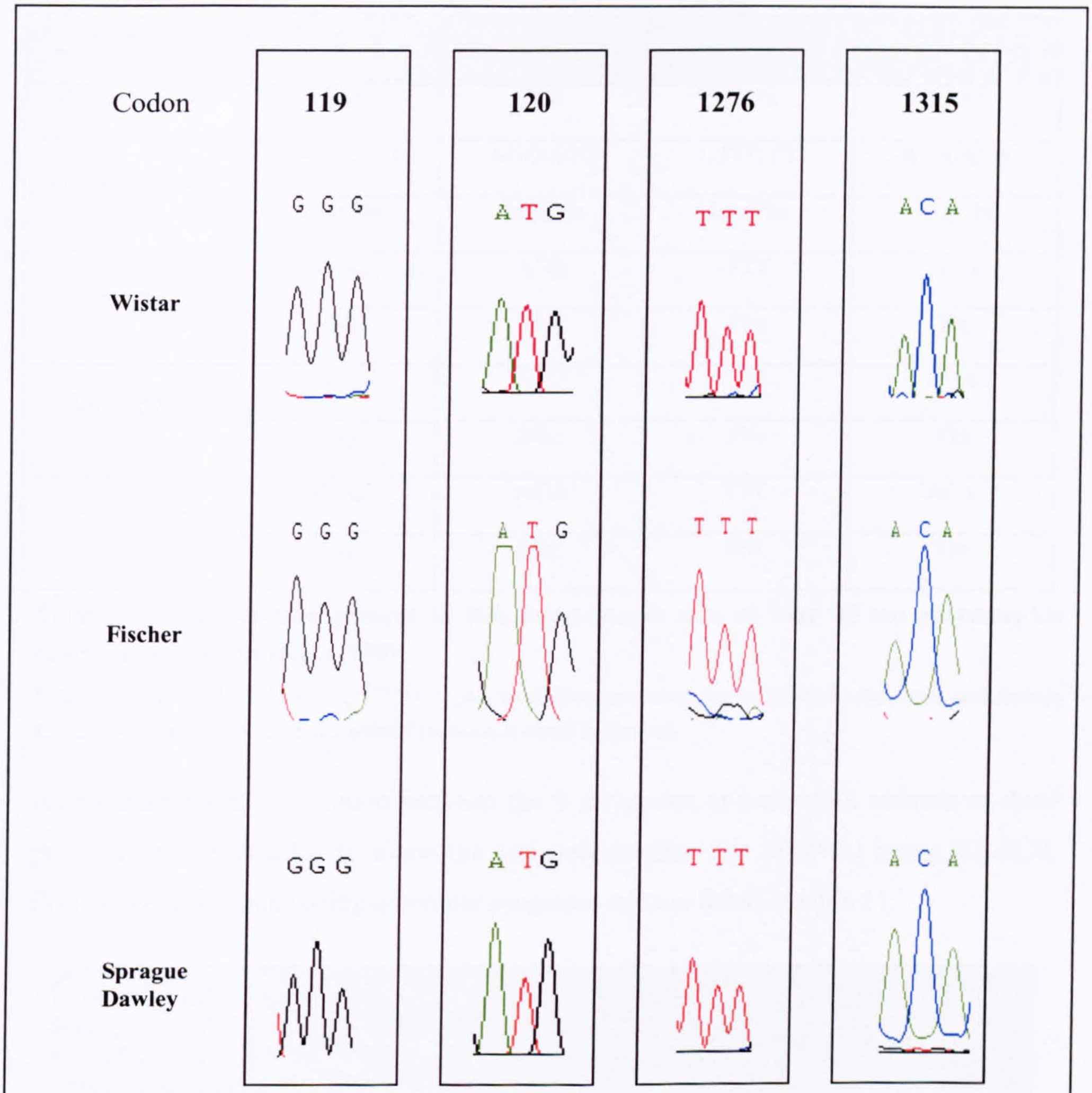

Figure 11 – Sequencing chromatograms illustrating the codon present in this laboratory's rat strains over four of the polymorphic sites found by Wright *et al.* (1999).

Chromatograms showing the codons representing the changes found by Wright et *al.* in the different strains of rat. As no interindividual or gender differences were observed only one representative chromatogram from each strain has been shown.

Table 10 compares the possible codons as described by Wright *et al.* with the codons found at four of the polymorphic sites in the Wistar, SD and Fischer strains of rat.

Exon	5	5	34	34
Codon Position	119	120	1,276	1,315
Possible codons*	GCG/GGG	AGG/ATG	CTT/TTT	AGA/ACA
	Ala/Gly	Arg/Met	Leu/Phe	Arg/Thr
SD rats	GGG	ATG	TTT	ACA
	Gly	Met	Phe	Thr
Wistar rats	GGG	ATG	TTT	ACA
	Gly	Met	Phe	Thr
Fischer rats	GGG	ATG	TTT	ACA
	Gly	Met	Phe	Thr

Table 10 – The codons present in this laboratory's rats at four of the polymorphic observed by Wright *et al.* (1999)

* As reported in (Wright *et al.*, 1999). As no differences were found between the male and female animals only one representative animal from each strain is shown.

As no differences were found between the 3 rat strains or individual animals at these positions it was decided to clone the last polymorphic site (T649A) using RT-PCR. Primers were designed using computer programs and are listed in table 11.

Primer Code	Primer Sequence*	bp at which primers start and finish**	Expected Product Size	Code for PCR product
RAO5F	GAAGGTGGAGTTCAAGAGGACC	1526	906 bp	RAO-5
RAO5R	GTGGTTCCTGAGCAGAGCATAC	2431		

Table 11 – Summary of primers designed for the RT-PCR amplification of rat aldehyde oxidase cDNA spanning codon 649.

This table shows the primers used, the sequence of the primers *reading 5`-3`, ** bp at which the 5` base of the primer binds, +1 represents the A of the ATG start codon. F and R signify sense and antisense primers respectively.

Table 12 shows a summary of the conditions used and the results obtained for the amplification of the rat AO cDNA clone encoding codon 649.

Primers used	Annealing temperature °C	Primer conc.**	$MgCl_2$ Conc.**	Fragments Generated
RAO5F/ RAO5R	47,49,51,53,55,57	0.5pM	1.5mM	Several fragments
	55,56,57,58	0.25pM	1.5mM	Two fragments
	55,56,57,58	0.5pM	2mM	Several fragments
	55,56,57,58	0.25pM	1mM	~900bp fragment

Table 12 – Summary of the conditions used and outcomes for the RT- PCR of the rat aldehyde oxidase cDNA RAO-5 clone.

This table shows the optimisation process for primer set RAO-5. It illustrates the temperatures used with each set of conditions and the outcomes from each set of conditions used. The optimal conditions for each primer pair are highlighted. ** concentration.

The cDNA product was then sequenced from two Wistar and Fischer animals and four SD animals. Figure 12 shows a representative sequencing chromatogram over the polymorphic codon 649 for each of the three rat strains.

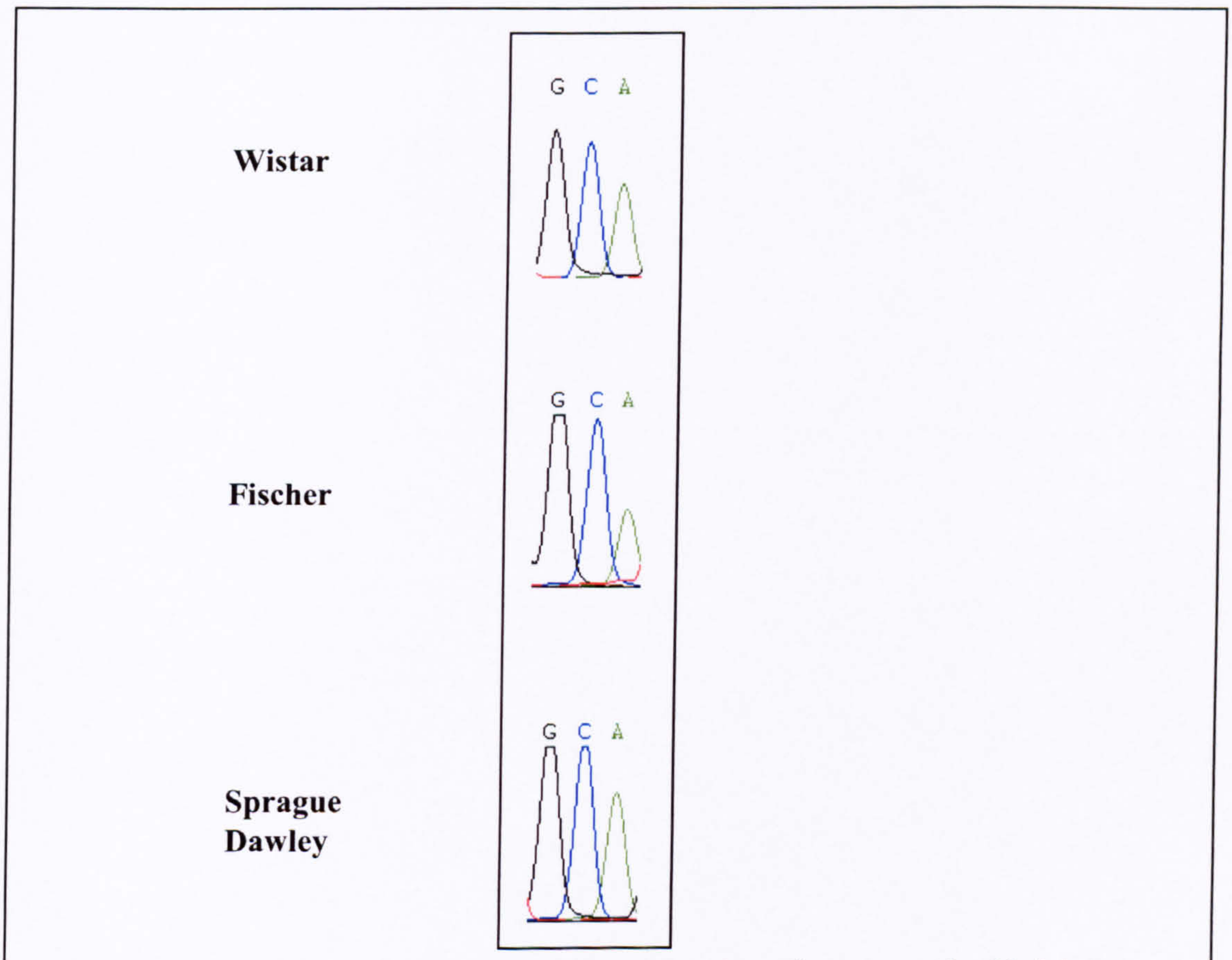

Figure 12 – Sequencing chromatograms illustrating the codon present in this laboratory's rat strains at codon 649.

Chromatograms showing the nucleotide sequence of codons 649 in the different strains of rat. As no gender differences were observed only one representative chromatogram from each strain has been shown.

Comparison of the possible codons (ACA/GCA) as found by Wright *et al.* (1999) encoding for threonine and alanine at position 649 in the Wistar, SD and Fischer rat, revealed that in all three rats strains a GCA codon was present, which resulted in an alanine residue at position 649 in the predicted protein sequence.

In conclusion the data showed no differences between the three strains of rat at the five polymorphic positions studied. All rat strains possessed a glycine, methionine, arginine, phenylalanine and threonine codon at positions 119, 120, 649, 1276 and 1315 respectively. It was therefore concluded that the differences observed by Wright *et al* (1999) did not correlate with the deficiency found in these rat strains.

3.3.Cloning and sequencing of aldehyde oxidase cDNA from Wistar, Sprague Dawley and Fischer rat strains.

As none of the changes observed by Wright *et al.* (1999) correlated with the genetic deficiency of AO in these rat strains. It was decided to clone the whole AO mRNA sequence using RT-PCR. Male and female rats were sequenced as Wright *et al.* (1999) had suggested a difference in their male and female SD rats (Wright *et al.*, 1999).

3.3.1 Design of PCR primers for the amplification of the rat aldehyde oxidase cDNA.

Primers were selected from the published SD rat AO cDNA sequence using the computer programs as previously carried out. Several primer sets were selected which amplified the cDNA with an overlap between individual clones (table 13 and figure 13). RAO-5 had already been designed and optimised for the study of the T649A change (tables 11 and 12).

Primer Code	Primer Sequence*	bp at which primers start and finish**	Expected Product Size	Code for PCR product
RAO1aF	ATCTACTAGGGACCTGCTAGG	-28	502 bp	RAO-1
RAO1R	CGTCAATTATGGGCCTGTATC	474		
RAO2F	AAGAACCTCCGACTCACG	93	903 bp	RAO-2
RAO2R	ATGTCTGTGTCGTCTCTTCTGG	996		
RAO3F	CTGGAGGAACTTGTGGAAGC	741	730 bp	RAO-3
RAO3R	GTGTCCAGCATCTCTTCATTCC	1471		
RAO4F	GTCTTGGTCTCAGTGAACATCC	1224	699 bp	RAO-4
RAO4R	TAATGATGTCCACCACGCCTGG	1923		
RAO6F	TCTACCGAGACTTGGAGC	2071	938 bp	RAO-6
RAO6R	CGGCCATTCCCCTCTTC	3009		
RAO7F	GCTGGTCACCGAAGCCTGTG	2771	629 bp	RAO-7
RAO7R	CTGGTCAAAAGCAGTCTGGG	3400		
RAO6F	TATCTTGATGGCTCTGC	3081	922 bp	RAO-8
RAO6R	TTCACTCACACAGGTATGTTCC	4003		

Table 13 – Summary of the primers designed for the RT-PCR amplification of rat aldehyde oxidase cDNA.

*reading 5`-3` ** bp at which the 5` base of the primer binds, +1 represents the A of the ATG start codon. F and R signify sense and antisense primers respectively.

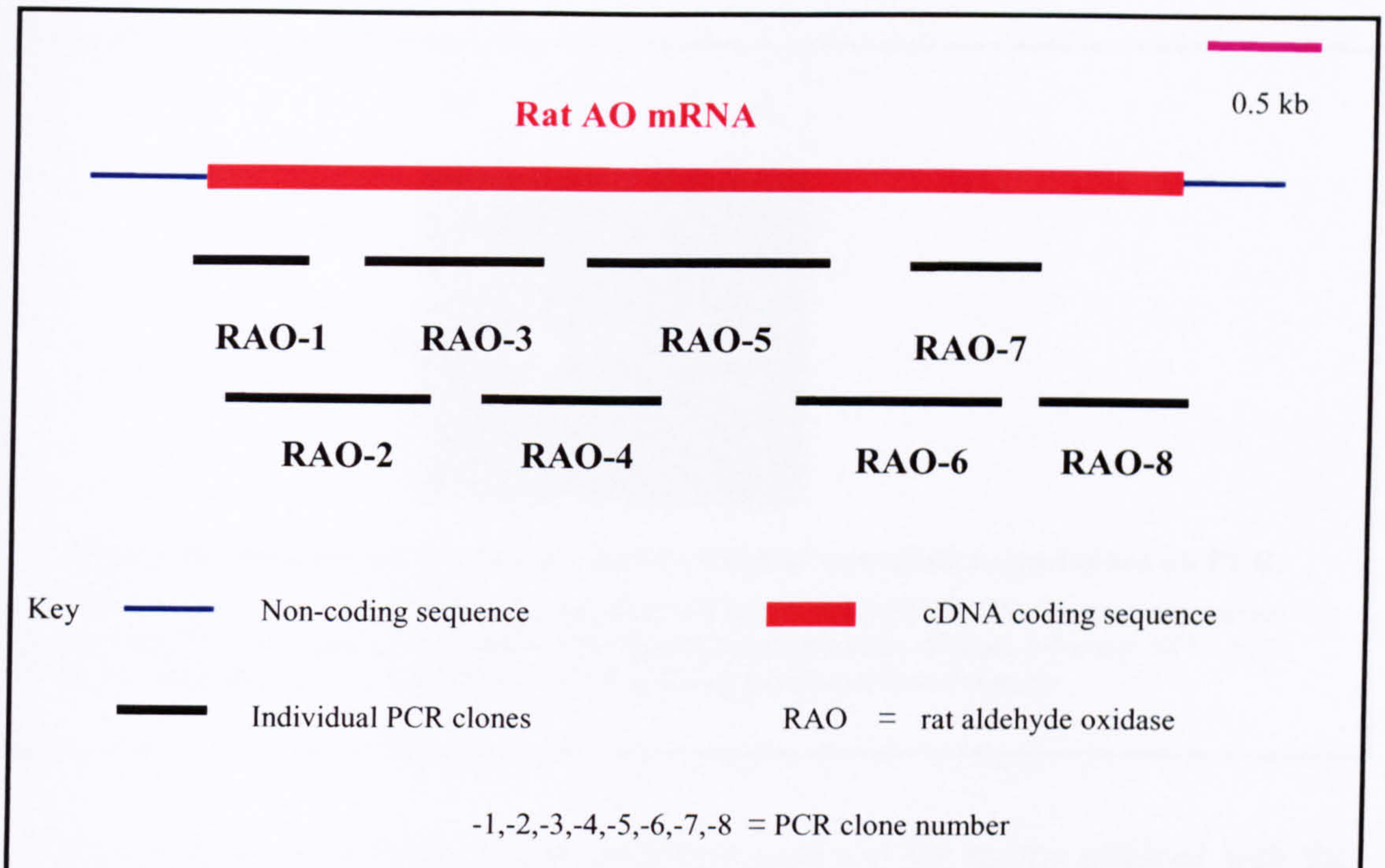

Figure 13 – Diagram showing the position and degree of overlap between the predicted rat aldehyde oxidase PCR clones.

3.3.2 Optimisation of the RT-PCR primers for amplification of the individual clones of rat aldehyde oxidase cDNA.

The PCR was then optimised in the same manner as for the genomic DNA amplification. As mentioned previously, the agarose gel images are too numerous to show so only a gel displaying an example of the optimisation process is shown. Figure 14 shows how critical annealing temperature can be in the successful amplification of the PCR reaction changing just one degree under or above the optimum results in the formation of non-specific products.

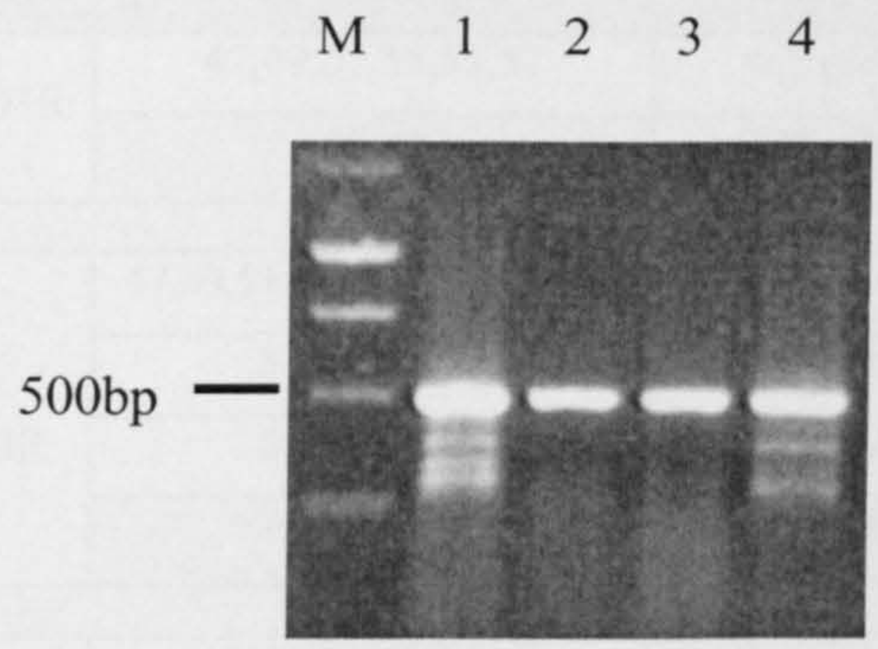

Figure 14 - Agarose gel image showing the effect of annealing temperature on PCR.

The PCR amplification was carried out using primers RAO1F and RAO1R. The reaction was carried out using 0.25 pM primer and 1.5 mM $MgCl_2$. The annealing temperatures of lanes 1-4 are at 55°C, 56°C, 57°C and 58°C respectively. Lane M is 1 kb DNA ladder purchased from Promega.

Table 14 shows a summary of the conditions used and the results obtained with the optimal conditions for each primer pair highlighted.

Primers used	Annealing temperatures °C	Primer conc.**	$MgCl_2$ Conc.**	Fragments Generated
RAO1aF/ RAO1R	47,49,51,53,55,57	0.5 pM	1.5 mM	Several fragments
	56,57	0.25 pM	1.5 mM	~500 bp fragment
RAO2F/RAO2R	47,49,51,53,55,57,59,61.63	0.25 pM	1.5 mM	Several fragments
	57,58,59,60	0.5 pM	2 mM	Several fragments
	55,56,57,58	0.25 pM	1 mM	No fragments
	52,53,54,55	0.5 pM	1.5 mM	~900 bp fragment
RAO3F/ RAO3R	47,49,51,53,55,57	0.5 pM	1.5 mM	Several fragments
	55,54,55,56,57,58	0.25 pM	1.5 mM	~750 bp fragment
RAO4F/ RAO4R	47,49,51,53,55,57	0.5 pM	1.5 mM	Several fragments
	56,57,58,59	0.5 pM	2 mM	Several fragments
	54,55,56,57	0.25 pM	1 mM	Several fragments
	58,59,60,61	0.25 pM	1.5 mM	Two fragments
	58,59,60,61	0.25 pM	2 mM	Two fragments
	58,59,60,61	0.25 pM	1 mM	~700 bp fragment
RAO6F/RAO6R	52,54,56,58,60,62	0.25 pM	1.5 mM	Several fragments
	52,54,56,58,60	0.5 pM	1.5 mM	~950 bp fragment
RAO7F/ RAO7R	52,54,56,58,60,62	0.25 pM	1.5 mM	~600 bp fragment
RAO8F/ RAO8R	52,54,56,58,60,62	0.25 pM	1.5 mM	~ 900 bp fragment

Table 14 – Summary of the conditions used and outcomes for the RT-PCR of the rat aldehyde oxidase cDNA clones.

This table shows the optimisation process for primer sets RAO-1, RAO-2, RAO-3, RAO-4, RAO-6, RAO-7 and RAO-8. It illustrates the range of annealing temperatures used with each set of conditions and the outcomes from each set of conditions used. The optimal conditions for each primer pair are highlighted. ** Concentration.

3.3.3 Nucleotide differences in the aldehyde oxidase cDNA identified between different rat strains.

Once optimised the primers were used to amplify the entire AO cDNA in male and female animals of the 3 different strains. These clones were then subjected to DNA sequencing and the sequences obtained were used to make a contig of the complete cDNA sequence from each strain. Figure 15 shows the sequence of rat liver AO obtained from our SD strain. The differences found between the strains are indicated as

are the various cofactor binding sites and domains. The sequences obtained from the different rat strains were aligned and the differences found are shown in figure 16 and table 15. The next two pages (figure 16) show the cDNA sequence obtained interleaved with the predicted amino acid sequence. The four different binding sites of the cofactors are highlighted and changes found both in our strains and Wright *et al's.* (1999) SD strain are indicated beneath the sequence.

```
    Met Asp Pro Pro Gln Leu Leu Phe Tyr Val Asn Gly Gln Lys Val Val Glu Asn Asn Val Asp Pro Glu Met Met Leu Leu Pro      28
  1 ATG GAT CCC CCG CAG CTG CTC TTC TAC GTG AAT GGC CAG AAG GTG GTA GAA AAC AAT GTT GAT CCT GAG ATG ATG CTT TTA CCG
                                                                                                          Pro
                                                                                                          CCA

    Tyr Leu Arg Lys Asn Leu Arg Leu Thr Gly Thr Lys Tyr Gly Cys Gly Gly Gly Gly Cys Gly Ala Cys Thr Val Met Ile Ser      56
 85 TAC CTG AGG AAG AAC CTC CGA CTC ACG GGA ACT AAG TAT GGC TGT GGA GGC GGC GGC TGC GGT GCC TGC ACA GTG ATG ATC TCA

    Arg Tyr Asn Pro Ser Thr Lys Ser Ile Arg His His Pro Val Asn Ala Cys Leu Thr Pro Ile Cys Ser Leu Tyr Gly Thr Ala      84
169 CGG TAC AAC CCC AGC ACC AAG AGC ATC AGG CAT CAT CCT GTC AAT GCC TGT CTG ACC CCC ATC TGC TCT CTG TAC GGT ACA GCA

    Val Thr Thr Val Glu Gly Ile Gly Asn Thr Arg Thr Arg Leu His Pro Val Gln Glu Arg Ile Ala Lys Cys His Ser Thr Gln     112
253 GTC ACC ACA GTA GAG GGC ATA GGC AAC ACC AGG ACC AGA CTT CAT CCT GTT CAG GAG AGG ATC GCC AAG TGT CAC AGC ACC CAG
                                                                                                  Gly
                                                                                                  GGC

    Cys Gly Phe Cys Thr Pro Gly Met Val Met Ser Met Tyr Ala Leu Leu Arg Asn His Pro Glu Pro Ser Leu Asp Gln Leu Thr     140
337 TGT GGG TTC TGT ACC CCT GGG ATG GTG ATG TCC ATG TAT GCT CTG CTC AGG AAC CAC CCA GAG CCC TCT CTA GAT CAG TTA ACT
                          Ala Arg
                          GCG AGG

    Asp Ala Leu Gly Gly Asn Leu Cys Arg Cys Thr Gly Tyr Arg Pro Ile Ile Asp Ala Cys Lys Thr Phe Cys Arg Ala Ser Gly     168
421 GAT GCC CTT GGG GGG AAT CTG TGC CGC TGT ACC GGA TAC AGG CCC ATA ATT GAC GCT TGC AAG ACT TTC TGT AGA GCT TCT GGT

    Cys Cys Glu Ser Lys Glu Asn Gly Val Cys Cys Leu Asp Gln Gly Ile Asn Gly Ser Ala Glu Phe Gln Glu Gly Asp Glu Thr     196
505 TGC TGT GAA AGT AAA GAA AAT GGG GTG TGC TGT TTG GAT CAA GGA ATA AAT GGA TCG GCA GAA TTT CAG GAA GGA GAT GAG ACA

    Ser Pro Glu Leu Phe Ser Glu Lys Glu Phe Gln Pro Leu Asp Pro Thr Gln Glu Leu Ile Phe Pro Pro Glu Leu Met Arg Ile     224
589 AGT CCA GAA CTG TTC TCG GAA AAG GAA TTT CAG CCA CTG GAC CCA ACC CAA GAG CTG ATA TTT CCT CCA GAG CTA ATG AGA ATA

    Ala Glu Lys Gln Pro Pro Lys Thr Arg Val Phe Tyr Ser Asn Arg Met Thr Trp Ile Ser Pro Val Thr Leu Glu Glu Leu Val     252
673 GCC GAG AAA CAG CCA CCA AAG ACC AGA GTG TTC TAC AGT AAT AGA ATG ACA TGG ATC TCC CCG GTG ACC CTG GAG GAA CTT GTG

    Glu Ala Lys Phe Lys Tyr Pro Gly Ala Pro Ile Val Met Gly Tyr Thr Ser Val Gly Pro Glu Val Lys Phe Lys Gly Val Phe     280
757 GAA GCT AAG TTC AAG TAT CCT GGG GCC CCC ATT GTC ATG GGG TAC ACC TCT GTG GGG CCT GAA GTA AAG TTT AAA GGT GTC TTC

    His Pro Ile Ile Ile Ser Pro Asp Arg Ile Glu Glu Leu Ser Ile Ile Asn Gln Thr Gly Asp Gly Leu Thr Leu Gly Ala Gly     308
841 CAC CCC ATC ATA ATT TCT CCT GAC AGA ATT GAA GAG CTG AGT ATC ATA AAC CAG ACT GGG GAT GGG CTG ACC CTG GGT GCT GGC

    Leu Ser Leu Asp Gln Val Lys Asp Ile Leu Thr Asp Val Val Gln Lys Leu Pro Glu Glu Thr Thr Gln Thr Tyr Arg Ala Leu     336
925 CTC AGC CTG GAC CAG GTG AAG GAC ATT CTC ACT GAC GTG GTC CAG AAG CTT CCA GAA GAG ACG ACA CAG ACA TAC CGT GCG CTC

    Leu Lys His Leu Arg Thr Leu Ala Gly Ser Gln Ile Arg Asn Met Ala Ser Leu Gly Gly His Ile Val Ser Arg His Leu Asp     364
1009 CTG AAG CAC CTG AGA ACT CTG GCT GGC TCT CAG ATC AGG AAT ATG GCT TCT TTA GGG GGC CAC ATC GTG AGC AGA CAT CTG GAC

    Ser Asp Leu Asn Pro Leu Leu Ala Val Gly Asn Cys Thr Leu Asn Leu Leu Ser Lys Asp Gly Lys Arg Gln Ile Pro Leu Ser     392
1093 TCG GAT CTG AAT CCC CTT CTG GCT GTG GGT AAT TGT ACC CTC AAC TTA CTA TCC AAA GAT GGA AAA CGG CAG ATC CCT TTA AGT

    Glu Gln Phe Leu Arg Lys Cys Pro Asp Ser Asp Leu Lys Pro Gln Glu Val Leu Val Ser Val Asn Ile Pro Cys Ser Arg Lys     420
1177 GAG CAG TTT CTC CGC AAG TGT CCT GAC TCG GAT CTT AAG CCT CAG GAA GTC TTG GTC TCA GTG AAC ATC CCC TGT TCC AGG AAG

    Trp Glu Phe Val Ser Ala Phe Arg Gln Ala Gln Arg Gln Gln Asn Ala Leu Ala Ile Val Asn Ser Gly Met Arg Val Leu Phe     448
1261 TGG GAG TTT GTG TCA GCC TTC CGA CAA GCC CAG AGA CAG CAG AAT GCA CTA GCG ATT GTC AAC TCT GGA ATG AGA GTC CTT TTT

    Arg Glu Gly Gly Gly Val Ile Lys Glu Leu Ser Ile Leu Tyr Gly Gly Val Gly Pro Thr Thr Ile Gly Ala Lys Asn Ser Cys     476
1345 AGA GAA GGA GGT GGC GTC ATT AAA GAG TTA TCC ATT TTG TAT GGA GGT GTC GGT CCA ACC ACC ATC GGT GCC AAG AAC TCC TGT

    Gln Lys Leu Ile Gly Arg Pro Trp Asn Glu Glu Met Leu Asp Thr Ala Cys Arg Leu Val Leu Asp Glu Val Thr Leu Ala Gly     504
1429 CAG AAA CTC ATT GGA AGG CCC TGG AAT GAA GAG ATG CTG GAC ACA GCA TGC AGG CTG GTT TTG GAT GAA GTC ACC CTT GCA GGT

    Ser Ala Pro Gly Gly Lys Val Glu Phe Lys Arg Thr Leu Ile Ile Ser Phe Leu Phe Lys Phe Tyr Leu Glu Val Leu Gln Gly     532
1513 TCA GCT CCT GGT GGG AAG GTG GAG TTC AAG AGG ACC CTC ATC ATC AGC TTC CTT TTC AAG TTC TAC CTG GAG GTG CTG CAG GGT

    Leu Lys Arg Glu Asp Pro Gly His Tyr Pro Ser Leu Thr Asn Asn Tyr Glu Ser Ala Leu Glu Asp Leu His Ser Lys His His     560
1597 CTG AAG AGG GAG GAC CCA GGT CAC TAT CCT AGC TTG ACA AAC AAT TAT GAG AGT GCT TTA GAA GAT CTC CAT TCA AAA CAT CAC
                                               Leu
                                               CTG

    Trp Arg Thr Leu Thr His Gln Asn Val Asp Ser Met Gln Leu Pro Gln Asp Pro Ile Gly Arg Pro Ile Met His Leu Ser Gly     588
1681 TGG AGA ACA TTA ACC CAC CAG AAC GTG GAC TCG ATG CAG CTT CCT CAG GAC CCA ATT GGC CGT CCC ATC ATG CAC CTT TCT GGT

    Ile Lys His Ala Thr Gly Glu Ala Ile Tyr Cys Asp Asp Met Pro Ala Val Asp Arg Glu Leu Phe Leu Thr Phe Val Thr Ser     616
1765 ATT AAG CAC GCT ACC GGC GAG GCC ATC TAC TGT GAC GAC ATG CCT GCA GTA GAC CGG GAG CTT TTC CTG ACT TTT GTA ACA AGT

    Ser Arg Ala His Ala Lys Ile Val Ser Ile Asp Leu Ser Glu Ala Leu Ser Leu Pro Gly Val Val Asp Ile Ile Thr Ala Asp     644
1849 TCA AGA GCA CAC GCT AAG ATT GTG TCC ATT GAT CTG TCA GAA GCT CTC AGC CTG CCA GGC GTG GTG GAC ATC ATT ACT GCG GAT

    His Leu Gln Asp Thr Thr Thr Phe Gly Thr Glu Thr Leu Leu Thr Thr Asp Lys Val His Cys Val Gly Gln Leu Val Cys Ala     672
1933 CAT CTT CAG GAC ACA ACC ACC TTC GGC ACA GAG ACG CTT CTG ACC ACA GAT AAG GTC CAC TGC GTG GGC CAA CTT GTC TGT GCC
                                                        Ala
                                                        GCC
```

```
     Val Ile Ala Asp Ser Glu Thr Arg Ala Lys Gln Ala Ala Lys His Val Lys Val Val Tyr Arg Asp Leu Glu Pro Leu Ile Leu    700
2017 GTG ATT GCG GAT TCT GAG ACA CGG GCA AAG CAA GCG GCG AAG CAC GTG AAG GTG GTC TAC CGA GAC TTG GAG CCT CTG ATC CTA

     Thr Ile Glu Glu Ala Ile Gln His Lys Ser Phe Phe Glu Ser Glu Arg Lys Leu Glu Cys Gly Asn Val Asp Glu Ala Phe Lys    728
2101 ACT ATT GAG GAA GCT ATA CAA CAC AAG TCC TTC TTC GAG TCA GAA CGG AAG CTG GAG TGT GGA AAT GTT GAT GAA GCG TTT AAA

     Ile Ala Asp Gln Ile Leu Glu Gly Glu Ile His Ile Gly Gly Gln Glu His Phe Tyr Met Glu Thr Gln Ser Met Leu Val Val    756
2185 ATT GCT GAT CAA ATT CTT GAA GGT GAG ATA CAC ATA GGC GGC CAG GAA CAT TTT TAT ATG GAA ACC CAA AGC ATG CTT GTT GTC

     Pro Lys Gly Glu Asp Gly Glu Ile Asp Ile Tyr Val Ser Thr Gln Phe Pro Lys His Ile Gln Asp Ile Val Ala Ala Thr Leu    784
2269 CCC AAA GGA GAG GAC GGA GAG ATT GAC ATC TAT GTG TCC ACA CAG TTC CCC AAG CAT ATA CAG GAT ATA GTT GCT GCA ACC TTG

     Lys Leu Ser Val Asn Lys Val Met Cys His Val Arg Arg Val Gly Gly Ala Phe Gly Gly Lys Val Gly Lys Thr Ser Ile Met    812
2353 AAG CTT TCA GTC AAC AAG GTC ATG TGT CAT GTA AGG CGT GTT GGT GGG GCG TTC GGA GGG AAG GTA GGC AAG ACC AGC ATC ATG

     Ala Ala Ile Thr Ala Phe Ala Ala Ser Lys His Gly Arg Ala Val Arg Cys Thr Leu Glu Arg Gly Glu Asp Met Leu Ile Thr    840
2437 GCG GCC ATC ACT GCA TTC GCT GCC AGC AAA CAC GGT CGC GCG GTC CGC TGC ACT CTG GAA CGA GGG GAA GAC ATG TTA ATA ACT

     Gly Gly Arg His Pro Tyr Leu Gly Lys Tyr Lys Val Gly Phe Met Arg Asp Gly Arg Ile Val Ala Leu Asp Val Glu His Tyr    868
2521 GGG GGC CGC CAT CCT TAC CTT GGA AAG TAT AAA GTT GGA TTC ATG AGG GAC GGC AGA ATC GTG GCC CTG GAT GTG GAG CAC TAT
                                                                                                  Ala
                                                                                                  GCT

     Cys Asn Gly Gly Ser Ser Leu Asp Glu Ser Leu Trp Val Ile Glu Met Gly Leu Leu Lys Met Asp Asn Ala Tyr Lys Phe Pro    896
2605 TGC AAT GGA GGG AGC TCC CTG GAT GAG TCC TTA TGG GTG ATA GAA ATG GGG CTT CTG AAG ATG GAC AAC GCT TAC AAG TTT CCC

     Asn Leu Arg Cys Arg Gly Trp Ala Cys Arg Thr Asn Leu Pro Ser Asn Thr Ala Leu Arg Gly Phe Gly Phe Pro Gln Ala Gly    924
2689 AAT CTA CGC TGC CGG GGC TGG GCC TGC AGA ACC AAC CTC CCG TCC AAC ACT GCT CTG CGT GGG TTT GGC TTT CCT CAG GCA GGG

     Leu Val Thr Glu Ala Cys Val Thr Glu Val Ala Ile Arg Cys Gly Leu Ser Pro Glu Gln Val Arg Thr Ile Asn Met Tyr Lys    952
2773 CTG GTC ACC GAA GCC TGT GTC ACA GAA GTG GCA ATC AGA TGT GGC CTG TCC CCT GAG CAG GTT CGA ACC ATA AAT ATG TAC AAG

     Gln Ile Asp Asn Thr His Tyr Lys Gln Glu Phe Ser Ala Lys Thr Leu Phe Glu Cys Trp Arg Glu Cys Met Ala Lys Cys Ser    980
2857 CAA ATT GAT AAT ACC CAT TAC AAG CAA GAA TTC AGC GCC AAG ACC CTC TTT GAG TGC TGG AGA GAA TGC ATG GCC AAG TGT TCC
                                       Glu
                                       GAG

     Tyr Ser Glu Arg Lys Thr Ala Val Gly Lys Phe Asn Ala Glu Asn Ser Trp Lys Lys Arg Gly Met Ala Val Ile Pro Leu Lys   1008
2941 TAC TCT GAG AGG AAA ACG GCT GTA GGA AAA TTC AAT GCA GAG AAT TCC TGG AAG AAG AGG GGA ATG GCC GTG ATT CCA TTG AAG

     Phe Pro Val Gly Val Gly Ser Val Ala Met Gly Gln Ala Ala Ala Leu Val His Ile Tyr Leu Asp Gly Ser Ala Leu Val Ser   1036
3025 TTT CCT GTG GGT GTT GGC TCA GTA GCC ATG GGA CAG GCG GCT GCC CTG GTC CAT ATT TAT CTT GAT GGC TCT GCA CTG GTC TCT

     His Gly Gly Ile Glu Met Gly Gln Gly Val His Thr Lys Met Ile Gln Val Val Ser Arg Glu Leu Lys Met Pro Met Ser Ser   1064
3109 CAC GGT GGG ATT GAG ATG GGG CAG GGT GTC CAC ACT AAA ATG ATC CAG GTG GTC AGC CGG GAA TTA AAG ATG CCA ATG TCG AGT

     Val His Leu Arg Gly Thr Ser Thr Glu Thr Val Pro Asn Thr Asn Ala Ser Gly Gly Ser Val Val Ala Asp Leu Asn Gly Leu   1092
3193 GTC CAC CTG CGT GGG ACA AGC ACA GAA ACC GTC CCC AAC ACC AAT GCA TCT GGA GGC TCT GTG GTG GCA GAT CTC AAT GGA TTG

     Ala Val Lys Asp Ala Cys Gln Thr Leu Leu Lys Arg Leu Glu Pro Ile Ile Ser Lys Asn Pro Gln Gly Thr Trp Lys Asp Trp   1120
3277 GCA GTA AAG GAT GCT TGC CAG ACC CTT CTA AAA CGC CTT GAG CCC ATC ATC AGC AAG AAC CCC CAG GGA ACT TGG AAG GAT TGG

     Ala Gln Thr Ala Phe Asp Gln Ser Val Ser Leu Ser Ala Val Gly Tyr Phe Arg Gly Tyr Glu Ser Asn Ile Asn Trp Glu Lys   1148
3361 GCC CAG ACT GCT TTT GAC CAG AGC GTC AGT CTC TCG GCT GTT GGA TAT TTC AGG GGC TAC GAG TCG AAT ATA AAC TGG GAG AAA

     Gly Glu Gly His Pro Phe Glu Tyr Phe Val Tyr Gly Ala Ala Cys Ser Glu Val Glu Ile Asp Cys Leu Thr Gly Asp His Lys   1176
3445 GGG GAA GGC CAT CCC TTC GAA TAC TTT GTG TAT GGA GCT GCC TGC TCA GAG GTT GAA ATA GAC TGC CTG ACC GGG GAC CAT AAG

     Asn Ile Arg Thr Asp Ile Val Met Asp Val Gly His Ser Ile Asn Pro Ala Leu Asp Ile Gly Gln Val Glu Gly Ala Phe Ile   1204
3529 AAT ATC AGA ACA GAC ATC GTG ATG GAT GTT GGC CAC AGC ATA AAC CCA GCC CTT GAC ATA GGC CAG GTT GAA GGT GCA TTT ATT

     Gln Gly Met Gly Leu Tyr Thr Ile Glu Glu Leu Ser Tyr Ser Pro Gln Gly Ile Leu Tyr Ser Arg Gly Pro Asn Gln Tyr Lys   1232
3613 CAA GGA ATG GGA CTT TAC ACG ATA GAG GAG CTG AGC TAC TCT CCT CAG GGC ATT CTG TAC AGT CGT GGT CCA AAC CAG TAC AAG
                                                                                                  Gln
                                                                                                  CAA

     Ile Pro Ala Ile Cys Asp Ile Pro Thr Glu Met His Ile Ser Phe Leu Pro Pro Ser Glu His Ser Asn Thr Leu Tyr Ser Ser   1260
3697 ATC CCT GCC ATC TGC GAC ATC CCC ACC GAG ATG CAC ATT TCT TTT TTG CCC CCA TCC GAA CAC TCA AAC ACC CTG TAT TCA TCT

     Lys Gly Leu Gly Glu Ser Gly Val Phe Leu Gly Cys Ser Val Phe Phe Ala Ile His Asp Ala Val Arg Ala Ala Arg Gln Glu   1288
3781 AAG GGT CTG GGA GAG TCT GGG GTG TTC CTG GGC TGT TCG GTA TTT TTT GCC ATC CAT GAC GCA GTG AGG GCA GCG CGG CAG GAG
                                                  Leu
                                                  CTT

     Arg Gly Ile Ser Gly Pro Trp Lys Leu Thr Ser Pro Leu Thr Pro Glu Lys Ile Arg Met Ala Cys Glu Asp Lys Phe Thr Lys   1316
3865 AGA GGC ATC TCT GGA CCA TGG AAG CTC ACT AGT CCT CTG ACT CCA GAG AAA ATC AGA ATG GCT TGT GAA GAT AAG TTC ACA AAA
                                                                                                  Arg
                                                                                                  AGA

     Met Ile Pro Arg Asp Glu Pro Gly Ser Tyr Val Pro Trp Asn Ile Pro Val                                              1333
3949 ATG ATT CCA AGA GAT GAA CCT GGA TCC TAT GTT CCC TGG AAC ATA CCT GTG TGA
```

Figure 15 – Sprague Dawley aldehyde oxidase cDNA sequence interleaved with the deduced amino acid sequence.

The iron-sulphur, FAD and MoCo binding sites are highlighted in yellow, grey and blue respectively (Terao *et al.*, 2000). Nucleotide changes leading to amino acid differences between the SD and Wistar rats are indicated in purple. Nucleotide changes not resulting in an amino acid change are indicated in green. The difference between the SD and the other two strains is indicated in pink. Changes found by Wright *et al* (1999) are shown in brown.

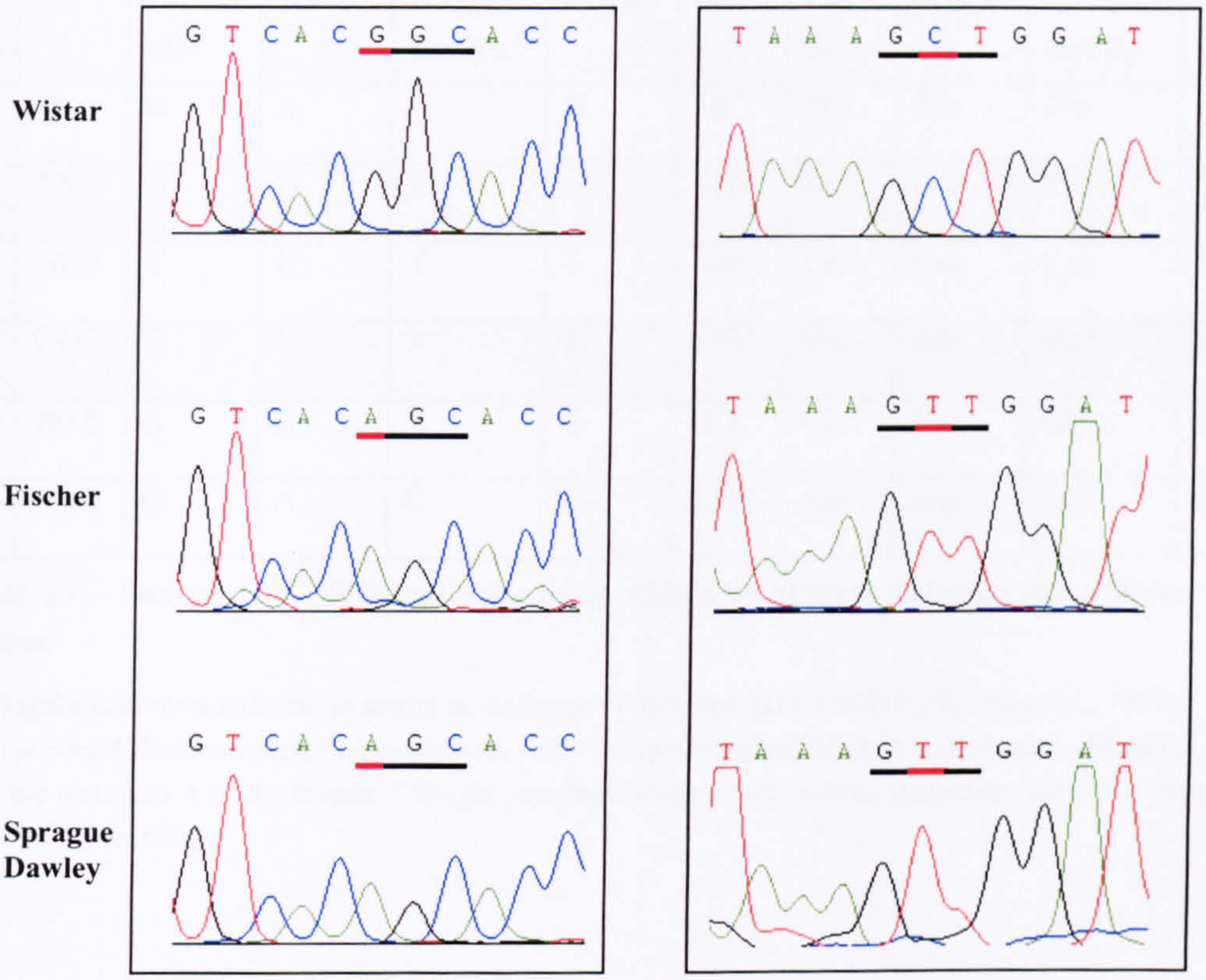

Figure 16 – Sequencing chromatograms showing the codon differences between the different rat strains.

As no gender differences were observed only one representative chromatogram from each strain has been shown.

Table 15 summarises all the differences found between the strains in the nucleotide sequence of the rat AO cDNA. Changes predicted to cause an amino acid change in the translated sequence are highlighted in yellow.

No	Nucleotide					Amino Acid				
	Site	Pub SD*	Wistar	Sprague Dawley	Fischer	Site	Pub SD*	Wistar	Sprague Dawley	Fischer
1[a]	84	G	A	G	G	28	Pro	Pro	Pro	Pro
2	328	A	G	A	A	110	Ser	Gly	Ser	Ser
3[b]	1630	T	C	T	T	544	Leu	Leu	Leu	Leu
4	2555	T	C	T	T	852	Val	Ala	Val	Val
5	2886	A	A	A	G	962	Glu	Glu	Glu	Glu
6	3690	G	A	G	G	1230	Asp	Asp	Asp	Asp

Table 15 – Summary of differences found in aldehyde oxidase between the different rat strains.

The highlighted rows indicate an amino acid change *Published SD rat cDNA (Wright *et al.*, 1999). **no gender differences were observed in our rats. [a] Wright reported this as a male/female difference with G in the male and A in the female. [b] Wright reported this as a male/female difference with T in the male and C in the female.

3.4 Cloning and sequencing of aldehyde oxidase homologue 1 cDNA from Wistar, Sprague Dawley and Fischer rat strains.

During the course of this investigation two AO homologues were discovered to be present in mice (September 2000) (Terao *et al.*, 2000). One of these (AOH1) was found in liver and was therefore of a concern to this study as even though differences were found between the AO-active Wistar strain and the AO-deficient strains in the AO cDNA sequence, if AOH1 is present in rats this enzyme may also be involved in the deficiency.

3.4.1 Characterisation of aldehyde oxidase and aldehyde oxidase homologue 1 in the different strains of rats using cellulose acetate electrophoresis.

The research publication on the mouse AO homologues used cellulose acetate electrophoresis to demonstrate that two polypeptides were found in mouse liver, which they designated AO and AOH1. (Terao *et al.*, 2000). In order to determine if there were AO homologues in rat liver the same cellulose acetate electrophoresis method was used to characterise rat liver cytosol from the SD, Wistar and Fischer strains (figure 17). This revealed that there were two enzymes present in wild type Wistar rat liver when stained with benzaldehyde but only one polypeptide stained in the SD and Fischer strains. Staining with phenanthridine as substrate indicated that only the furthest migrating polypeptide showed phenanthridine oxidising activity (figure 17) and confirmed that this enzyme is missing in the SD and Fischer rats. This band corresponded to the furthest migrating polypeptide in mice suggesting that AOH1 is responsible solely for the activity of phenanthridine oxidation in rat liver.

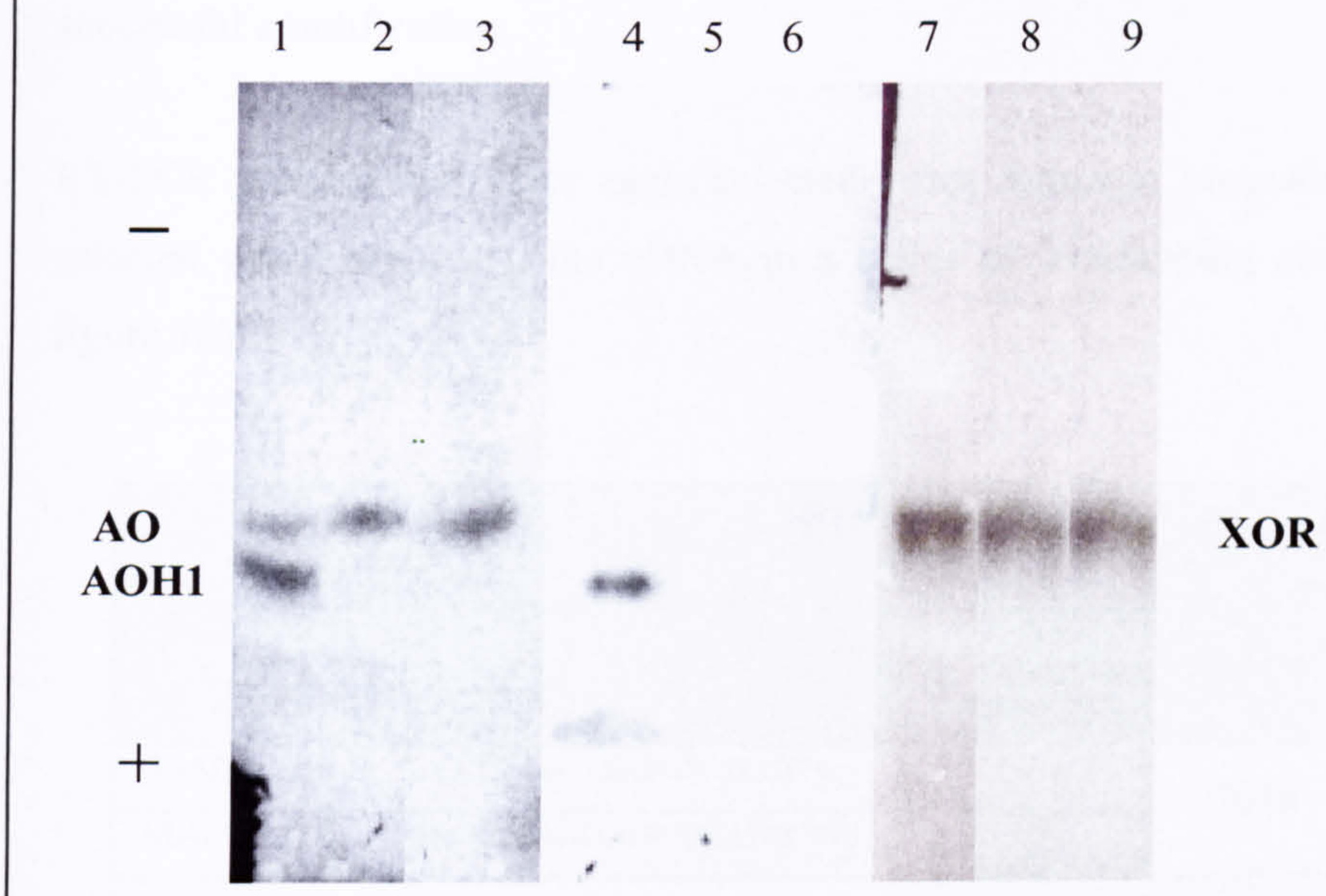

Figure 17 – Cellulose acetate zymogram of molybdenum hydroxylases in the different rat strains.

Lanes 1, 2and 3 were stained using benzaldehyde, Lanes 4, 5 and 6 were stained using phenanthridine, and lanes 7, 8 and 9 were stained using hypoxanthine as described in materials and methods section 2.6. Lanes 1, 4 and 7 are Wistar rat cytosol. Lanes 2, 5 and 8 are SD rat cytosol and lanes 3, 6 and 9 are Fischer rat cytosol. The direction of migration is from the anode (-) to the cathode (+) as indicated on the left.

3.4.2 The cloning of aldehyde oxidase homologue 1 cDNAs from different rat strains.

As the zymograms in figure 17 demonstrated that the AO holoenzyme is present in the SD and Fischer rats but AOH1 activity is absent it was decided to clone the AOH1 enzyme from rat liver to establish if any differences in its amino acid sequence could account for the lack of N-heterocyclic oxidase activity in the SD and Fischer rats.

As the only mammalian cDNA sequence available for AOH1 was the mouse cDNA, primers were designed to the mouse AOH1 sequence with care being taken not to select primers, which bound to any regions of high nucleotide identity between AO and AOH1. As the mouse and rat are evolutionary very closely related and the AO cDNAs are 92% identical, it would be reasonable to presume that most of the primers designed

to the mouse AOH1 cDNA sequence would bind to the rat sequence and produce a successful amplification.

RT-PCR primers were once again selected using computer programs and several sets selected which amplified the cDNA in a series of overlapping clones (table 16 and figure 18).

Primer Code	Primer Sequence*	bp at which primers start and finish**	Predicted product Size***	Code for PCR product
MAOH11F	CCTCAAGTAATGTCTCCTTC	-9	770 bp	MAOH1-1a
MAOH11aR	GAGTGGAGCGCTGGGATGCTTC	761		
MAOH11aF	CAGCCCCTGGATCCAACTCAGG	621	866 bp	MAOH1-2
MAOH11R	CATCTTGCCAGCATCATCCAGC	1487		
MAOH12F	GCATCAACAGAAGGAATACAGC	1143	909 bp	MAOH1-3
MAOH12aR	CCTGCTGGGCATGAGCATAAG	2052		
MAOH12aF	GGTAACCAGCAGGAAGTCAC	1841	996 kb	MAOH1-4
MAOH12R	AACCTTCTCTGGTGGTAAGCGG	2837		
MAOH13F	ATGTGTCAAGCCAGGATGCTGC	2292	949 bp	MAOH1-5a
MAOH13aR	GTAACCGTGTTGGGGACGGTCAC	3241		
MAOH13aF	CGCTTTGGTCCAGATCTACA	3068	942 bp	MAOH1-6
MAOH13R	CTAGGCAACTGGGATGGACC	4010		

Table 16 – Summary of the primers designed for the RT-PCR amplification of aldehyde oxidase homologue 1 cDNA.

*reading 5`-3` from left to right ** bp at which the 5` base of the primer binds, +1 represents the A of the ATG start codon. ***based on mouse AOH1 cDNA sequence (Terao *et al.*, 2000). F and R signify sense and antisense primers respectively.

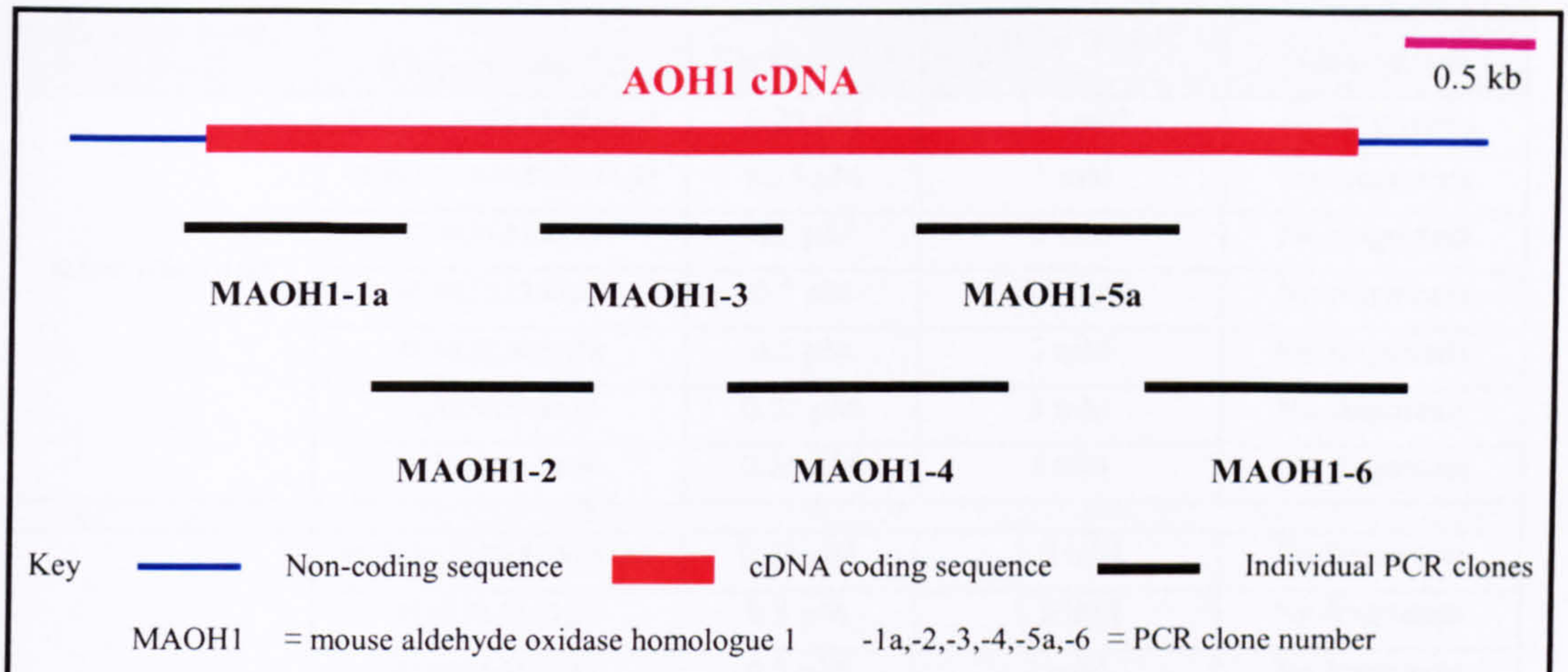

Figure 18 – Diagram showing the degree of overlap between the predicted aldehyde oxidase homologue 1 PCR clones.

3.4.3 Optimization of the RT-PCR primers for amplification of the individual clones of rat aldehyde oxidase homologue 1 cDNA.

The cDNA was cloned from the Wistar rat RNA in the first instance as the cellulose acetate electrophoresis (figure 17) demonstrated the presence of the enzyme therefore the AOH1 mRNA should also be present. As the enzyme activity was absent in the SD and Fischer strains it was possible that this was due to the lack of AOH1 mRNA synthesis. The primers were then optimised in a similar manner as for the DNA amplification. Table 17 shows a summary of the conditions used and the results obtained with the optimal conditions for each primer pair are highlighted.

Despite many different conditions being used to attempt to clone the MAOH1-1a and the MAOH1-5 fragments these could not be optimised. As the primers were designed to the mouse AOH1 cDNA sequence and not the rat it is reasonable to presume that one of the primers is binding in a non-conserved region. Therefore new primers needed to be designed in the hope that they will bind in a conserved region resulting in a successful amplification.

Primers used	Annealing temperatures °C	Primer conc.**	$MgCl_2$ Conc.**	Fragments Generated
MAO11F/ MAO11aR	47,49,51,53,55,57,59,61,63	0.25 pM	1.5 mM	No fragments
	47,49,51,53,55,57,59,61,63	0.25 pM	1 mM	No fragments
	47,49,51,53,55,57	0.5 pM	2 mM	No fragments
	47,49,51,53,55,57	0.5 pM	2.5 mM	No fragments
	48,50,52,54,56,58	0.5 pM	3 mM	No fragments
	53,55,57,59,61,63	0.25 pM	3 mM	No fragments
	50,52,54,56,58,60	0.25 pM	2 mM	No fragments
MAOH11aF/ MAOH11R	47,49,51,53,55,57,59,61,63	0.25 pM	1.5 mM	No fragments
	47,49,51,53,55,57	0.5 pM	1.5 mM	No fragments
	47,49,51,53,55,57	0.5 pM	2 mM	No fragments
	47,49,51,53,55,57	0.5 pM	2.5 mM	Several fragments
	48.50.52.54.56.58	0.5 pM	3 mM	No Fragments
	53,55,57,59,61,63	0.25 pM	2.5 mM	~800 bp fragment
MAOH12F/ MAOH12aR	47,49,51,53,55,57	0.25 pM	1.5 mM	~900 bp fragment
MAOH12aF/ MAOH12R	47,49,51,53,55,57	0.25 pM	1.5 mM	~1 kb fragment
MAOH13F/ MAOH13aR	47,49,51,53,55,57,59,61,63	0.25 pM	1.5 mM	Several fragments
	47,49,51,53,55,57	0.25 pM	1 mM	Several fragments
	47,49,51,53,55,57	0.5 pM	2 mM	Several fragments
	47,49,51,53,55,57	0.5 pM	2.5 mM	Several fragments
	48,50,52,54,56,58	0.5 pM	3 mM	Several fragments
	50,52,54,56,58,60	0.25 pM	2 mM	Several fragments
	53,55,57,59,61,63	0.25 pM	3 mM	No fragments
MAOH13aF/ MAOH13R	47,49,51,53,55,57,59,61,63	0.25 pM	1.5 mM	No fragments
	47,49,51,53,55,57	0.25 pM	1mM	Several fragments
	47,49,51,53,55,57	0.5 pM	2 mM	Several fragments
	47,49,51,53,55,57	0.5 pM	2 mM	Several fragments
	48,50,52,54,56,58	0.5 pM	3 mM	Several fragments
	53,55,57,59,61,63	0.25 pM	3 mM	Several fragments
	50,52,54,56,58,60	0.25 pM	3 mM	Several fragments
	57, 59,61,63,65,67	0.25 pM	1 mM	~950 bp fragment

Table 17 – Summary of the conditions used and outcomes for PCR of the aldehyde oxidase homologue 1 cDNA clones.

This table shows the optimisation process for primer sets MAOH-1a, MAOH1-2, MAOH1-3, MAOH1-4, MAOH1-5a and MAOH1-6. It illustrates the annealing temperatures used with each set of conditions and the outcomes from each set of conditions used. The optimal conditions for each primer pair are highlighted. ** concentration.

3.4.4 Design of the new RT-PCR primers for amplification of the individual clones of rat aldehyde oxidase homologue 1 cDNA.

As MAOH-1a fragment could not be optimised new primers were designed using the rat AOH1 cDNA sequence obtained from product MAOH1-2 to design the reverse primer. The mouse AOH1 sequence had to be used for the forward primer, as this was the only information available for the start of the sequence. New primers were designed for MAOH1-5 from the Wistar sequence obtained from MAOH1-4 and MAOH1-6 cDNA clones (table 18 and figure 19).

Primer Code	Primer Sequence*	bp at which primers start and finish**	Expected product Size	Code for PCR product
MAOH11cF	AGAGCACAGCAGTTCCATCTGAG	-81	856 bp ***	MAOH1-1b
RAOH11bR	GTGTTGCCAATCACGAGTGGAC	775		
RAOH5F	ATCAAGGCAGCAGACATCCA	2780	772 bp	RAOH1-5
RAOH5R	CAGTCACCATTAGGATTCTGG	3552		

Table 18 – Summary of the primers designed for the RT-PCR amplification of rat aldehyde oxidase homologue 1 cDNA (revised).

*reading 5`-3` from left to right ** bp at which the 5` base of the primer binds, +1 represents the A of the ATG start codon.***if similar to mouse AOH1 (Terao *et al.*, 2000). F and R signify sense and antisense primers respectively.

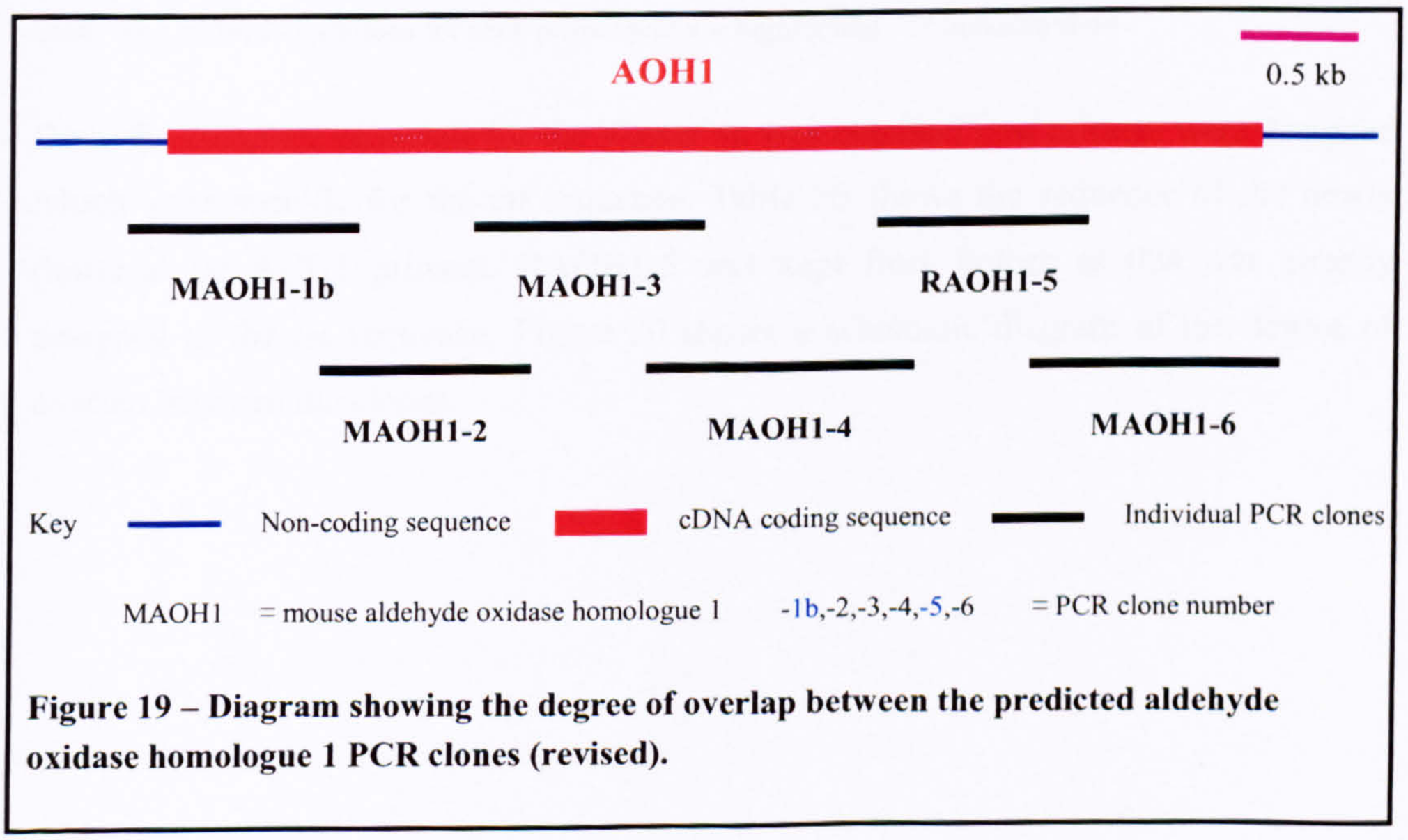

Figure 19 – Diagram showing the degree of overlap between the predicted aldehyde oxidase homologue 1 PCR clones (revised).

3.4.5 Optimization of the new RT-PCR primers for amplification of the individual clones of rat aldehyde oxidase homologue 1 cDNA.

The new primers were then optimised in the same way as for the previous amplifications (table 19). Once again the optimal conditions for each primer pair are highlighted in yellow.

Primers used	Annealing temperatures °C	Primer conc.**	$MgCl_2$ Conc.**	Fragments Generated
MAOH11cF/ RAOH11bR	52,54,56,58,60,62	0.25pM	1.5mM	No fragments
	52,54,56,58,60,62	0.5pM	1.5mM	Many fragments
	52,54,56,58,60,62	0.25pM	1mM	No fragments
	48,50,52,54,56,58	0.25pM	1mM	No fragments
	52,54,56,58,60,62	0.5pM	1mM	No fragments
	53,55,57,59,61,63	0.5pM	2mM	~900bp fragment
RAOH5F/ RAOH5R	48,50,52,54,56,58	0.25pM	1.5mM	~750bp fragment

Table 19 Summary of the conditions used and outcomes for PCR of the MAOH1-1b and RAOH1-5 cDNA clones.

This table shows the optimisation process for primer sets MAOH-1b and RAOH1-5. It illustrates the annealing temperatures used with each set of conditions and the outcomes from each set of conditions used. The optimal conditions for each primer pair are highlighted. ** concentration

Once the complete sequence for the Wistar rat was obtained new primers were designed which were specific for the rat sequence. Table 20 shows the sequence of the newly designed rat AOH1 primers. RAOH1-5 was kept from before as this was already designed to the rat sequence. Figure 20 shows a schematic diagram of the degree of overlap between the clones.

Primer Code	Primer Sequence*	bp at which primers start and finish**	Expected product Size	Code for PCR product
MAOH11bF	CGTCTGTCTATTGAACAACG	-52	512bp	RAOH1-A
RAOH11cR	GAGTTAGGGATGAAACTTCTCG	564		
RAOH11F	TACAGTAGAAGGCATAGGAAGC	270	897 bp	RAOH1-1
RAOH11R	TTGCTGTGTTCCTTCTGTTG	1167		
RAOH12F	TCTCCTGAAGCACCTGAG	1008	852 bp	RAOH1-2
RAOH12R	ATGTGGCTTGCTGCTGGTTACC	1860		
RAOH13F	ACACCATTACAGACTTGAGC	1361	676 bp	RAOH1-3
RAOH13R	AGCATACGAGTCAGCAGC	2037		
RAOH14F	GTGTGGTTGATGTGATAACAGC	1907	747 bp	RAOH1-4
RAOH14R	GCATACTCTATCACCAGTTCAG	2654		
RAOH16F	ACTGGTGCCGATGTCAAC	3253	590 bp	RAOH1-6
RAOH16R	GGCAGCAGCAATAGCGAAGAAC	3843		

Table 20 – Summary of the primers designed for the RT-PCR amplification of rat aldehyde oxidase homologue 1 cDNA.

*reading 5`-3` from left to right, ** bp at which the 5` base of the primer binds, +1 represents the A of the ATG start codon. F and R signify sense and antisense primers respectively.

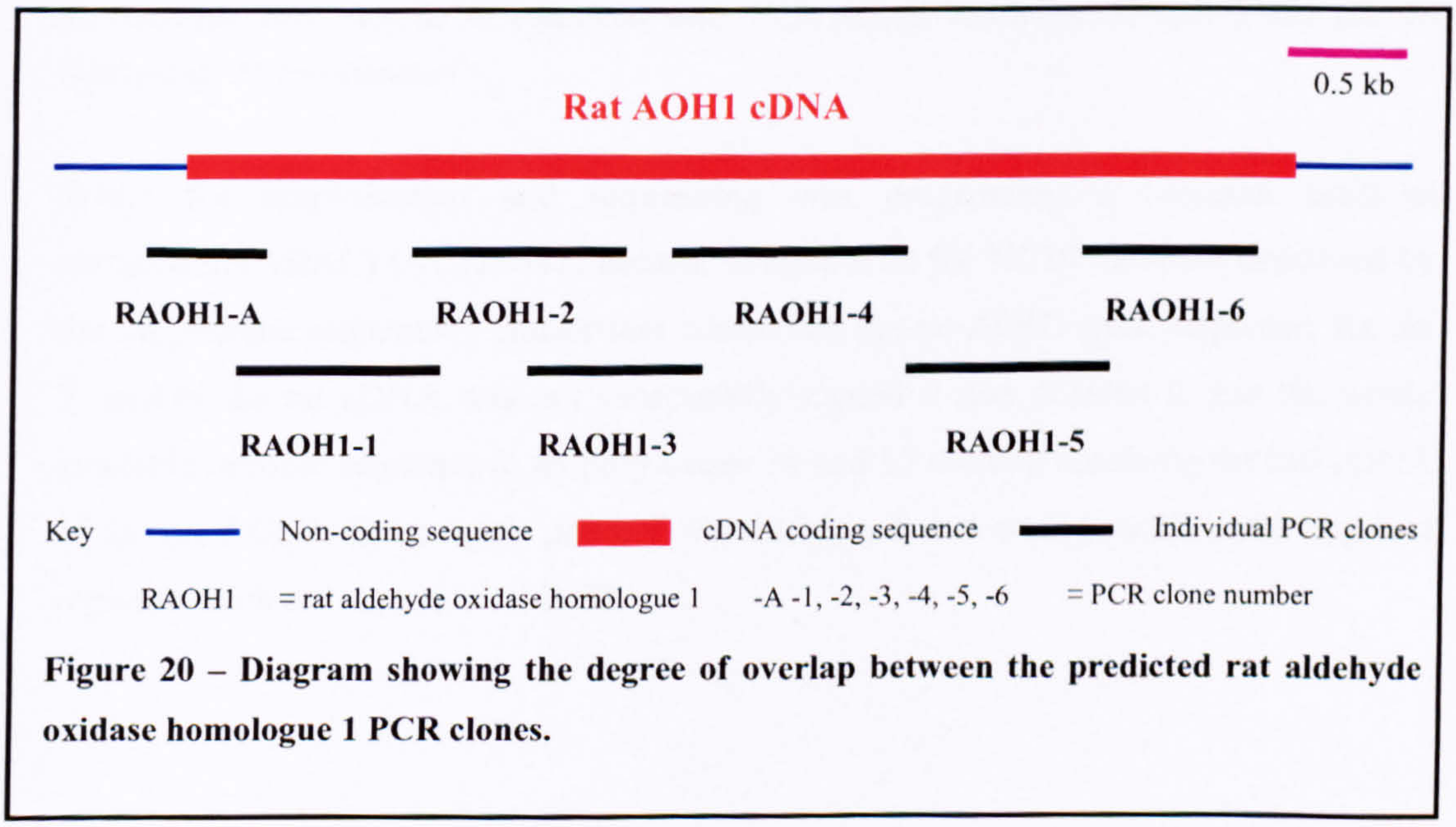

Figure 20 – Diagram showing the degree of overlap between the predicted rat aldehyde oxidase homologue 1 PCR clones.

The primers were then optimised in the same way as for the DNA amplifications (table 21). The highlighted rows indicate the optimal conditions for each primer pair.

Primers used	Annealing temperatures °C	Primer conc.**	$MgCl_2$ Conc.**	Fragments Generated
MAO11cF/ RAO11cR	51,53,55,57,59,61,63	0.25 pM	1.5 mM	No fragments
	51,53,55,57,59,61,63	0.25 pM	1 mM	No fragments
	47,49,51,53,55,57	0.5 pM	1 mM	~ 500 bp fragment
RAOH11F/RAOH11R	51,53,55,57,59,61,63	0.25 pM	1.5 mM	No fragments
	51,53,55,57,59,61,63	0.25 pM	1 mM	No fragments
	48,50,52,54	0.5 pM	1 mM	~900 bp fragment
RAOH12F/RAOH12R	51,53,55,57,59,61,63	0.25 pM	1.5 mM	No fragments
	47,49,	0.25 pM	1.5 mM	~850 bp fragment
RAOH13F/RAOH13R	54,56,58,60,62	0.25 pM	1.5 mM	~700 bp fragment
RAOH14F/RAOH14R	51,53,55,57,59,61,63	0.25 pM	1.5 mM	~750 bp fragment
RAOH16F/RAOH16R	51,53,55,57,59,61,63	0.25 pM	1.5 mM	~600 bp fragment

Table 21 - Summary of the conditions used and outcomes for the RT-PCR of the RAOH1-A, RAOH1-1 to RAOH1-4 and RAOH1-6 cDNA clones.

This table shows the optimisation process for primer sets RAOH1-A, RAOH1-1, RAOH1-2, RAOH1-3, RAOH1-4 and RAOH1-6. It illustrates the annealing temperatures used with each set of conditions and the outcomes from each set of conditions used. The optimal conditions for each primer pair are highlighted. ** concentration

While the amplification and sequencing was progressing a bacterial artificial chromosome (BAC) (AC126841) became available on the NCBI database deposited by the rat genome sequencing consortium containing the rat AOH1 gene sequence. As the 3` end of the rat cDNA was not successfully cloned it was decided to use the newly available intronic sequence to amplify exons 34 and 35 thereby acquiring the full cDNA of the rat AOH1. Once again primers were designed that would amplify the required regions which are shown in table 22.

Primer Code	Primer Sequence*	exon covered	Expected product Size	Code for PCR product
RAOH1E34F	TCTTCAGAGTCACTGCGTCAGC	34	476 bp	RAOH1E34
RAOH1E34R	GGTGAAGAAGGTAGATTGTGAC			
RAOH1E35F	TTGCCTTACTATGCCAAG	35	543 bp	RAOH1E35
RAOH1E35R	TACACACAGCATCACAATACCG			

Table 22 – Summary of the primers designed for the PCR amplification of rat aldehyde oxidase homologue 1 exons 34 and 35.

*reading 5`-3`. F and R signify sense and antisense primers respectively

Once again these primers were optimised in the same way as before and the optimal conditions are highlighted in yellow in table 23.

Primers used	Annealing temperatures °C	Primer conc.**	$MgCl_2$ Conc.**	Fragments Generated
RAOH1E34F/ RAOH1E34F	48,50,52,54,56,58	0.25 pM	1.5 mM	~500bp fragment
RAOH1E35F/ RAOH1E35F	48,50,52,54,56,58	0.25 pM	1.5 mM	~550bp fragment

Table 23 - Summary of the conditions used and outcomes for PCR amplification of exons 34 and 35 of rat aldehyde oxidase homologue 1.

This table shows the optimisation process for primer sets RAOH1E34 and RAOH1E35. It illustrates the annealing temperatures used with each set of conditions and the outcomes from each set of conditions used. The optimal conditions for each primer pair are highlighted. ** concentration.

3.4.6 Differences found between Sprague Dawley and Wistar strains of rat in the aldehyde oxidase homologue 1 cDNA.

The optimised RT-PCR conditions were used to amplify Wistar, Fischer and SD rat liver cDNA in both male and female animals. These clones were then subjected to DNA sequencing and the sequences obtained were used to make a contig of the complete cDNA sequence from each strain. The sequences obtained from the different rat strains were aligned and the changes found were noted (figures 21 and 22, table 24). Figure 21 over the next two pages shows the sequence of rat liver AOH1 obtained from the Wistar strain. The differences found between the strains are indicated as are the various cofactor binding sites and domains.

```
   Met Ser Arg Ser Lys Glu Ser Asp Glu Leu Ile Phe Phe Val Asn Gly Lys Lys Val Ile Glu Arg Asn Ala Asp Pro Glu Val     28
 1 ATG TCT CGT TCT AAG GAG TCA GAT GAG CTC ATT TTC TTT GTG AAT GGG AAA AAA GTC ATT GAG AGG AAT GCA GAC CCT GAG GTT

   Asn Leu Leu Phe Tyr Leu Arg Lys Ile Ile Arg Leu Thr Gly Thr Lys Tyr Gly Cys Gly Gly Gly Asp Cys Gly Ala Cys Thr     56
 85 AAT TTA TTG TTC TAT TTG AGA AAA ATC ATC CGA CTC ACA GGG ACA AAG TAT GGC TGT GGA GGA GGT GAC TGT GGC GCC TGC ACA
                                          Gln                                                   Gly
                                          CAA                                                   GGT

   Val Met Ile Ser Arg Tyr Asn Pro Ile Ser Lys Lys Ile Ser His Phe Ser Ala Ala Ala Cys Leu Val Pro Ile Cys Ser Leu     84
169 GTG ATG ATC TCA AGA TAC AAC CCC ATC TCC AAA AAG ATC AGT CAT TTC TCC GCC GCT GCC TGC CTG GTC CCC ATC TGC TCT CTC

   His Gly Ala Ala Val Thr Thr Val Glu Gly Ile Gly Ser Thr Lys Thr Arg Ile His Pro Val Gln Glu Arg Ile Ala Lys Gly    112
253 CAT GGG GCT GCT GTC ACT ACA GTA GAA GGC ATA GGA AGC ACC AAA ACC AGA ATA CAC CCT GTC CAG GAA AGG ATT GCT AAA GGC

   His Gly Thr Gln Cys Gly Phe Cys Thr Pro Gly Met Val Met Ser Ile Tyr Thr Leu Leu Arg Asn His Pro Glu Pro Ser Thr    140
337 CAT GGT ACC CAG TGT GGA TTC TGC ACT CCC GGG ATG GTG ATG AGC ATC TAC ACT CTC CTG AGA AAC CAC CCG GAG CCC TCC ACG

   Glu Gln Ile Met Glu Thr Leu Gly Gly Asn Leu Cys Arg Cys Thr Gly Tyr Arg Pro Ile Val Glu Ser Ala Arg Ser Phe Ser    168
421 GAA CAG ATA ATG GAA ACC TTG GGT GGG AAT CTA TGC CGT TGC ACT GGA TAC AGG CCC ATT GTG GAG AGT GCG AGA AGT TTC AGC
                                             His
                                             CAT

   Pro Asn Ser Ala Cys Cys Pro Met Asn Glu Lys Trp Lys Cys Cys Leu Asp Glu Gly Lys Asn Glu Pro Glu Arg Lys Asn Ser    196
505 CCT AAC TCA GCT TGC TGC CCG ATG AAT GAG AAA TGG AAA TGT TGC TTG GAT GAA GGA AAA AAC GAG CCT GAG AGA AAA AAC AGT

   Val Cys Thr Lys Leu Tyr Glu Lys Glu Glu Phe Gln Pro Leu Asp Pro Thr Gln Glu Leu Ile Phe Pro Pro Glu Leu Met Arg    224
589 GTT TGC ACC AAG TTA TAT GAA AAA GAA GAA TTT CAA CCC TTG GAC CCA ACT CAG GAG CTT ATA TTT CCA CCT GAA CTG ATG AGA

   Met Ala Glu Asp Ser Pro Asn Thr Val Leu Thr Phe Arg Gly Glu Arg Thr Thr Trp Ile Ala Pro Gly Thr Leu Asn Asp Leu    252
673 ATG GCA GAG GAT TCC CCA AAT ACA GTT CTG ACT TTC CGT GGG GAA AGG ACG ACC TGG ATT GCC CCA GGA ACC CTA AAT GAC CTT

   Leu Glu Leu Lys Met Glu Tyr Pro Ser Ala Pro Leu Val Ile Gly Asn Thr Cys Leu Gly Leu Asp Met Lys Phe Lys Asp Val    280
757 CTG GAA CTG AAA ATG GAG TAC CCC AGT GCT CCG CTC GTG ATC GGC AAC ACG TGT CTT GGG CTT GAT ATG AAG TTC AAA GAC GTT

   Ser Tyr Pro Ile Ile Ile Ser Pro Ala Arg Ile Leu Glu Leu Phe Val Val Thr Asn Thr Asn Glu Gly Leu Thr Leu Gly Ala    308
841 TCT TAT CCA ATT ATC ATC TCT CCT GCA AGG ATC TTA GAA TTA TTT GTG GTG ACT AAT ACA AAT GAA GGG CTG ACA CTG GGC GCT

   Gly Leu Ser Leu Thr Gln Val Lys Asn Ile Leu Ser Asp Val Val Ser Arg Leu Pro Lys Glu Arg Thr Gln Thr Tyr Arg Ala    336
925 GGC CTC AGC CTG ACC CAG GTG AAG AAT ATC TTG TCT GAT GTG GTC TCC AGG CTC CCG AAG GAG AGG ACG CAG ACA TAC CGT GCT

   Leu Leu Lys His Leu Arg Thr Leu Ala Gly Gln Gln Ile Arg Asn Val Ala Ser Leu Gly Gly His Ile Ile Ser Arg Leu Pro    364
1009 CTC CTG AAG CAC CTG AGG ACT CTG GCT GGG CAG CAG ATC AGG AAT GTG GCT TCC TTA GGT GGT CAT ATT ATC AGT AGA CTG CCG
                                          Gln
                                          CAA

   Thr Ser Asp Leu Asn Pro Ile Phe Gly Val Gly Asn Cys Lys Leu Asn Val Ala Ser Thr Glu Gly Thr Gln Gln Ile Pro Leu    392
1093 ACC TCT GAC CTC AAC CCT ATT TTC GGT GTA GGC AAT TGC AAA CTC AAT GTT GCT TCA ACA GAA GGA ACA CAG CAA ATC CCT CTG

   Asn Asp His Phe Leu Ala Gly Val Pro Glu Ala Ile Leu Lys Pro Glu Gln Val Leu Ile Ser Val Phe Val Pro Leu Ser Arg    420
1177 AAC GAT CAT TTT CTC GCT GGA GTC CCA GAA GCC ATC CTG AAG CCA GAG CAA GTG CTC ATC TCG GTT TTC GTG CCC CTC TCC AGG
                                       Glu
                                       GAG

   Lys Trp Glu Phe Val Ser Ala Phe Arg Gln Ala Pro Arg Gln Gln Asn Ala Phe Ala Ile Val Asn Ala Gly Met Arg Val Ala    448
1261 AAG TGG GAG TTC GTA TCA GCT TTC AGA CAG GCC CCG CGT CAG CAA AAT GCG TTT GCG ATA GTG AAT GCT GGA ATG CGA GTC GCT

   Phe Lys Glu Asp Thr Asn Thr Ile Thr Asp Leu Ser Ile Leu Tyr Gly Gly Ile Gly Ala Thr Val Val Ser Ala Lys Ser Cys    476
1345 TTC AAA GAG GAT ACA AAC ACC ATT ACA GAC TTG AGC ATC TTA TAT GGA GGG ATC GGT GCC ACT GTA GTC AGC GCC AAG TCC TGC
                                                            Ile
                                                            ATT

   Gln Gln Leu Ile Gly Arg Cys Trp Asp Glu Glu Met Leu Asp Asp Ala Gly Arg Met Ile Arg Glu Glu Val Ser Leu Leu Thr    504
1429 CAG CAG CTG ATT GGA AGG TGT TGG GAT GAG GAA ATG CTG GAT GAC GCT GGC CGG ATG ATT CGT GAA GAA GTC TCC CTC CTC ACA

   Ala Ala Pro Gly Gly Met Val Glu Tyr Arg Lys Thr Leu Ala Ile Ser Phe Leu Phe Lys Phe Tyr Leu Asp Val Leu Lys Gln    532
1513 GCA GCC CCC GGA GGA ATG GTG GAA TAC CGG AAG ACC CTT GCC ATC AGT TTC CTC TTC AAG TTT TAC TTA GAT GTG TTG AAG CAG

   Leu Lys Arg Arg Asn Pro His Arg Cys Pro Asp Ile Ser Gln Lys Leu Leu Gln Val Leu Glu Asp Phe Pro Leu Thr Met Pro    560
1597 CTA AAG AGG AGG AAT CCC CAT AGG TGC CCT GAC ATC TCG CAG AAA CTC CTA CAG GTT CTG GAA GAC TTT CCT TTG ACC ATG CCT
                                                   Ser
                                                   TCA

   His Gly Thr Gln Ser Phe Lys Asp Val Asp Ser Gln Gln Pro Leu Gln Asp Pro Val Gly Arg Pro Ile Met His Gln Ser Gly    588
1681 CAT GGG ACA CAG TCA TTT AAA GAT GTA GAC TCC CAG CAG CCT CTG CAA GAC CCA GTC GGG CGT CCC ATC ATG CAT CAG TCC GGC
                                                                                          Ser
                                                                                          TCT

   Ile Lys His Ala Thr Gly Glu Ala Val Phe Cys Asp Asp Met Ser Val Leu Ala Gly Glu Leu Phe Leu Ala Val Val Thr Ser    616
1765 ATC AAA CAC GCC ACA GGG GAG GCC GTA TTT TGT GAT GAT ATG TCT GTG TTG GCA GGG GAA CTC TTC TTG GCT GTG GTA ACC AGC

   Ser Lys Pro His Ala Arg Ile Ile Ser Leu Asp Ala Ser Glu Ala Leu Ala Ser Pro Gly Val Val Asp Val Ile Thr Ala Gln    644
1849 AGC AAG CCA CAT GCT AGA ATC ATC TCC CTC GAT GCC TCC GAG GCC TTG GCA TCA CCT GGT GTG GTT GAT GTG ATA ACA GCT CAA

   Asp Val Pro Gly Asp Asn Gly Arg Glu Glu Glu Ser Leu Tyr Ala Gln Asp Glu Val Ile Cys Val Gly Gln Ile Val Cys Ala    672
1933 GAT GTG CCT GGT GAC AAT GGC AGA GAA GAG GAA AGC CTG TAT GCA CAG GAT GAG GTG ATC TGC GTG GGT CAG ATT GTC TGC GCC

   Val Ala Ala Asp Ser Tyr Ala Arg Ala Lys Gln Ala Thr Lys Lys Val Lys Ile Val Tyr Glu Asp Met Glu Pro Met Ile Val    700
2017 GTG GCT GCT GAC TCG TAT GCT CGC GCC AAG CAG GCC ACA AAA AAA GTA AAG ATT GTC TAT GAA GAC ATG GAG CCC ATG ATT GTG

   Thr Val Gln Asp Ala Leu Gln His Glu Ser Phe Ile Gly Pro Glu Lys Lys Leu Glu Gln Gly Asn Val Gln Leu Ala Phe Gln    728
2101 ACG GTT CAG GAT GCA CTG CAA CAT GAA TCA TTC ATT GGA CCT GAA AAA AAA CTA GAA CAA GGA AAT GTC CAG TTA GCA TTT CAA

   Ser Ala Asp Gln Ile Leu Glu Gly Glu Val His Leu Gly Gly Gln Glu His Phe Tyr Met Glu Thr Gln Ser Val Arg Val Ile    756
2185 AGT GCT GAT CAA ATC CTC GAA GGG GAA GTG CAC TTG GGA GGC CAG GAG CAT TTT TAC ATG GAG ACT CAA AGC GTA CGA GTG ATC
           Asp
           GAC

   Pro Lys Gly Glu Asp Met Glu Met Asp Ile Tyr Val Ser Ser Gln Asp Ala Ala Phe Thr Gln Glu Met Val Ala Arg Thr Leu    784
2269 CCC AAG GGA GAG GAC ATG GAG ATG GAC ATA TAT GTG TCC AGC CAG GAT GCA GCG TTT ACC CAG GAA ATG GTG GCT CGA ACC TTG
```

```
     Gly Ile Pro Lys Asn Arg Ile Thr Cys His Val Lys Arg Val Gly Gly Ala Phe Gly Gly Lys Thr Ser Lys Pro Gly Leu Leu   812
2353 GGC ATC CCA AAG AAC AGG ATC ACC TGC CAC GTG AAA AGG GTT GGT GGA GCC TTC GGA GGG AAA ACG AGC AAA CCT GGG CTC CTG
     Asp
     GAC

     Ala Ser Val Ala Ala Val Ala Ala Gln Lys Thr Gly Arg Pro Ile Arg Phe Ile Leu Glu Arg Gly Asp Asp Met Leu Ile Thr   840
2437 GCA TCA GTG GCA GCT GTG GCC GCA CAG AAG ACC GGC CGC CCA ATC CGT TTT ATT CTA GAG CGT GGG GAT GAC ATG TTG ATA ACG
         Ser
         TCG

     Gly Gly Arg His Pro Leu Leu Gly Lys Tyr Arg Val Gly Phe Met Asn Asn Gly Lys Ile Lys Ala Ala Asp Ile Gln Leu Tyr   868
2521 GGA GGA CGT CAC CCA CTA CTC GGG AAA TAC AGG GTT GGC TTC ATG AAC AAT GGG AAA ATC AAG GCA GCA GAC ATC CAG CTT TAT
                                                             Lys
                                                             AAG

     Ile Asn Gly Gly Cys Thr Pro Asp Asp Ser Glu Leu Val Ile Glu Tyr Ala Leu Leu Lys Leu Glu Asn Ala Tyr Lys Ile Pro   896
2605 ATC AAC GGA GGC TGC ACC CCA GAT GAT TCT GAA CTG GTG ATA GAA TAT GCT TTG CTC AAA CTG GAA AAT GCG TAC AAG ATC CCC

     Asn Leu Arg Val Arg Gly Arg Val Cys Lys Thr Asn Leu Pro Ser Asn Thr Ala Phe Arg Gly Phe Gly Phe Pro Gln Gly Ala   924
2689 AAC CTC CGT GTC CGA GGT CGC GTC TGT AAG ACC AAC TTG CCA TCC AAT ACA GCA TTT CGG GGA TTT GGT TTT CCC CAG GGG GCA
                                                             AlA
                                                             GCG

     Phe Val Thr Glu Thr Trp Val Ser Ala Val Ala Ala Gln Cys His Leu Pro Pro Glu Lys Val Arg Glu Leu Asn Met Tyr Lys   952
2773 TTC GTA ACA GAA ACC TGG GTG TCA GCT GTG GCA GCC CAA TGC CAC TTG CCA CCA GAG AAG GTT CGA GAG TTA AAC ATG TAC AAA
                                                   Lys
                                                   AAA

     Thr Ile Asp Arg Thr Ile His Lys Gln Glu Phe Asp Pro Thr Asn Leu Ile Lys Cys Trp Glu Thr Cys Met Glu Asn Ser Ser   980
2857 ACA ATC GAC AGG ACA ATT CAC AAG CAA GAA TTT GAC CCA ACG AAT CTG ATA AAG TGC TGG GAG ACA TGT ATG GAA AAT TCT TCC

     Tyr Tyr Ser Arg Lys Lys Ala Val Asp Glu Phe Asn Gln Gln Ser Phe Trp Lys Lys Arg Gly Ile Ala Ile Ile Pro Met Lys  1008
2941 TAC TAC AGC AGA AAG AAG GCT GTA GAT GAA TTT AAC CAG CAG AGT TTT TGG AAG AAG AGA GGA ATT GCC ATC ATC CCC ATG AAG

     Phe Ser Val Gly Phe Pro Lys Thr Phe Tyr His Gln Ala Ala Ala Leu Val Gln Ile Tyr Thr Asp Gly Ser Val Leu Val Ala  1036
3025 TTC TCA GTT GGA TTT CCA AAG ACA TTT TAT CAT CAG GCT GCT GCT TTG GTC CAG ATC TAC ACA GAT GGG TCT GTG CTA GTT GCT
                                                                                          Val
                                                                                          GTA

     His Gly Gly Val Glu Leu Gly Gln Gly Ile Asn Thr Lys Met Ile Gln Val Ala Ser Arg Glu Leu Lys Ile Pro Met Ser Tyr  1064
3109 CAT GGT GGT GTT GAA CTG GGA CAA GGT ATT AAC ACC AAA ATG ATA CAG GTG GCC AGC CGT GAA TTA AAA ATA CCA ATG TCT TAT
                                                             Ala
                                                             GCT

     Ile His Leu Asp Glu Met Asn Thr Met Thr Val Pro Asn Met Ile Thr Thr Gly Gly Ser Thr Gly Ala Asp Val Asn Gly Arg  1092
3193 ATA CAC CTG GAT GAA ATG AAC ACT ATG ACC GTC CCC AAC ATG ATT ACC ACT GGA GGC TCC ACT GGT GCC GAT GTC AAC GGG AGA
                                                   Thr
                                                   ACG

     Ala Val Gln Asn Ala Cys Gln Ile Leu Met Lys Arg Leu Glu Pro Ile Ile Ser Gln Asn Pro Asn Gly Asp Trp Glu Glu Trp  1120
3277 GCT GTT CAG AAT GCC TGT CAG ATC CTC ATG AAG CGC CTG GAA CCC ATC ATC AGC CAG AAT CCT AAT GGT GAC TGG GAA GAG TGG

     Ile Asn Glu Ala Phe Ile Gln Ser Ile Ser Leu Ser Ala Thr Gly Tyr Phe Arg Gly Tyr Gln Ala Asp Met Asp Trp Glu Lys  1148
3361 ATT AAT GAA GCT TTC ATT CAA AGC ATT AGC CTC TCT GCC ACT GGA TAT TTT AGG GGT TAC CAA GCT GAC ATG GAC TGG GAG AAG

     Gly Glu Gly Asp Ile Tyr Pro Tyr Phe Val Phe Gly Ala Ala Cys Ser Glu Val Glu Ile Asp Cys Leu Thr Gly Ala His Lys  1176
3445 GGA GAA GGT GAC ATT TAT CCC TAT TTT GTT TTT GGA GCT GCC TGT TCT GAG GTT GAA ATT GAT TGT CTG ACG GGA GCT CAC AAG

     Asn Ile Arg Thr Asp Ile Val Met Asp Gly Ser Phe Ser Ile Asn Pro Ala Val Asp Ile Gly Gln Ile Glu Gly Ala Phe Val  1204
3529 AAC ATC AGA ACT GAC ATT GTC ATG GAT GGA TCT TTC AGT ATA AAC CCT GCT GTG GAC ATA GGC CAG ATC GAA GGG GCA TTT GTT

     Gln Gly Leu Gly Leu Tyr Thr Leu Glu Glu Leu Lys Tyr Ser Pro Glu Gly Val Leu Tyr Thr Arg Gly Pro His Gln Tyr Lys  1232
3613 CAA GGT CTT GGA CTT TAT ACT CTA GAG GAA CTG AAA TAT TCC CCT GAA GGA GTC CTA TAC ACC CGT GGT CCA CAC CAG TAC AAA

     Ile Ala Ser Val Ser Asp Ile Pro Glu Glu Phe His Val Ser Leu Leu Thr Pro Thr Gln Asn Pro Lys Ala Ile Tyr Ser Ser  1260
3697 ATA GCA TCA GTT AGC GAC ATC CCA GAA GAA TTC CAT GTA TCA TTG TTG ACA CCA ACC CAA AAC CCC AAA GCC ATC TAC TCT TCT

     Lys Gly Leu Gly Glu Ala Gly Met Phe Leu Gly Ser Ser Val Phe Phe Ala Ile Ala Ala Ala Val Ala Ala Ala Arg Lys Glu  1288
3781 AAG GGC CTT GGT GAA GCT GGA ATG TTT CTA GGT TCT TCT GTG TTC TTC GCT ATT GCT GCT GCC GTG GCT GCC GCC CGC AAG GAG

     Arg Gly Leu Pro Leu Ile Leu Ala Ile Asn Ser Pro Ala Thr Ala Glu Val Ile Arg Met Ala Cys Glu Asp Gln Phe Thr Asn  1316
3865 AGA GGC CTG CCC CTG ATT TTG GCC ATA AAC AGC CCT GCC ACA GCA GAA GTA ATT CGA ATG GCC TGT GAG GAC CAG TTT ACA AAC

     Leu Val Pro Lys Thr Asp Ser Lys Cys Cys Lys Pro Trp Ser Ile Pro Val Ala                                          1334
3949 CTG GTT CCA AAA ACG GAT TCT AAA TGC TGT AAG CCA TGG TCC ATC CCA GTT GCC TGA
```

Figure 21 – Wistar aldehyde oxidase homologue 1 cDNA sequence interleaved with the deduced amino acid sequence.

The iron-sulphur, FAD and MoCo binding sites are highlighted in yellow, grey and blue respectively (Terao *et al.*, 2000). Nucleotide changes leading to an amino acid change present between Wistar and both AO-deficient strains are indicated in purple. Nucleotide changes leading to an amino acid change present between Wistar and Fisher only are indicated in blue. Nucleotide changes not leading to an amino acid change present between Wistar and both AO-deficient strains are indicated in green. Nucleotide changes not leading to an amino acid change present between Wistar and Fisher only are indicated in pink

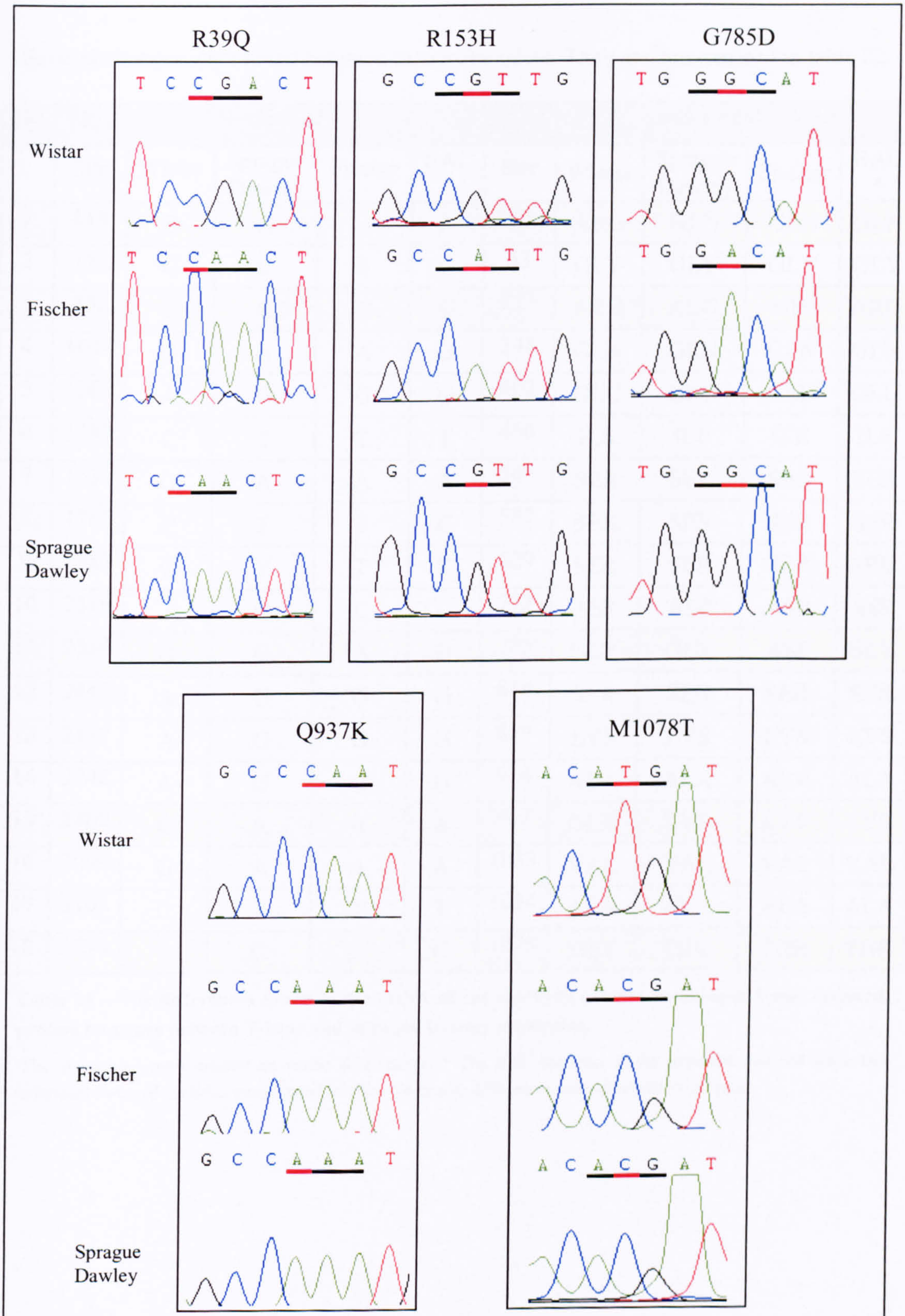

Figure 22 – Sequencing chromatogram showing the codon changes found between rat strains in the aldehyde oxidase homologue 1 cDNA.

Several changes were noted between the strains of rat. They are summarised in table 22.

No	Nucleotide					Amino Acid				
	Site	Wistar	Sprague Dawley	Fischer	BAC *	Site	Wistar	Sprague Dawley	Fischer	BAC *
1	116	G	A	A	A	39	ARG	GLN	GLN	GLN
2	159	C	C	T	C	53	GLY	GLY	GLY	GLY
3	458	G	G	A	G	153	ARG	ARG	HIS	ARG
4	1044	G	A	A	G	348	GLN	GLN	GLN	GLN
5	1206	A	G	G	G	402	GLU	GLU	GLU	GLU
6	1398	C	T	T	T	466	ILE	ILE	ILE	ILE
7	1635	G	A	A	A	545	SER	SER	SER	SER
8	1761	C	T	T	C	587	SER	SER	SER	SER
9	1887	C	T	T	T	629	SER	SER	SER	SER
10	2316	T	C	C	C	772	ASP	ASP	ASP	ASP
11	2354	G	G	A	G	785	GLY	GLY	ASP	GLY
12	2442	A	G	G	G	814	SER	SER	SER	SER
13	2577	A	G	G	G	859	LYS	LYS	LYS	LYS
14	2742	A	G	G	G	914	ALA	ALA	ALA	ALA
15	2809	C	A	A	A	937	GLN	LYS	LYS	LYS
16	3099	G	A	A	A	1033	VAL	VAL	VAL	VAL
17	3162	C	T	T	T	1054	ALA	ALA	ALA	ALA
18	3233	T	C	C	C	1078	MET	THR	THR	THR

Table 24 – The differences found in the cDNA of rat aldehyde oxidase homologue 1 and deduced protein sequence between Wistar and Sprague Dawley rat strains.

The highlighted rows indicate an amino acid change. * The BAC sequence is the sequence obtained when the individual exons of the BAC were ligated *in silico* No gender differences were observed in our rats.

3.4.7 Comparison of levels of aldehyde oxidase and aldehyde oxidase homologue 1 mRNA in the different rat strains.

During the course of the RT-PCR amplifications no significant differences were noted between the different strains in either the amount of RNA needed for a successful amplification or the amounts of product formed, however it was decided to amplify one segment of both AO and AOH1 with identical amounts of RNA simultaneously in each strain to confirm that different mRNA levels were not responsible for the differences in levels of enzyme activity, Published glyceraldehydes-3-phosphate dehydrogenase (GAPDH) primers were used to normalize for the amount of RNA in the reaction mixture. Primer sets RAO-8 and RAOH1-4 were used for amplification of AO and AOH1 mRNA respectively (figure 23). Visual inspection of the result indicated that there were no differences significant enough that would account for the loss of N-heterocycle activity in Fischer and SD rat strains.

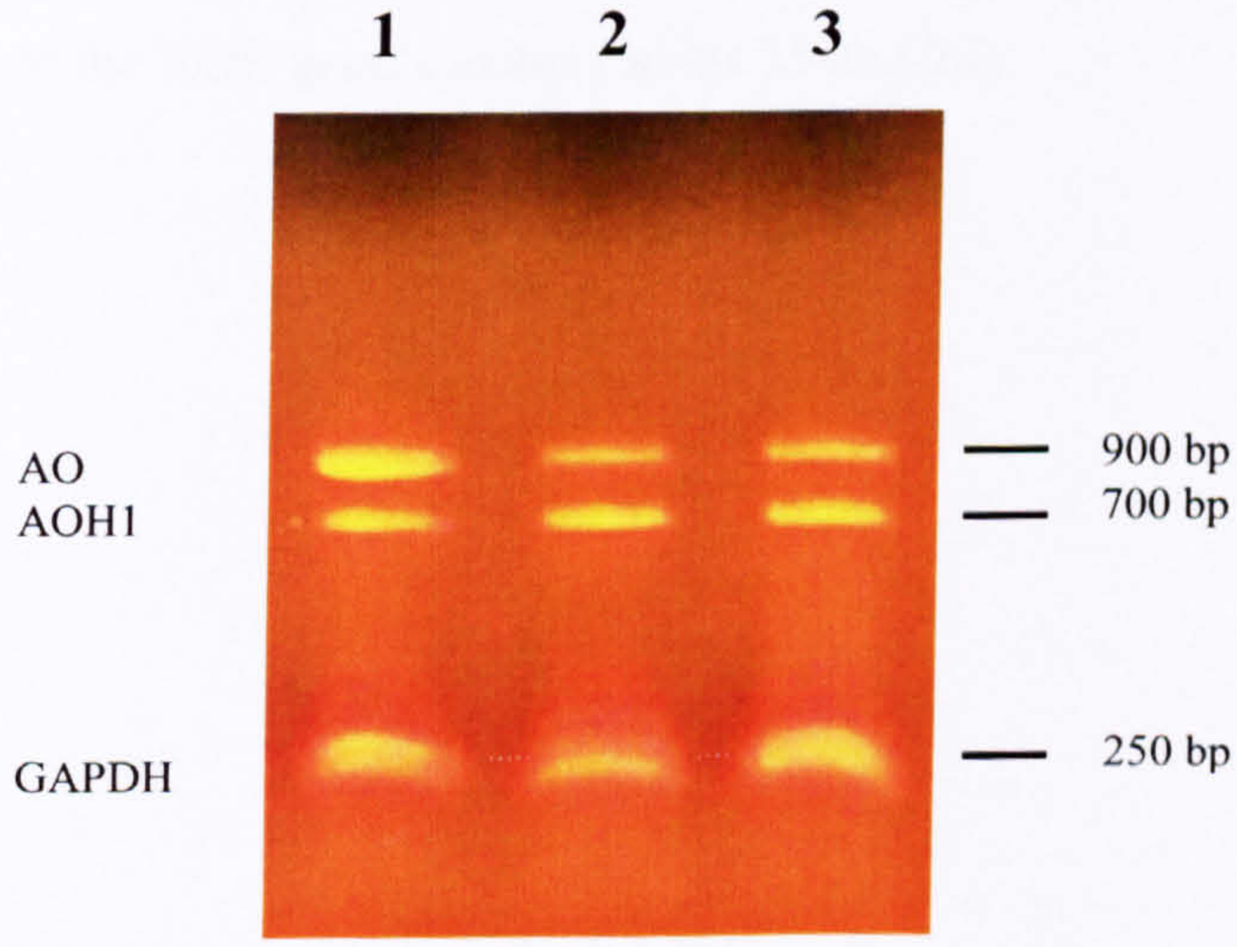

Figure 23 – Agarose gel image showing the comparison of mRNA levels of aldehyde oxidase and aldehyde oxidase homologue 1 in the different strains of rat.

Lanes 1, 2 and 3 are SD, Wistar and Fischer rat respectively The 900 bp product is AO and was amplified from primer set RAO-8, the 700 bp product is AOH1 and was amplified from primer set RAOH1-4, the 250 bp is GAPDH and was amplified using published primers as detailed in the materials and methods. The conditions used were 0.25 pM primer, 1.5 mM $MgCl_2$ at 58°C.
Published primers (Hoen *et al.*, 2000) were used for the glyceraldehydes-3-phosphate dehydrogenase (GAPDH) the sequence of these primers are

GAPDHF	TTCAACGGCACAGTCAAG
GAPDHR	CACACCCATCACAAACAT

3.5 The molecular genetic basis of hereditary xanthinuria in a British patient.

The aim of this section was to identify the molecular genetic basis of hereditary xanthinuria in a British patient. To date no European patients have been studied for the molecular genetic basis of this disease.

3.5.1 Cloning and sequencing of the human xanthine oxidoreductase gene.

As the gene sequence for human XOR was available due to the human genome sequencing project it was decided to amplify each exon individually using primers, which bind in the intron sequence. This data was obtained from two bacterial artificial chromosomes (BAC) (accession numbers AL121654 and AL121657).

In order to delineate the intron/exon boundaries in the BAC sequence the human XOR mRNA sequence was aligned with each BAC and the exon highlighted. Computer programs were used (as described in materials and methods section 2.7) to find primers that would hybridise to regions located within approximately 1 kb of intronic sequence surrounding each of the XOR gene's exons (tables 25 and 26)

Primer Code	Primer Sequence *	bp of intron covered **	Expected product size bp	Code for PCR product[$]
HXD1F	AGTGCCAAGTCAACAACCTTAC	71	548	HXDEXON1 (23a)
HXD1R	GCCTCTGAGTATCTTGTCTGTG	211		
HXD2F	TTAAACATGAGATTTAGAGG	153	664	HXDEXON2 (23a)
HXD2R	TAGGATTCTTACCTCACG	453		
HXD3F	TCACACATAGAAGACCTCAACC	330	638	HXDEXON3 (23a)
HXD3R	TTATCAGCAGTTCGGAGCCTGG	212		
HXD4F	CACTGGTAGAAGAGACAAGAAC	142	511	HXDEXON4 (23a)
HXD4R	CACCAGATTCAGTTGGCCTCTT	270		
HXD5F	TAACACTGGCTGACTGCCTG	311	579	HXDEXON5 (23a)
HXD5R	ATCTTAGTCACCACCTTGTTGG	141		
HXD6F	CTGATAGGCTAACTGATGAAGC	291	528	HXDEXON6 (23a)
HXD6R	TAAGAATGGCAGACTCTACTCC	176		
HXD7/8F	AGTGGCCTTGTTGCTCCTAT	179 329	770	HXDEXON7/8 (23b)
HXD7/8R	GGACTCACAGTACAGACCCG	49		
HXD9F	CAATGGAGTTCCTGCCTC	166	539	HXDEXON9 (23a)
HXD9R	TGAGGTCACACATCCAGCAAGG	231		
HXD10F	CCCTGGTCTACTGAGTTTCC	201	403	HXDEXON10 (23a)
HXD10R	CTTTCCCTGTGCAAGGTGAG	140		
HXD11F	TTAGGTCACTCAACCACTCTGG	167	598	HXDEXON11 (23a)
HXD11R	ACAGAATGAAGCCTATGAGTCG	282		
HXD12F	GCCAAGTTACCAGGAAGTTCAG	420	582	HXDEXON12 (23a)
HXD12R	AATGACCTATCTGGTGAGAC	68		
HXD13F	CCTACACGGAACTGGTTG	222	586	HXDEXON13 (23a)
HXD13R	ATGGCTCACTCAGGACCAAGT	255		
HXD14F	GAATGTTATCTGGAACCTCTCC	194	525	HXDEXON14 (23a)
HXD14R	TAGCAGTAGTAGCAGCAGTAGC	147		
HXD15F	ATGAGGAAACAGGCTCAATG	178	510	HXDEXON15 (23a)
HXD15R	GGTCACTCCCATTTCCAAGC	157		
HXD16F	CAAGGAAGGAGGAGAAGG	329	496	HXDEXON16 (23a)
HXD16R	AGTCATTAGCCGATGGTCAGCC	84		
HXD17F	CCTTGCTATCACTTATGCAC	175	560	HXDEXON17 (23a)
HXD17R	CATACCCTGCTTGTGCCTTA	215		
HXD18F	CCAGCAACATTCAGCTAGTGGC	219	705	HXDEXON18 (23a)
HXD18R	CACGTAGTGGTGGTATTGTG	362		
HXD19F	CCTCAATCAGTAGGATAAGG	162 483	871	HXDEXON19 (23c)
HXD19R	CAGCTCTACCTGACACAACAT	9		
HXD20F	CCATCTGGTCCTTGTGGTATTC	251	871	HXDEXON20 (23a)
HXD20R	AGAGGTAAGGCTGTCAGGC	301		

Table 25 – Summary of the primers designed for the amplification of human xanthine oxidoreductase exons 1-20.

* reading 5`-3` ** red = position of 5` nucleotide of forward primer before the start of the exon blue = position of 3` nucleotide of reverse primer after the end of the exon green = size of the intron between the exons [$] the numbers in brackets refers to figure 24 showing the binding of the primers. F and R signify sense and antisense primers respectively.

Primer Code	Primer Sequence*	bp of intron covered **	Expected product size bp	Code for PCR product[$]
HXD21F	TAGCCATTGCTTCCTGCC	110	416	HXDEXON21 (23a)
HXD21R	ATGGAACAAGGTCAGTGATACC	182		
HXD22F	AGTATTCTGTGACCAACTGC	244	783	HXDEXON22 (23a)
HXD22R	GTTACCGACAGTGTTAGAAGCC	425		
HXD23F	TATTCTGTGACCAACTGCTTGC	224	543	HXDEXON23 (23a)
HXD23R	ATCCACAGAAGTCACGAATGCC	230		
HXD24F	ATCTCTCCTACTGGCTGTGAGC	161	525	HXDEXON24 (23a)
HXD24R	ATCCACAGAAGTCACGAATGCC	279		
HXD25/26F	CAGCCCTCAAAGTTCCTACT	79 199	760	HXDEXON25/26 (23b)
HXD25/26R	AAGAGATGGCTGTGAATGAG	142		
HXD27F	GGAAGAAGAGTGTTGACAAGAC	168	544	HXDEXON27 (23a)
HXD27R	ATCTGTCCTCACTCTGTAAG	296		
HXD28F	GCTGCTGGTTCTCTTGTTCCTG	101	746	HXDEXON28 (23a)
HXD28R	GACAGGATTCACATTCACTGTTAC	549		
HXD29F	AACTCCACCAAGTGCTCC	180	719	HXDEXON29 (23a)
HXD29R	CCAGAGAGGTGTCTTCTTCC	411		
HXD30F	CATTGCTTGGAGGTAGCCTTGC	99	579	HXDEXON30 (23a)
HXD30R	TAGACTCAGACTCAAGAGATGG	406		
HXD31F	TCAGATAATGAGGACCTGGTGC	184	458	HXDEXON31 (23a)
HXD31R	GGTCTTCTGACACACAGC	222		
HXD32F	CAGTCCTGAAGACCTTGGATTC	379	719	HXDEXON32 (23a)
HXD32R	TGCTGTCACACTTCAATGGTAG	225		
HXD33F	GAACTCTACCATTGAAGTGTGAC	590	754	HXDEXON33 (23a)
HXD33R	GACAACCTTGGACAACAT	99		
HXD34F	TTGTGTCCATTGTGGCAAGTGG	79	483	HXDEXON34 (23a)
HXD34R	TACTAAGGTGCTCTCCTCAACC	216		
HXD35F	GCTTGATTGTTCTTAGCC	195	466	HXDEXON35 (23a)
HXD35R	CCAACACCTCTCCTCTGTG	144		
HXD36F	TTGGAATGATGGTTGGCAGTGG	102	498	HXDEXON36 (23a)
HXD36R	CAGACACCATCAGAACTTGAGG	18		

Table 26 – Summary of the primers designed for the amplification of human xanthine oxidoreductase exons 21-36.

* reading 5`-3` ** red = position of 5` nucleotide of forward primer before the start of the exon blue = position of 3` nucleotide of reverse primer after the end of the exon green = size of the intron between the exons. [$] the numbers in brackets refers to figure diagram showing the binding of the primers. F and R signify sense and antisense primers respectively.

Figure 24 shows a schematic representation of the primer binding in relation to the XOR gene exons for each of three different situations, primers spanning one exon, primers spanning two exons and primers spanning the splice site junction of the neighbouring exon (exon 19).

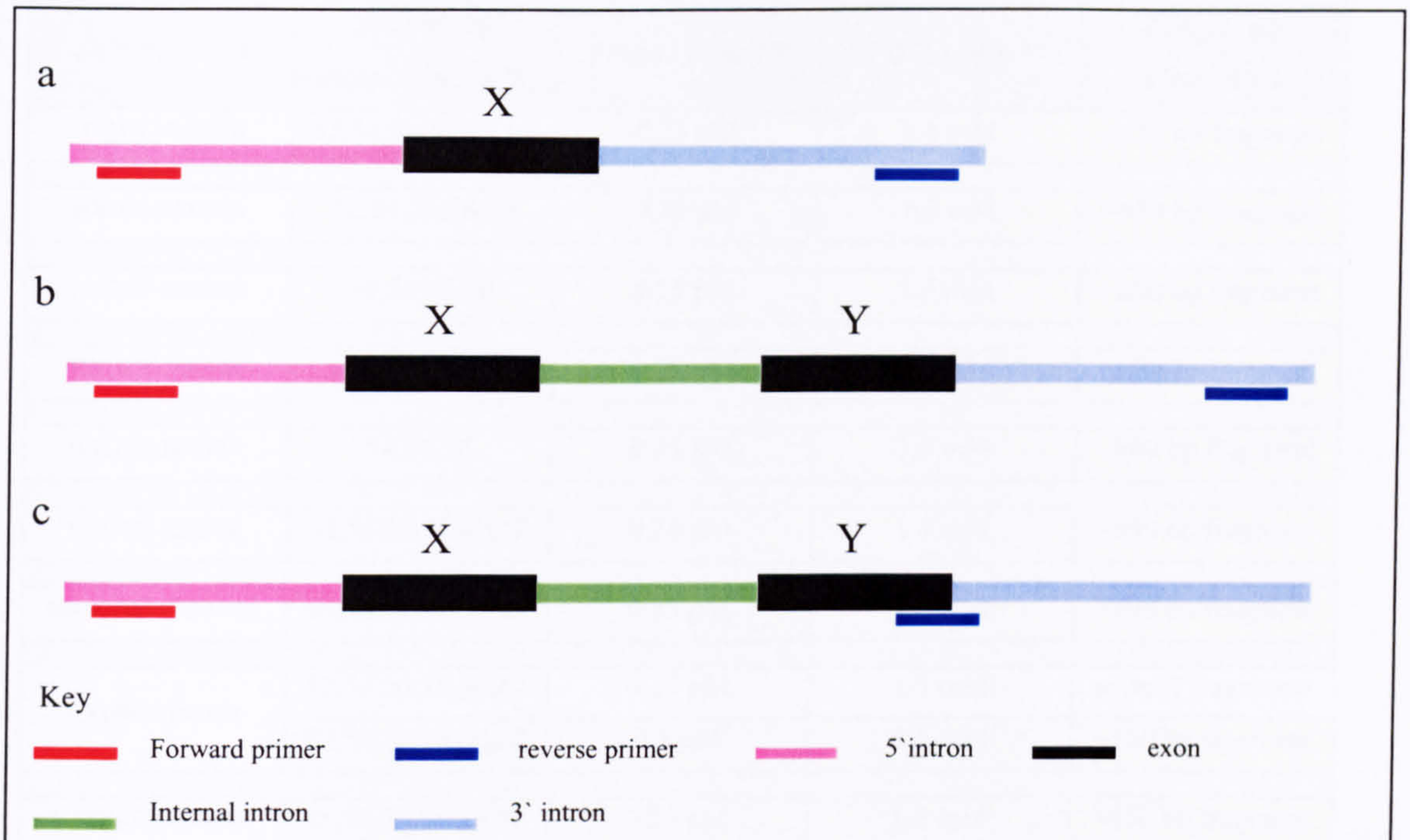

Figure 24 – Schematic diagram showing the primer binding within the introns of the xanthine oxidoreductase gene.

a Schematic representation of PCR spanning exons 1-6, 9-18, 20-24 and 27-36. X represents the exon number.

b Schematic representation of PCR spanning exons 7/8 and 25/26. X and Y represent exons 7 and 8 or 25 and 26 respectively.

c Schematic representation of PCR spanning exon 19. X and Y represent exons 19 and 20 respectively. As no suitable primer pairs could be found in spanning exon 19 primers had to be designed encompassing intron 19. The same primer pair could not be used for amplification of exon 20 as the primer spanned the 3` splice site of exon 20.

3.5.2 Optimization of the PCR for the amplification of the individual exons of human xanthine oxidoreductase.

The PCRs were optimised in the same manner as for the rat AO and AOH1 cDNAs. Tables 27 and 28 show a summary of the conditions used and the results obtained with the optimal conditions for each primer pair highlighted.

Primers used	Annealing temperatures °C	Primer conc.**	$MgCl_2$ Conc.**	Fragments Generated
HXD1F/ HXD1R	52,54,56,58,60,62	0.25 pM	1.5 mM	~550 bp fragment
HXD2F/ HXD2R	52,54,56,58,60	0.25 pM	1.5 mM	~650 bp fragment
HXD3F/ HXD3R	54,56,58,60	0.25 pM	1.5 mM	~650 bp fragment
HXD4F/ HXD4R	54,56,58,60,62	0.25 pM	1.5 mM	~500 bp fragment
HXD5F/ HXD5R	54,56,58	0.25 pM	1.5 mM	~600 bp fragment
HXD6F/ HXD6R	52,54,56,58,60,62	0.25 pM	1.5 mM	~550 bp fragment
HXD7/8F/ HXD7/8R	48,50,52,54,56,58	0.25 pM	1.5 mM	~700 bp fragment
HXD9F/ HXD9R	52,54,56,58,60,62	0.25 pM	1.5 mM	several fragments
	52,54,56,58,60,62	0.5 pM	1.5 mM	~550 bp fragment
HXD10F/ HXD10R	48,50,52,54,56,58	0.25 pM	1.5 mM	~450 bp fragment
HXD11F/ HXD11R	52,54,56,58,60,62	0.25 pM	1.5 mM	~600 bp fragment
HXD12F/ HXD12R	52,54,56,58,60,62	0.25 pM	1.5 mM	several fragments
	48,50,52,54,56,58	0.25 pM	1.5 mM	2 fragments
	48,50,52,54,56,58	0.5 pM	1.5 mM	no fragments
	48,50,52,54,56,58	0.5 pM	2 mM	no fragments
	52,54,56,58,60,62	0.5 pM	1.5 mM	~600 bp fragment
HXD13F/ HXD13R	52,54,56,58	0.25 pM	1.5 mM	~600 bp fragment
HXD14F/ HXD14R	52,54,56,58,60,62	0.25 pM	1.5 mM	~500 bp fragment
HXD15F/ HXD15R	52,54,56,58,60,62	0.25 pM	1.5 mM	No fragments
	48,50	0.25 pM	1.5 mM	~600 bp fragment
HXD16F/ HXD16R	54,56	0.25 pM	1.5 mM	~500 bp fragment
HXD17F/ HXD17R	52,54,56,58,60,62	0.25 pM	1.5 mM	~550 bp fragment
HXD18aF/ HXD18aR	52,54,56,58,60,62	0.25 pM	1.5 mM	~700 bp fragment
HXD19F/ HXD19R	48,50,52,54	0.25 pM	1.5 mM	~850 bp fragment

Table 27- Summary of the conditions used and outcomes for PCR amplification of xanthine oxidoreductase exons 1-19.

This table shows the optimisation process for the amplification of exons 1-19. It illustrates the annealing temperatures used with each set of conditions and the outcomes from each set of conditions used. The optimal conditions for each primer pair are highlighted. ** concentration

Primers used	Annealing temperatures °C	Primer conc.**	$MgCl_2$ Conc.**	Fragments Generated
HXD20F/ HXD20R	52,54,56,58,60,62	0.25 pM	1.5 mM	~650 bp fragment
HXD21F/ HXD21R	48,50,52,54,56,58	0.25 pM	1.5 mM	~400 bp fragment
HXD22F/ HXD22R	52,54,56,58,60,62	0.5 pM	1.5 mM	~750 bp fragment
HXD23F/ HXD23R	52,54,56,58,60,62	0.25 pM	1.5 mM	~550 bp fragment
HXD24F/ HXD24R	48,50,52,54,56,58	0.25 pM	1.5 mM	two fragments
	48,50,52,54,56,58	0.25 pM	1 mM	No fragments
	48,50,52,54,56,58	0.5 pM	1.5 mM	~500 bp fragment
HXD25/26F/ HXD25/26R	48,50,52,54,56,58	0.25 pM	1.5 mM	~750 bp fragment
HXD27F/ HXD27R	48,50,52,54,56,58	0.25 pM	1.5 mM	~500 bp fragment
HXD28aF/ HXD28aR	48,50,52,54,56,58	0.25 pM	1.5 mM	~750 bp fragment
HXD29F/ HXD29R	48,50,52,54,56,58	0.25 pM	1.5 mM	~750 bp fragment
HXD30/ HXD30R	48,50,52,54,56,58	0.25 pM	1.5 mM	~600 bp fragment
HXD31F/ HXD31R	52,54,56,58,60,62	0.25 pM	1.5 mM	~450 bp fragment
HXD32F/ HXD32R	48,50,52,54,56,58	0.25 pM	1.5 mM	~700 bp fragment
HXD33F/ HXD33R	48,50,52,54,56,58	0.25 pM	1.5 mM	~750 bp fragment
HXD34F/ HXD34R	60,62	0.25 pM	1.5 mM	~500 bp fragment
HXD35F/ HXD35R	48,50,52,54,56,58	0.25 pM	1.5 mM	~450 bp fragment
HXD36F/ HXD36R	48,50,52,54,56,58	0.25 pM	1.5 mM	~500 bp fragment

Table 28- Summary of the conditions used and outcomes for PCR amplification of xanthine oxidoreductase exons 20-36.

This table shows the optimisation process for the amplification of exons 20-36. It illustrates the annealing temperatures used with each set of conditions and the outcomes from each set of conditions used. The optimal conditions for each primer pair are highlighted. ** concentration.

3.5.3 Comparison of the xanthinuric patient's and a normal subject's xanthine oxidoreductase gene sequences.

The DNA sequence obtained for the xanthinuric patient was compared to the published XOR sequence produced by Saksela and Raivio and the BAC sequences (accession numbers AL121654 and AL121657). Only one difference (33T>G) was identified in the coding region of the xanthinuric sample. This was predicted to cause an asparagine to lysine change at codon position 11. This change was also sequenced in a non-xanthinuric individual as comparison (figure 25).

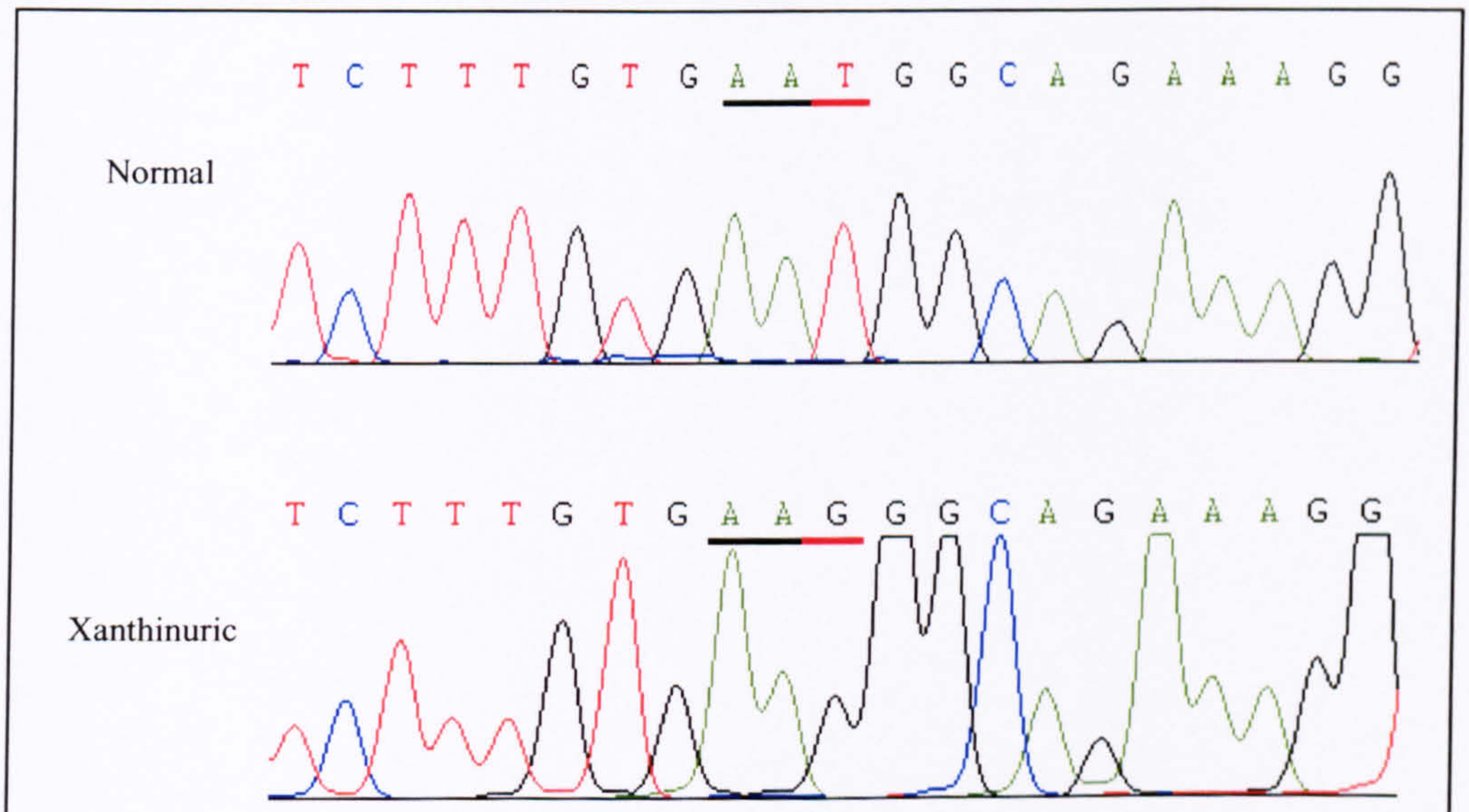

Figure 25 – Chromatogram showing the missense mutation found in the xanthinuric patient's xanthine oxidoreductase gene.

The codon changed is underlined with the change in red and the nucleotide change boxed.

As well as the difference found in the coding region seven intronic changes were found between the BAC sequences and our xanthinuric patient's DNA (table 29). These are not predicted to affect the expression of the enzyme, as they are not present at the splice sites. In addition no differences were found in the promoter region (224 bp upstream of the ATG) (Martelin *et al.*, 2000) of the xanthinuric patient when compared to the BAC sequence.

Intron	Normal > xanthinuric patient
7	IVS7+64C>T
8	IVS8-25T>G
11	IVS11-273G>A
15	IVS15+137T>G
18	IVS18+39A>G
23	IVS23+22T>A
32	IVS32-153G>A

Table 29 – Nucleotide differences found in the intronic sequence of the xanthine oxidoreductase gene of the xanthinuric patient.

4. DISCUSSION

4.Discussion

This discussion section follows the order of the results section with sections 4.1 – 4.4 describing the phenotyping and genotyping of the rat strains with enzyme assays and cloning of AO and AOH1 cDNA. The final section (4.5) discusses the significance of a novel mutation found in the XOR gene of a patient with hereditary xanthinuria.

4.1 Phenotyping the rat strains for molybdenum hydroxylase activities.

Assays using phenanthridine as substrate demonstrated that SD and Fischer rats were unable to oxidise this N-heterocycle. Unlike the SD strains studied elsewhere that display a discontinuous variation in N-heterocycle activity, all SD rats (n=24) examined in this laboratory (studies reported in this thesis and Clarke, D.J., Marshall, L., and Meehan, W., unpublished results) were completely devoid of N-heterocycle oxidase activity (table 3). Assays using the aldehyde DMAC as substrate showed that the SD and Fischer rats studied in this laboratory all had low levels of DMAC oxidase, which were approximately four-fold and six-fold lower than Wistar rat activity in SD and Fischer rats respectively (table 4). In order to determine whether the AO deficiency found in these rat strains was due to a defect in molybdenum cofactor synthesis, which would also cause a defect in XOR activity as has been demonstrated in man (Reiss & Johnson, 2003) and plants (Mendel & Schwarz, 1999), the XOR activity in the AO-deficient rat strains was compared to the Wistar strain. The presence of XOR activity at similar levels in all the rat strains indicated that the AO deficiency was not due to a defect in any cofactor synthesis. This suggested that the cause of the AO deficiency was most likely to be due to a mutation in the gene for AO.

4.2. Cloning of polymorphic areas of the aldehyde oxidase gene in rats.

As mentioned in the introduction at the time the project was initiated it was thought that only one aldehyde oxidase gene existed. Five SNPs that resulted in non-synonymous amino acid substitutions in the AO cDNA, (A119G, R120M, T649A, L1276F and R1315T), had been reported in a SD colony of rats in the Webb-Waring Antioxidant Research Institute in Colorado, however no functional analysis has been carried out to determine the effects of these polymorphisms. It was therefore decided to clone these polymorphic areas of the AO gene, to identify if any of the changes observed correlated with the AO deficiency found in the SD and Fischer rat strains. This was achieved by PCR or RT-PCR and DNA sequence analysis of the relevant areas of the AO gene and cDNA. The data showed no differences between the strains at the five positions studied (figures 11 and 12, table 10). It was therefore concluded that the differences observed by Wright *et al* (1999) did not correlate with the deficiency found in the rat strains examined in this study. Possible reasons why Wright *et al* (1999) found a discontinuous variation of nucleotide polymorphisms in their colony of SD rats and we did not could be because we had a different substrain of SD rat in our laboratory or that Wright *et al* (1999) did not have a pure SD colony. It is also possible that the changes found by Wright *et al* (1999) were induced by the cloning method they used as they amplified large stretches of cDNA (~2 kb), which can result in mistakes being made by the Taq polymerase enzyme.

4.3 Cloning and sequencing of aldehyde oxidase cDNA from Wistar, Sprague Dawley and Fischer rat strains.

As the polymorphisms identified by Wright *et al.* (1999) did not correlate with the deficiency found between the strains, the whole coding region of the AO gene was cloned. This was achieved by using RT-PCR to clone the AO cDNA from the different rat strains. This revealed that six nucleotide differences existed between the Wistar and the two AO-deficient strains (84A>G, 328G>A, 1630C>T, 2555C>T, 2886A>G and 3690A>G) (table 15). Five of these differences (84A>G, 328G>A, 1630C>T, 2555C>T and 3690A>G) were conserved between the SD and Fischer rat strains (figure 15, table 15). Two differences, 328G>A and 2555C>T, resulted in the amino acid changes, G110S and A852V, respectively, both of which are conserved between the SD and Fischer strains (figures 15 and 16, table 15). The other four changes (84A>G, 1630C>T, 2886A>G and 3690A>G) had no effect on the predicted amino acid sequence (figure 15, table 15).

In order to speculate the effect of the G110S and A852V amino acid differences on the activity of AO, the relevant regions were aligned with other molybdenum hydroxylases to identify the degree of sequence conservation. Their position in relation to the cofactor binding domains was also investigated. The first difference (G110S) consists of a serine present in the published SD rat AO sequence and both our AO-deficient rat strains and a glycine present in the Wistar rat sequence. Both glycine and serine are aliphatic amino acids although serine contains a hydroxyl side chain which results in it being highly hydrophilic in comparison to glycine and these two amino acids are not considered interchangeable (Bordo & Argos, 1991). When aligned with the related bovine XOR sequence and the corresponding amino acid position examined in the 3-D structure (Enroth *et al.*, 2000) this residue was found to be situated in a highly conserved region linking a α-helix (residues 100-107) and a β-turn (residues 111-114). Due to the close proximity to two of the cysteines responsible for the binding of the second iron-sulphur molecule to the protein, the 28.9 $Å^3$ increase in size (Zamyatin, 1972) and increased hydrophilicity (due to this substitution), could disrupt the folding of this region and therefore interfere with the iron-sulphur cofactor binding that may affect the activity of the enzyme. Comparison of this residue through alignment with other molybdenum

hydroxylases from an evolutionary diverse range of species revealed that this glycine is conserved between all non-plant molybdenum hydroxylases (figure 26). The degree of conservation and positioning suggests that this glycine is a very important residue.

The second difference (A852V) observed between the Wistar and shared in the AO-deficient strains is situated in the molybdenum cofactor binding domain between the MoCoI and MoCoII binding sites (figure 15) and consists of an alanine present in the Wistar sequence and a valine present in the published SD AO sequence and both AO-deficient strains. Both alanine and valine contain a small non-polar side chain and may be substituted with 95% confidence (Bordo & Argos, 1991). A comparison of molybdenum hydroxylases illustrated that globally all eukaryotic molybdenum hydroxylases have a non-polar amino acid (alanine, valine or isoleucine), which are considered interchangeable at this position (figure 27).

In conclusion it is more likely that G110S might be responsible for the reduced activity seen in the SD and Fischer strains, however in order to determine this the AO enzyme would need to be expressed in a cell culture system and the wild type enzyme mutated separately at these two positions to determine definitively which change is responsible for the deficiency.

			*	
AO	Rat Wistar	96	TRLHPVQERIAKCHGTQCGFCTPGMVMSM	125
AO	Rat SD	96	TRLHPVQERIAKCHSTQCGFCTPGMVMSM	125
AO	Rat Fischer	96	TRLHPVQERIAKCHSTQCGFCTPGMVMSM	125
AO	Rat SD published	96	TRLHPVQERIAKCHSTQCGFCTPGMVMSM	125
AO	Mouse	96	TRLHPIQERIAKCHGTQCGFCTPGMVMSM	125
AO	Rabbit	97	TRLHPVQERIAKFHGTQCGFCTPGMVMSM	126
AO	Bovine	97	TRIHPVQERIAKCHGTQCGFCTPGMVMSL	126
AO	Human	97	TRIHPVQERIAKCHGTQCGFCTPGMVMSI	126
AOH1	Wistar	100	TRIHPVQERIAKGHGTQCGFCTPGMVMSI	129
AOH1	Mouse	100	TRIHPVQERIRKGHGTQCGFCTPGMVMSI	129
AOH2	Mouse	100	KRVHPVRERLAKCHGTQCGFCSPGMVMSI	129
XOR	Rat	96	-KLHPVQERIARSHGSQCGFCTPGIVMSM	124
XOR	Mouse	99	-KLHPVQERIAKSHGSQCGFCTPGIVMSM	127
XOR	Cat	96	SRLHPVQERIAKSHGSQCGFCTPGIVMSM	125
XOR	Bovine **	96	TRLHPVQERIAKSHGSQCGFCTPGIVMSM	125
XOR	Human	96	TRLHPVQERIAKSHGSQCGFCTPGIVMSM	125
XOR	Chicken	100	SRLHPAQERIAKSHGSQCGFCTPGIVMSM	129
XDH	*D.melanogaster*	96	TRLHPVQERLPKAHGSQCGFCTPGIVMSM	125
XDH	Silkworm	107	TKLHPVQERIAKAHGSQCGFCTPGIVMSM	136
XDH	*E.nidulans*	126	-NPHAIQQRLAIGNGSQCGFCTPGIVMSL	154
XDH	*A.thaliana*	109	LGLHPLQESLASSHGSQCGFCTPGFVMSM	138
XDH	*R.capsulates*	85	GRLHPVQQAMIDHHGSQCGFCTPGFIVSM	114
AO	*A.thaliana*	113	VGFHAVHERIAGFHATQCGFCTPGMSVSM	142
AOR	*D.Gigas*	83	-NLHPLQKAWVLHGGAQCGFCSPGFIVSA	111

Figure 26 – Rat aldehyde oxidase deduced amino acid sequences aligned with representative molybdenum hydroxylases from other species over the region flanking G110S.

Residues coloured red are conserved at the same position, residues coloured blue are synonymous to other amino acids at the same position and residues coloured black possess different properties to the other amino acids at the same position. Sequences, which are underlined, are the sequences obtained in this research study. **The α-helix (residues PVQERIA) and β-pleated sheet (residues SQCG) shown in the crystal structure of bovine XOR are also underlined.

The point where the change occurs is highlighted in yellow and marked with *

The second iron sulphur binding site is shaded grey (Terao *et al.*, 2000).

D. melanogaster – Drosophila melanogaster. E. nidulans –Emericella nidulans,

A. thaliana – Arabidopsis thaliana, R. capsulatus – Rhodobacter capsulatus,

D. gigas – Desulfovibrio gigas.

			*	
AO	Rat Wistar	838	ITGGRHPYLGKYKAGFMRDGRIVALDVE	867
AO	Rat SD	838	ITGGRHPYLGKYKVGFMRDGRIVALDVE	867
AO	Rat Fischer	838	ITGGRHPYLGKYKVGFMRDGRIVALDVE	867
AO	Rat SD Published	838	ITGGRHPYLGKYKVGFMRDGRIVALDVE	867
AO	Mouse	838	ITGGRHPYLGKYKAGFMNEGRILALDVE	867
AO	Rabbit	839	ITGGRHPYLGKYKAGFMNDGRIVALDVE	869
AO	Bovine	844	ITGGRHPYLGKYKAGFMNDGRILALDME	873
AO	Human	843	ITGGRHPYLGKYKAGFMNDGRILALDME	872
AOH1	Wistar	838	ITGGRHPLLGKYRVGFMNNGKIKAADIQ	867
AOH1	Mouse	839	ITGGRHPLLGKYKIGFMNNGKIKAADIQ	868
AOH2	Mouse	841	ITAGRHPLLGKYKIGFMNNGEIRAADVE	870
XOR	Rat	834	ITGGRHPFLAKYKVGFMKTGTVVALEVA	863
XOR	Mouse	837	ITGGRHPFLAKYKVGFMKTGTIVALEVA	866
XOR	Cat	833	ITGGRHPFLARYKVGFMKTGRVVALKVE	862
XOR	Bovine	834	ITGGRHPFLARYKVGFMKTGTIVALEVD	863
XOR	Human	835	ITGGRHPFLARYKVGFMKTGTVVALEVD	864
XOR	Chicken	863	ISGGRHPFLGRYKVGFMKNGKIKSLEVS	892
XDH	Bluebottle	857	ITGTRHPFLFKYKIAFTSEGRLTGCYIE	886
XDH	*D. melanogaster*	839	ITGTRHPFLFKYKVGFTKEGLITACDIE	868
XDH	Silkworm	861	MTGTRHPFLIKYKAAATKEGKIVGAVVN	890
XDH	*E. nidulans*	865	TSGQRHPFYCKWKVGVTREGKLLALDAD	894
XDH	*A. thaliana*	866	ITGHRHSFVGKYKVGFTNEGKILALDLE	895
XDH	*R. capsulates*	264	ITGKRHDFRIRYRIGADASGKLLGADFV	293
AO	Mosquito	809	AVGKRASCISNYQIEVDEDGRICKLLNN	838
AO	*A. thaliana*	868	TTGGRHPMKVTYSVGFKSNGKITALDVE	897
AOR	*D. gigas*	455	YTGKRSPWEMNVKFAAKKDGTLLAMESD	484

Figure 27 – Rat aldehyde oxidase cDNA sequences aligned with representative molybdenum hydroxylases from other species over the region flanking A852V.

Residues coloured red are conserved at the same position, residues coloured blue are synonymous to other amino acids at the same position and residues coloured black possess different properties to the other amino acids at the same position. Sequences, which are underlined, are the sequences obtained in this research study. The point where the change occurs is highlighted in yellow and marked with *

D. melanogaster – Drosophila melanogaster. *E. nidulans –Emericella nidulans,*

A. thaliana – Arabidopsis thaliana, *R. capsulatus – Rhodobacter capsulatus,*

D. gigas – Desulfovibrio gigas.

4.4 Evidence for aldehyde oxidase homologue 1 deficiency in Sprague Dawley and Fischer rats.

Following the publication of the AOH1 homologue in mice (Terao *et al.*, 2000) the presence of this enzyme in rat liver was investigated. The same method as Terao *et al* used to establish the presence of AOH1 in mice was used to establish the presence of more than one AO in rat liver. Using benzaldehyde as substrate this technique suggested that there were two AOs present in the Wistar rat strain (figure 17). As mouse AO and rat AO are 95% identical, mouse AOH1and rat AOH1 are 93% identical (section 3.4) and mouse XOR and rat XOR are 96% identical at the amino acid level it is reasonable to suggest that the slowest and fastest migrating benzaldehyde staining polypeptide in rat liver cytosol probably corresponded to AO and AOH1 respectively as with the zymograms generated from mouse liver extract (Terao *et al.*, 2000). Staining with benzaldehyde also revealed that only the slowest migrating band (thought to be AO) was present in the SD and Fischer strains (figure 17). When the staining was repeated with phenanthridine (figure 17) it was established that the fastest migrating band (thought to be AOH1) was responsible for N-heterocyclic oxidase activity in Wistar rat liver and that no polypeptides stained with this substrate in the AO-deficient strains. It was also noted that surprisingly the intensity of the slowest migrating benzaldehyde staining polypeptide was similar in all strains despite the fact that the DMAC oxidase activity was up to 6 fold higher in the wild type Wistar strain. It is possible that this may be due to the majority of the benzaldehyde staining being due to XOR as it is documented that benzaldehyde is also a substrate for XOR as well as AO (Beedham., 1987), and staining with hypoxanthine revealed that XOR comigrated with the slowest AO migrating polypeptide on these plates (figure 17). In order for this conflict to be resolved each polypeptide would need to be individually expressed in a cell culture system and analysed using cellulose acetate electrophoresis, as was carried out with the mouse liver enzymes (Terao *et al.*, 2000).

In order to determine whether the lack of AO or AOH1 transcripts was the cause of the deficiency RT-PCR was performed as described in the results (sections 3.3 and 3.4). This indicated that the levels of transcription of the AO and AOH1 genes did not account for the loss of activity in the AO-deficient strains (figure 17). This suggested

that mutations in either or both AO and AOH1 may be the cause of the AO deficiency in SD and Fischer rat strains.

4.5 Cloning and sequencing of the aldehyde oxidase homologue 1 cDNAs from rat strains.

As the cellulose acetate zymogram suggested that AOH1 was absent in the AO-deficient rats (Figure 17), AOH1 cDNA was cloned from the three rat strains.
This was achieved by RT-PCR first using primers to the mouse AOH1 cDNA ortholog then by using specific rat AOH1 cDNA primers as described in the results section 3.4. This enabled the cloning of the entire 3999 bp coding region of AOH1 from the three rat strains. Comparison of the Wistar rat AOH1 cDNA with other known rat molybdenum hydroxylases established that the predicted amino acid sequence was 60 % and 50 % identical to AO and XOR respectively.

Comparison of the AOH1 cDNA sequences obtained for Wistar and SD rat strains revealed 14 changes (figures 21, 22 and table 25) 3 of which resulted in a deduced amino acid difference between the protein sequences (R39Q, Q937K and M1078T). The first two differences to be discussed (Q937K and M1078T) are surprising as the changes found are opposite to what would be expected. In each case comparison with other molybdenum hydroxylases established that the deficient rat strains have an amino acid which shows more conservation than the Wistar strain's amino acid at these positions (figure 28 and 29).

The amino acid difference Q937K consists of a glutamine codon in the Wistar AOH1 cDNA sequence changing to a lysine codon in the SD AOH1 cDNA sequences. These two amino acids may be substituted for each other with 95% confidence (Bordo & Argos, 1991). Alignment of the rat AOH1 sequences with other molybdenum hydroxylases reveals that this lysine residue is conserved in the mouse AOH1, bovine AO, human AO and rabbit AO, however rat AO possesses an arginine at this position. Mammalian XORs possess a threonine at this position but less evolved species in evolution possess a variety of amino acids at this position (figure 28). The amino acid difference closest to the amino terminus of the protein (M1078T) consists of a methionine present in the Wistar AOH1 and a threonine present in the SD AOH1 predicted protein sequences. The AO-deficient strains have a threonine at position 1078 that is highly conserved in mammalian molybdenum hydroxylases, from bacteria to humans which all possess either a threonine or the highly related amino acid serine at

this position (figure 29). As these two differences show the wild type Wistar strain differing from the others it appears that these differences cannot be detrimental to the activity of the enzyme otherwise reduced AOH1 activity would be apparent in the Wistar strain.

Of the three differences found between SD and Wistar the R39Q difference, which consists of the substitution of an arginine in the Wistar by a glutamine in the SD appeared to be the most significant. Arginine contains a basic side chain, which is positively charged making it highly hydrophilic. Glutamine contains an acidic side chain, however the overall charge on this amino acid is negated. Aligning the rat AOH1 protein sequence with the bovine XOR sequence and examining the corresponding amino acid position in the 3-D structure (Enroth *et al.*, 2000) indicated that this residue was situated five amino acids after a α-helix and just two amino acids before a β-turn. The amino acids comprising the β-turn are 100% conserved between the rat AOH1 and bovine XOR sequences suggesting that the β-turn could be conserved between the two enzymes. In addition this change is situated seven amino acids prior to the start of the first iron-sulphur binding site so the loss of the positive charge and the reduction in volume of the amino acid by 29.6 $Å^3$ (Lagziel *et al.*, 2001), could disrupt the complex folding of this region possibly resulting in disruption of the iron-sulphur cofactor which may inactivate the protein. Comparison of this residue with other molybdenum hydroxylases found that all mammalian AOs characterised to date, with the exception of one (mouse AOH2) possess an arginine in this position (figure 30). However *D. Gigas* AO possesses a glycine in this position, as do most of the XORs. The conservation in mammalian AO enzymes suggests that this residue is important for activity at this position in mammalian AOs.

Comparison of Wistar and Fischer AOH1 deduced amino acid sequences revealed the same three non-synonymous codon differences as found in the SD rat strain, but in addition a further two non-synonymous codon differences were also found. The additional differences were an arginine codon changing to a histidine codon at position 153 and a glycine codon to asparagine codon at position 785 in Wistar and Fischer AOH1 predicted protein sequences respectively.

Arginine is a basic hydrophilic positively charged molecule whilst histidine contains a basic side chain, which can be either positively charged or uncharged depending upon its surroundings. Figure 31 illustrates that this amino acid is very conserved between molybdenum hydroxylases of all the evolutionary diverse species from bacteria to humans suggesting that an arginine is essential at this position. This difference is situated in the unique iron-sulphur binding site (figure 5) between the second two cysteine residues (CXC), which are responsible for binding the iron-sulphur cofactor to the protein (Figure 5). Interestingly a mutation of this residue had been reported to cause xanthinuria in humans in which the arginine residue in the non-afflicted human XOR protein was found to be a cysteine in the xanthinuric individual (Sakamoto *et al.*, 2001).

The second additional codon change found between Wistar and Fischer AOH1 deduced amino acid sequences, consists of a glycine present in the Wistar strain changing to an aspartate at codon position 785 in the Fischer strain's AOH1 predicted protein. Glycine is the smallest of all the amino acids and contains an aliphatic side chain while aspartate contains a negatively charged acidic side chain. Aspartate is almost double the size of glycine (111.1 and 60.1 $Å^3$ respectively) (Zamyatin, 1972), which coupled with the addition of a negative charge could be detrimental to the enzyme activity. Glycine is conserved in the mouse AOH1, mammalian XORs, and plant molybdenum hydroxylases but not in mammalian AOs (figure 32), which indicates that it may be important for the activity of AOH1 and XOR. As these two additional changes are not conserved between the SD and Fischer sequences it is likely that these mutations were acquired after the strains diverged rather than being the original mutation, which is responsible for causing the deficiency in these strains of rat.

In conclusion these results suggest that the R39Q codon difference found between the Wistar and both the AO-deficient strains (SD and Fischer) was the ancestral mutation which resulted in the loss of AOH1 activity in the AO-deficient strains of rat.

This difference coupled with the G110S difference found in the AO cDNA could result in the AO phenotype seen in these strains. However as it has not been conclusively determined which polypeptide is responsible for AO and AOH1 activity it could be that the R39Q difference is responsible for the reduced DMAC oxidase activity and the G110S difference is responsible for the lack of phenanthridine oxidase activity.

			*	
AOH1	Rat Wistar	923	GAFVTETWVSAVAAQCHLPPEKVRELNM	951
AOH1	Rat SD	923	GAFVTETWVSAVAAKCHLPPEKVRELNM	951
AOH1	Rat Fischer	923	GAFVTETWVSAVAAKCHLPPEKVRELNM	951
AOH1	Mouse	922	GAFVTETCMSAVAAKCRLPPEKVRELNM	950
AO	Rat Wistar	923	AGLVTEACVTEVAIRCGLSPEQVRTINM	951
AO	Mouse	923	AGLVTEACITEVAIKCGLSPEQVRTINM	951
AO	Rabbit	922	AGLITECCITEVAAKCGLSPEKVRAINF	950
AO	Bovine	929	AGLITEACITEVAAKCGLPPEKVRMINM	957
AO	Human	928	AVLITESCITEVAAKCGLSPEKVRIINM	956
AOH2	Mouse	926	ATVVVEAYIAAVASKCNLLPEEVREINM	954
XOR	Rat	919	GMLIAEYWMSEVAITCGLPAEEVRRKNM	947
XOR	Mouse	922	GMLIAEYWMSEVAVTCGLPAEEVRRKNM	950
XOR	Cat	918	GMLIAEHWMSEVAVTCGLPAEEVRRKNM	946
XOR	Bovine	919	ALFIAENWMSEVAVTCGLPAEEVRWKNM	947
XOR	Human	920	GMLIAECWMSEVAVTCGMPAEEVRRKNL	948
XOR	Chicken	948	GMMIAECWMSDLARKCGLPPEEVRKINL	976
XOR	*D. melanogaster*	924	GMYAGEHIIRDVARIVGRDVVDVMRLNF	952
XOR	Silkworm	946	GMFGAENMVREIAHRLGKSPEEISRLNL	974
XOR	*E. nidulans*	950	GLFFAESIISEVADHLDLQVEQLRILNM	978
XOR	*A. thaliana*	951	GMLITENWIQRIAAELDKIPEEIKEMNF	979
XOR	*R. capsulates*	349	GALGMERAIEHLARGMGRDPAELRALNF	377
AO	*A. thaliana*	952	GSYIGEAIIEKVASYLSVDVDEIRKVNL	980
AOR	*D. gigas*	540	SMFASECLMDMLAEKLGMDPLELRYKNA	568

Figure 28 – Rat aldehyde oxidase homologue 1 deduced amino acid sequences aligned with representative molybdenum hydroxylases from other species over the region flanking Q937K.

Residues coloured red are conserved at the same position, residues coloured blue are synonymous to other amino acids at the same position and residues coloured black possess different properties to the other amino acids at the same position. Sequences, which are underlined, are the sequences obtained in this research study. The point where the change occurs is highlighted in yellow and marked with *

D. melanogaster – *Drosophila melanogaster.* *E. nidulans* – *Emericella nidulans,*
A. thaliana – *Arabidopsis thaliana,* *R. capsulatus* – *Rhodobacter capsulatus,*
D. gigas – *Desulfovibrio gigas.*

			*	
AOH1	Rat Wistar	1064	YIHLDEMNTMTVPNMITTGGSTGADVNGRA	1094
AOH1	Rat SD	1064	YIHLDEMNTMTVPNTITTGGSTGADVNGRA	1094
AOH1	Rat Fischer	1064	YIHLDEMNTMTVPNTITTGGSTGADVNGRA	1094
AOH1	Mouse	1065	YIHLDEMSTVTVPNTVTTGASTGADVNGRA	1095
AO	Wistar	1064	SVHLRGTSTETVPNTNASGGSVVADLNGLA	1094
AO	Mouse	1064	SVHLRGTSTETVPNTNASGGSVVADLNGLA	1094
AO	Rabbit	1065	NVHLRGTSTETVPNTNASGGSVVADLNGLA	1095
AO	Bovine	1070	SIHLRGTSTETIPNTNPSGGSVVADLNGLA	1100
AO	Human	1069	NVHLRGTSTETVPNANISGGSVVADLNGLA	1099
AOH2	Mouse	1067	YVHFSETSTTTVPNSAFTAGSMGADINGKA	1097
XOR	Rat	1060	KIHISETSTNTVPNTSPTAASASADLNGQG	1090
XOR	Mouse	1063	KIHITETSTNTVPNTSPTAASASADLNGQA	1093
XOR	Cat	1059	KIYISETSTNTVPNTSPTAASVSTDINGQA	1089
XOR	Bovine	1030	KIYISETSTNTVPNSSPTAASVSTDIYGQA	1060
XOR	Human	1061	KIYISETSTNTVPNTSPTAASVSADLNGQA	1091
XOR	Chicken	1089	KIYISETSTNTVPNTSPTAASVSADINGMA	1119
XOR	Guppy	1062	KIFLSETSTGTVPNTCPSAASFGTDANGMA	1092
XOR	*D. melanogaster*	1065	LIHISETATDKVPNTSPTAASVGSDLNGMA	1096
XOR	Silkworm	1087	KIHISETSTDKVPNTSATAASAGSDLNGMA	1117
XOR	*E. nidulans*	1091	DVFISETATNTVANTSSTAASASSDLNGYA	1121
XOR	*A. thaliana*	1092	SVFVSETSTDKVPNASPTAASASSDMYGAA	1122
XOR	*R. capsulates*	510	QVRITATDTSKVPNTSATAASSGADMNGMA	540
AO	*A. thaliana*	1092	KIRVIQSDTLSMVQGSMTAGSTTSEASSEA	1122
AOR	*D. gigas*	675	KIKFTWPNTATTPNSGPSGGSRQQVMTGNA	705

Figure 29 - Rat aldehyde oxidase homologue 1 deduced amino acid sequences aligned with representative molybdenum hydroxylases from other species over the region flanking M1078T.

Residues coloured red are conserved at the same position, residues coloured blue are synonymous to other amino acids at the same position and residues coloured black possess different properties to the other amino acids at the same position. Sequences, which are underlined, are the sequences obtained in this research study. The point where the change occurs is highlighted in yellow and marked with *

D. melanogaster – *Drosophila melanogaster.* *E. nidulans* – *Emericella nidulans,*
A. thaliana – *Arabidopsis thaliana,* *R. capsulatus* – *Rhodobacter capsulatus,*
D. gigas – *Desulfovibrio gigas.*

			*	
AOH1	Rat Wistar	25	DPEVNLLFYLRKIIRLTGTKYGCGGGDCGA	55
AOH1	Rat SD	25	DPEVNLLFYLRKIIQLTGTKYGCGGGDCGA	55
AOH1	Rat Fischer	25	DPEVNLLFYLRKIIQLTGTKYGCGGGDCGA	55
AOH1	Mouse	25	DPEVNLLFYLRKVIRLTGTKYGCGGGDCGA	55
AO	Rat Wistar	21	DPEMMLLPYLRKNLRLTGTKYGCGGGGCGA	51
AO	Mouse	21	DPEMMLLPYLRKNLRLTGTKYGCGGGGCGA	51
AO	Rabbit	22	DPETMLLPYLRKKLRLTGTKYGCGGGGCGA	52
AO	Bovine	22	DPETMLLPYLRKKLRLTGTKYGCGGGGCGA	52
AO	Human	22	DPETMLLPYLRKKLRLTGTPYGCGGGGCGA	52
AOH2	Mouse	25	DPEKNLLFYTRKVLNLTGTKYSCGTGGCGA	55
XOR	Rat	21	DPETTLLVYLRRKLGLCGTKLGCGEGGCGA	51
XOR	Mouse	24	DPETTLLVYLRRKLGLCGTKLGCGEGGCGA	54
XOR	Cat	21	DPETTLLAYLRRKLGLSGTKLGCGEGGCGA	51
XOR	Bovine	21	DPETTLLAYLRRKLGLRGTKLGCGEGGCGA	51
XOR	Human	21	DPETTLLAYLRRKLGLSGTKLGCGEGGCGA	51
XOR	Chicken	27	DPETTLLTYLRRKLGLCGTKLGCGEGGCGA	57
XOR	*D. melanogaster*	21	DPECTLLTFLREKLRLCGTKLGCAEGGCGA	51
XOR	Silkworm	32	DPEWTLLWYLRKKLRLTGTKLGCAEGGCGA	62
XOR	*E. nidulans*	52	DPEITLLEYLRG-IGLTGTKLGCAEGGCGA	82
XOR	*A. thaliana*	24	LAHMTLLEYLR---GLTGTKLGCGEGGCGS	54
XOR	*R. capsulates*	17	DPTQSLLELLRA-EGLTGTKEGCNEGDCGA	37
AO	*A. thaliana*	38	DPSTTLVDFLRNKTPFKSVKLGCGEGGCGA	68

Figure 30 – Rat aldehyde oxidase homologue deduced amino acid sequences aligned with representative molybdenum hydroxylases from other species over the region flanking R39Q.

Residues coloured red are conserved at the same position, residues coloured blue are synonymous to other amino acids at the same position and residues coloured black possess different properties to the other amino acids at the same position. Sequences, which are underlined, are the sequences obtained in this research study. The point where the change occurs is highlighted in yellow and marked with *

**The α-helix (residues DPETMLLPY) and β-turn (residues TGTKY) shown in the crystal structure of bovine XOR are underlined.

The second iron sulphur binding site is shaded grey (Terao *et al.*, 2000)

D. melanogaster – Drosophila melanogaster. *E. nidulans – Emericella nidulans,*

A. thaliana – Arabidopsis thaliana, *R. capsulatus – Rhodobacter capsulatus,*

D. gigas – Desulfovibrio gigas.

			*	
AOH1	Rat Wistar	138	PSTEQIMETLGGNLCRCTGYRPIVESARSFSPN	171
AOH1	Rat SD	138	PSTEQIMETLGGNLCRCTGYRPIVESARSFSPN	171
AOH1	Rat Fischer	138	PSTEQIMETLGGNLCHCTGYRPIVESARSFSPN	171
AOH1	Mouse	138	PSTEQIMETLGGNLCRCTGYRPIVESAKSFCPS	171
AO	Rat Wistar	134	PSLDQLTDALGGNLCRCTGYRPIIDACKTFCRA	167
AO	Mouse	134	PTLDQLTDALGGNLCRCTGYRPIIDACKTFCKA	167
AO	Rabbit	135	PTLDQLADALGGNLCRCTGYRPIIEAYKTFCKT	168
AO	Bovine	135	PTLTQLNDALGGNLCRCTGYRPIINACKTFCKT	168
AO	Human	135	PTLDQLTDALGGNLCRCHGYRPIIDACKTFCKT	168
AOH2	Mouse	138	PTPDQITEALGGNLCRCTGYRPIVESGKTFSQK	171
XOR	Rat	133	PTVEEIENAFQGNLCRCTGYRPILQGFRTFAKD	166
XOR	Mouse	136	PTVEEIENAFQGNLCRCTGYRPILQGFRTFAKD	169
XOR	Cat	134	PTIEEIEDAFQGNLCRCTGYRPILQGFRTFARD	167
XOR	Bovine	134	PTVEEIEDAFQGNLCRCTGYRPILQGFRTFAKN	167
XOR	Human	134	PTMEEIENAFQGNLCRCTGYRPILQGFRTFARD	167
XOR	Chicken	138	PKMEDIEDAFQGNLCRCTGYRPILEGYRTFAVD	171
XOR	*D. melanogaster*	134	PSMRDLEVAFQGNLCRCTGYRPILEGYKTFTKE	167
XOR	Silkworm	145	IQYSDLEVAFQGNLCRCTGYRAIIEGYKTFIED	178
XOR	*E. nidulans*	163	PSEHAVEEAFDGNLCRCTGYRPILDAAQSFTSP	196
XOR	*A. thaliana*	147	PSEEEIEECLAGNLCRCTGYRPIIDAFRVFAKS	180
XOR	*R. capsulates*	119	RDRKDYDDLLAGNLCRCTGYAPILRA-------	152
AO	*A. thaliana*	151	LTAVEAEKAVSGNLCRCTGYRPLVDACKSFAAD	184
AOR	*D. gigas*	121	--DVRDWFQKHRNACRCTGYKPLVD--------	154

Figure 31 – Rat aldehyde oxidase homologue 1 deduced amino acid sequences aligned with representative molybdenum hydroxylases from other species over the region flanking R153H.

Residues coloured red are conserved at the same position, residues coloured blue are synonymous to other amino acids at the same position and residues coloured black possess different properties to the other amino acids at the same position. Sequences, which are underlined, are the sequences obtained in this research study. The point where the change occurs is highlighted in yellow and marked with *

The iron sulphur binding site is shaded grey (Terao *et al.*, 2000)

D. melanogaster – *Drosophila melanogaster.* *E. nidulans* – *Emericella nidulans,*

A. thaliana – *Arabidopsis thaliana,* *R. capsulatus* – *Rhodobacter capsulatus,*

D. gigas – *Desulfovibrio gigas.*

			*	
AOH1	Rat Wistar	755	SQDAAFTQEMVARTLGIPKNRITCHVKRVG	785
AOH1	Rat SD	755	SQDAAFTQEMVARTLGIPKNRITCHVKRVG	785
AOH1	Rat Fischer	755	SQDAAFTQEMVARTLDIPKNRITCHVKRVG	785
AOH1	Mouse	756	SQDAAFTQEMVARTLGIPKNRINCHVKRVG	786
AO	Rat Wistar	755	TQFPKHIQDIVAATLKLSVNKVMCHVRRVG	785
AO	Mouse	755	TQFPKYIQDIVAATLKLSANKVMCHVRRVG	785
AO	Rabbit	756	TQFPKYIQDMVAAVLKLPVNKVMCHVKRVG	786
AO	Bovine	761	AQFPKYIQDITASVLKVSANKVMCHVKRVG	791
AO	Human	760	TQFPKYIQDIVASTLKLPANKVMCHVRRVG	790
AOH2	Mouse	758	TQFPTHVQEFVSAALNVPRSRIACHMKRAG	788
XOR	Rat	751	TQNTMKTQSFVAKMLGVPDNRIVVRVKRMG	781
XOR	Mouse	754	TQNTMKTQSFIAKMLGVPDNRIVVRVKRMG	784
XOR	Cat	750	TQNTTKTQSFVANMLGVPANRILVRVKRMG	780
XOR	Bovine	751	TQNAMKTQSFVAKMLGVPVNRILVRVKRMG	781
XOR	Human	752	TQNTMKTQSFVAKMLGVPANRIVVRVKRMG	782
XOR	Chicken	780	TQNLMKTQEFTASALGVPSNRIVVRVKRMG	810
XOR	*D. melanogaster*	757	TQHPSEVQKLVAHVTALPAHRVVCRAKRLG	787
XOR	Silkworm	778	SQHPSEIAKLVSHILHVPMNRIVARVKRMG	808
XOR	*E. nidulans*	782	TQNPTETQSYVAQVTGVAANKIVSRVKRLG	818
XOR	*A. thaliana*	783	TQAPQQHQKYVSHVLGLPMSKVVCKTKRLG	813
XOR	*R. capsulates*	183	SQHPSEIQHKVAHALGLAFHDVRVEMRRMG	213
AO	*A.thaliana*	786	TQTPEFVHQTIAGCLGVPENNVRVITRRVG	816
AOR	*D. gigas*	375	SIGVHLHLYMIAPGVGLEPDQLVLVANPMG	405

Figure 32 – Rat aldehyde oxidase homologue 1 deduced amino acid sequences aligned with representative molybdenum hydroxylases from other species over the region flanking G785D.

Residues coloured red are conserved at the same position, residues coloured blue are synonymous to other amino acids at the same position and residues coloured black possess different properties to the other amino acids at the same position. Sequences, which are underlined, are the sequences obtained in this research study. The point where the change occurs is highlighted in yellow and marked with *

D. melanogaster – Drosophila melanogaster. *E. nidulans – Emericella nidulans,*

A. thaliana – Arabidopsis thaliana, *R. capsulatus – Rhodobacter capsulatus,*

D. gigas – Desulfovibrio gigas.

4.6 Identification of a novel mutation in the xanthine oxidoreductase gene of a British xanthinuric patient.

As explained in the introduction (section 1.6.3) only 5 mutations causing hereditary xanthinuria are known worldwide and there has been no molecular genetic study of any European patients. The patient described in this thesis was a British female of 52 years of age at diagnosis. She was tested for purine metabolic disorders because of a persistently low plasma urate level that had been noted over seven years while she was undergoing investigation for a variety of clinical problems, which resulted in the diagnosis of idiopathic thrombocytopenic purpura.

Comparison of the biochemical features of this xanthinuric patient (table 30) with the normal British population indicated that the xanthine to hypoxanthine ratio was approximately 4 times the level of unaffected British females, which is typical of severe xanthinuria (Simmonds *et al.*, 1995) (table 30). The xanthine and hypoxanthine levels of this patient were 29-fold and 7-fold higher respectively than in the normal British population. As UK patients are not diagnosed by using XOR enzyme assays of duodenal mucosal biopsy as in Japan, we were unable to confirm the complete absence of XOR activity. However comparison of our patient with a Japanese patient, whose XOR activity in the duodenal mucosal was undetectable, indicated that our patient suffers from a more severe form of hereditary xanthinuria based on oxypurine levels in urine (table 30).

Subject	British xanthinuric patient	Japanese xanthinuric patient	Normal	Normal
Sex (male/female)	Female	Male	Female	Male
Age at presentation (Years)	52	60	N/A	N/A
Xanthine in urine (mmol/24hrs)	1.46	0.36	0.05	0.05
Hypoxanthine in urine (mmol/24hrs)	0.37	0.17	0.05	0.07
Uric Acid (mmol/24hrs)	N.D.	0.02	2.7	3.0
Oxypurines (mmol/24hrs)	1.83	0.53	0.1	0.12
Xanthine:hypoxanthine ratio	3.9	2.1	1	0.7
Duodenal XOR activity (nmol/hr/mg protein)	unknown	N.D.	N.S.	12.1
Type of xanthinuria	unknown	I	N/A	N/A
Mutation	N11K	R149C	N/A	N/A

Table 30 - Clinical data for xanthinuric and control subjects.

The data from the xanthinuric patient reported in this thesis is shaded pink. Data from a Japanese patient reported by Sakamoto *et al*, (Sakamoto *et al.*, 2001) is also listed. The normal male and female data represents the normal British population (Simmonds, A., 2003, personal communication). N.D not detected, N/A not applicable.

Unfortunately only one patient could be directly compared to our patient as most Japanese research groups use the xanthine to creatinine clearance ratio to study the excretion of oxypurines from the body. Personal communication with Dr A. Simmonds of the Purine Research Laboratory in Guy's Hospital, London revealed that the Japanese method is flawed as it does not take into account liquid consumption and sampling close to mealtimes which can affect the result and problems with oxypurine and creatinine clearance such as found in patients with diabetes (Ichida *et al.*, 1997). The 24 hour urine collection is a much more accurate way of determining excretion of oxypurines because these factors do not have an adverse effect on the result of the test (Simmonds, A., 2003, personal communication). Comparison of the biochemical features of the British patient with the one genetically characterised Japanese patient, that had a 24 hour urine test performed, revealed that the Japanese patient had much lower levels of oxypurines

in the urine and a lower xanthine to hypoxanthine ratio compared to the British patient. The total absence of uric acid in the urine of the British patient also suggests that the XOR enzyme was totally inactive further indicating the severity of the disease.

Cloning and DNA sequencing of the XOR promoter, exons and intron/exon splice sites in the British xanthinuric patient revealed a novel single nucleotide difference (33T>G) situated in the coding region of exon 1 between the xanthinuric patient's XOR gene and normal XOR sequence. This resulted in a codon substitution at position 11 consisting of an asparagine found in the normal XOR sequence changing to a lysine in the xanthinuric's XOR sequence. This codon difference is not one of the SNPs observed for the XOR gene in the normal population (Ichida *et al.*, 1993; Lagziel *et al.*, 2001)(SNP database, http://www.ncbi.nlm.nih.gov/) which suggests that this base change is not a common benign polymorphism.

With regards to the N11K substitution asparagine is a small uncharged polar molecule and lysine is a positively charged polar molecule. When aligned with other molybdenum hydroxylases from an evolutionary diverse range of species from bacteria to humans this asparagine residue shows 100% conservation (figure 33), this suggests that an asparagine is essential at this position. Comparison with the bovine XOR protein sequence and examination of this residue in the 3-D structure (Enroth *et al.*, 2000) found that this residue was situated in a β-turn. The change is positioned in the iron-sulphur binding domain 31 residues prior to the first iron-sulphur binding site (Garattini *et al.*, 2003). As lysine is 54.5 $Å^3$ larger (Zamyatin, 1972) than the asparagine, this size difference could disrupt the physical folding of the protein thereby disrupting the β-turn. Also the addition of a charge at this position could prove detrimental to the activity of the protein.

As the patient had not been tested for aldehyde oxidase activity and the nature of the xanthinuria not characterised, another member of this laboratory examined the human molybdenum cofactor sulphurase gene of this patient and found no mutations (Kelly, M. L., 2003, personal communication). This suggests that our patient suffers from hereditary xanthinuria type I.

In conclusion it seems likely that the N11K mutation in the XOR gene is responsible for the hereditary xanthinuria in this patient. Definitive proof will require the expression and assay of the N11K mutant XOR in a cell culture system.

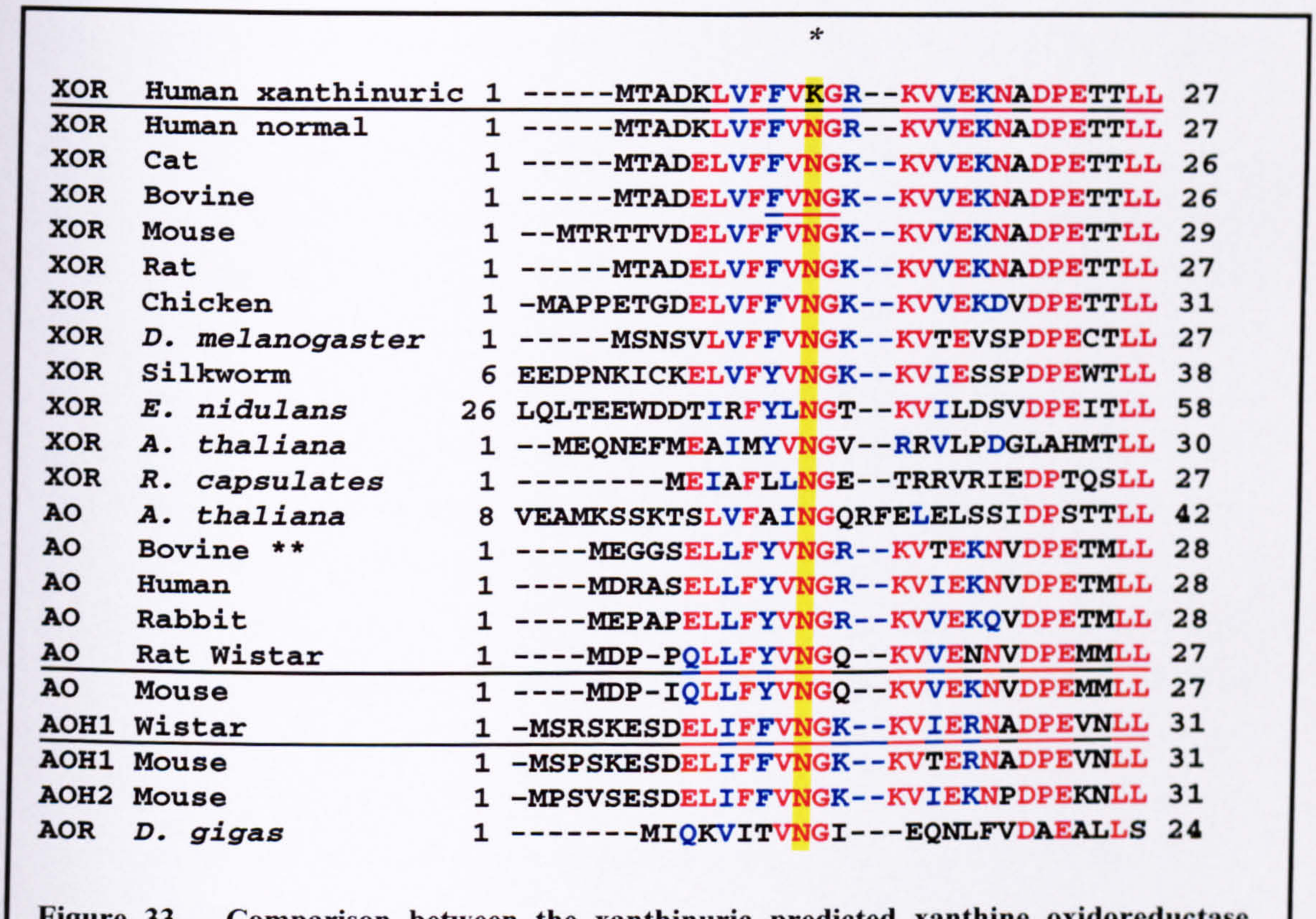

Figure 33 – Comparison between the xanthinuric predicted xanthine oxidoreductase sequence with representative molybdenum hydroxylases from a range of species.

Residues coloured red are conserved at the same position, residues coloured blue are synonymous to other amino acids at the same position and residues coloured black possess different properties to the other amino acids at the same position. Sequences, which are underlined, are the sequences obtained in this research study. The point where the change occurs is highlighted in yellow and marked with *

**The β-turn (residues FVNG) shown in the crystal structure of bovine XOR is underlined.

D. melanogaster – *Drosophila melanogaster.* *E. nidulans* – *Emericella nidulans,*
A. thaliana – *Arabidopsis thaliana,* *R. capsulatus* – *Rhodobacter capsulatus,*
D. gigas – *Desulfovibrio gigas.*

It should also be noted that although this patient appears to be homozygous for this mutation it is possible that only one allele was amplified during the PCR reactions and that another mutation exists in the other allele, which was not seen in this study.

Expression studies will determine if this mutation alone is enough to account for the deficiency observed in this patient.

4.7 Conclusions.

Phenotyping of the three rat strains revealed that the SD and Fischer rats possessed a 4-fold and 6-fold lower DMAC oxidase activity respectively in comparison with the wild type Wistar strain. It also revealed that the SD and Fischer rat strains were completely deficient in phenanthridine oxidase activity. The non-synonymous polymorphisms observed by Wright *et al.* (1999) did not correlate with the deficiency found in these strains of rat, therefore the entire coding region of the AO cDNA was cloned and two differences found. Comparison of the two differences with an evolutionary diverse range of molybdenum hydroxylases suggested that the G110S difference was most likely to cause the AO deficiency in the SD and Fischer strains. Cellulose acetate electrophoresis revealed two AO homologues present in Wistar rat liver and determined that AOH1 was absent in the SD and Fischer rat strains. Cloning of this novel AOH1 cDNA from rat liver revealed five predicted amino acid changes of which only three were conserved between the two AO-deficient strains. Comparison of these differences with an evolutionary diverse range of molybdenum hydroxylases suggested that the R39Q difference was most likely to be responsible for the AOH1 deficiency in the SD and Fischer rat strains.

In addition to the study of molybdenum hydroxylase deficiency in rat, a British patient with hereditary xanthinuria was analysed for mutations in the XOR gene. This revealed a N11K missense mutation in the coding region of the gene. Analysis of this difference with an evolutionary diverse range of molybdenum hydroxylases suggested that as the asparagine residue was 100% conserved through evolution the missense N11K mutation was the cause of hereditary xanthinuria in this patient.

4.8 Future work.

4.8.1 Identification of aldehyde oxidase and aldehyde oxidase homologue 1 in rat liver cytosol.

To definitively determine which polypeptide on the cellulose acetate electrophoresis zymograms is AO and which is AOH1 each cDNA would need to be individually expressed in a cell culture system and analysed using cellulose acetate electrophoresis as has been carried out for the mouse molybdenum hydroxylases (Terao *et al.*, 2000). Rather than use cellulose acetate electrophoresis isoelectric focusing might also help resolve the apparent comigration problem of AO and XOR polypeptides (see figure 17).

4.8.2 Identification of the effect of the codon differences found in rat aldehyde oxidase and aldehyde oxidase homologue 1 cDNAs.

To unequivocally determine the effect of the non-synonymous codon differences found in the AO and AOH1 cDNA sequences of the deficient rat strains, the enzymes will need to be expressed in a cell culture system. The wild type cDNA will need to be mutated at the relevant positions and the mutant enzymes expressed. Each of the amino acid differences would need to be studied individually to determine the effect of each change on the enzyme activity.

Each of the identified codon differences will also need to be determined in a larger number of animals to determine if there is any interindividual variation in the strains. This could be achieved by either restriction fragment length polymorphism (RFLP) or amplification refractory mutation system (ARMS) tests

4.8.3 Identification of the effect of the difference found in the xanthinuric patient.

To determine if the N11K missense mutation is definitely responsible for xanthinuria in the British patient the enzyme would need to be expressed in a cell culture system with the wild type cDNA sequence mutated at this position and cell extracts assayed for XOR activity. In order to determine that the N11K amino acid difference is not a benign polymorphism, the normal British population will also need to be screened to ensure

that this difference is a disease causing mutation. This could be achieved by RFLP or ARMS tests.

5. REFERENCES

5. References.

Amaya Y., Yamazaki K., Sato M., Noda K., and Nishino T. (1990). Proteolytic conversion of xanthine dehydrogenase from the NAD- dependent type to the O_2-dependent type: Amino acid sequence of rat liver xanthine dehydrogenase and identification of the cleavage sites of the enzyme protein during irreversible conversion by trypsin. *J. Biol. Chem.* **265:** 14170-14175.

Ambroziak W., Izaguirre G., and Pietruszko R. (1999). Metabolism of retinaldehyde and other aldehydes in soluble extracts of human liver and kidney. *J. Biol. Chem.* **274:** 33366-33373.

Barabas N. K., Omarov R. T., Erdei L., and Lips S. H. (2000). Distribution of the Mo-enzymes aldehyde oxidase, xanthine dehydrogenase and nitrate reductase in maize (*Zea mays L.*) nodal roots as affected by nitrogen and salinity. *Plant Sci.* **155:** 49-58.

Beedham C., Bruce S. E., and Rance D. J. (1987). Tissue distribution of the molybdenum hydroxylases, aldehyde oxidase and xanthine-oxidase, in male and female guinea-pigs. *Eur. J. Drug Metab. Pharmacokinet.* **12:** 303-306.

Beedham. C. (1985). Molybdenum hydroxylases as drug metabolizing enzymes. *Drug Metab. Rev.* **16:** 119-156.

Beedham. C. (1987). Molybdenum hydroxylases: biological distribution and substrate-inhibitor specificity. *In* "Progress in Medicinal Chemistry." (G. B. W. G.P. Ellis, Ed.), pp. 85-127.

Beedham. C. (1997). The role of non-P450 enzymes in drug oxidation. *Pharm. World Sci.* **19:** 1-9.

Bendotti C., Prosperini E., Kurosaki M., Garattini E., and Terao M. (1997). Selective localization of mouse aldehyde oxidase mRNA in the choroid plexus and motor neurons. *Neuroreport* **8:** 2343-2349.

Berger R., Mezey E., Clancy K. P., Harta G., Wright R. M., Repine J. E., Brown R. H., Brownstein M., and Patterson D. (1995). Analysis of aldehyde oxidase and

xanthine dehydrogenase oxidase as possible candidate genes for autosomal recessive familial amyotrophic-lateral-sclerosis. *Somat.Cell Mol.Genet.* **21:** 121-131.

Berglund L., Rasmussen J. T., Andersen M. D., Rasmussen M. S., and Petersen T. E. (1996). Purification of the bovine xanthine oxidoreductase from milk fat globule membranes and cloning of complementary deoxyribonucleic acid. *J. Dairy Sci.* **79:** 198-204.

Bertilsson L., Dahl M. L., Johansson I., Ingleman-Sundburg M., and Sjoqvist F. (1995). Interindividual and interethnic differences in polymorphic drug oxidation. Implications for drug therapy with focus on psychoactive drugs. *In* "Advances in Drug Metabolism in Man" (G. M. Pacifici, and G. N. Fracchia, Eds.), pp. 85-136, European Commision, Luxembourg.

Bordo D., and Argos P. (1991). Suggestions for "safe" residue substitutions in site directed mutagenesis. *J. Mol. Biol* **217:** 721-729.

Boukouvala S., Price N., and Sim E. (2002). Identification and functional characterization of novel polymorphisms associated with the genes for arylamine N- acatyltransferases in mice. *Pharmacogenetics* **12:** 385-394.

Brass C. A., Narciso J., and Gollan J. L. (1991). Enhanced activity of the free radical producing enzyme xanthine oxidase in hypoxic rat liver. *J. Clin. Invest.* **87:** 424-431.

Buters J. T. M., Doehmer J., and Gonzalez F. J. (1999). Cytochrome P450-null mice. *Drug Metab. Rev.* **31:** 437-447.

Calzi M. L., Raviolo C., Ghibaudi E., DeGioia L., Salmona M., Cazzaniga G., Kurosaki M., Terao M., and Garattini E. (1995). Purification, cDNA cloning, and tissue distribution of bovine liver aldehyde oxidase. *J. Biol. Chem.* **270:** 31037-31045.

Castro G. D., de Layno A., Costantini M. H., and Castro J. A. (2001). Cytosolic xanthine oxidoreductase mediated bioactivation of ethanol to acetaldehyde and free radicals in rat breast tissue. Its potential role in alcohol-promoted mammary cancer. *Toxicology* **160:** 11-18.

Christen S., Bifrare Y. D., Siegenthaler C., Leib S. L., and Tauber M. G. (2001). Marked elevation in cortical urate and xanthine oxidoreductase activity in experimental bacterial meningitis. *Brain Res.* **900:** 244-251.

Clarke S. E., Harrell A. W., and Chenery R. J. (1995). Role of aldehyde oxidase in the in-vitro conversion of famciclovir to penciclovir in human liver. *Drug Metab. Dispos.* **23:** 251-254.

de Morais S. M., and Wells P. G. (1988). Deficiency in bilirubin UDP-glucuronyl transferase as a genetic determinant of acetaminophen toxicity. *J. Pharmacol. Exp. Ther.* **247:** 323-331.

Demontis S., Kurosaki M., Saccone S., Motta S., Garattini E., and Terao M. (1999). The mouse aldehyde oxidase gene: Molecular cloning, chromosomal mapping and functional characterization of the 5 '-flanking region. *Biochim. Biophys. Acta.* **1489:** 207-222.

Dent C. E., and Philpot G. R. (1954). Xanthinuria: an inborn error (or deviation) of metabolism. *Lancet* **1:** 182.

Dietrich C. G., Ottenhoff R., de Waart D. R., and Oude Elferink R. P. J. (2001). Lack of UGT1 isoforms in Gunn rats changes metabolic ratio and facilitates excretion of the food-derived carcinogen 2-amino-1-methyl-6-phenylimadazo[4,5-*b*]pyridine. *Toxicol. Appl. Pharmacol.* **170:** 137-143.

Enroth C., Eger B. T., Okamoto K., Nishino T., and Pai E. F. (2000). Crystal structures of bovine milk xanthine dehydrogenase and xanthine oxidase: Structure-based mechanism of conversion. *Proc. Natl. Acad. Sci. U. S. A.* **97:** 10723-10728.

Garattini E., Mendel R., Romao M. J., Wright R., and Terao M. (2003). Mammalian molybdo-flavoenzymes, an expanding family of proteins: structure, genetics, regulation, function and pathophysiology. *Biochem. J.* **372:** 15-32.

Glatigny A., and Scazzocchio C. (1995). Cloning and molecular characterization of Hxa, the gene coding for the xanthine dehydrogenase (purine hydroxylase-I) of *Aspergillus-nidulans*. *J. Biol. Chem.* **270:** 3534-3550.

Gonzalez F. J., and Kimura S. (2001). Understanding the role of xenobiotic-metabolism in chemical carcinogenesis using gene knockout mice. *Mutat. Res.* **477:** 79-87.

Grosflam J., and Weinblatt M. E. (1991). Methotrexate: Mechanism of action, pharmacokinetics, clinical indications, and toxicity. *Curr. Opin. Rheumatol.* **3:** 363-3368.

Harrison R. (2002). Structure and function of xanthine oxidoreductase: where are we now. *Free Radic. Biol. Med.* **33:** 774-797.

Hille R., and Nishino T. (1995). Xanthine oxidase and xanthine dehydrogenase. *FASEB J.* **9:** 995-1003.

Hoen P. A., Commanduer J. N. M., Vermeulen N. P. E., Van Berkel T. J. C., and Bijsterbosch M. K. (2000). Selective induction of cytochrome P450 3A1 by dexamethasone in cultured rat hepatocytes. *Biochem. Pharmacol.* **60:** 1509-1518.

Holmes E. W., and Wyngaarden J. B. (1989). Hereditary xanthinuria. *In* "The Metabolic Bases of Inherited Disease" (C. R. Scriver, A. L. Beaudet, W. S. Sly, and D. Valle, Eds.), pp. 1085-1094, McGraw-Hill, New York.

Holmes R. S. (1978). Electrophoretic analysis of alcohol dehydrogenase, aldehyde oxidase, sorbitol dehydrogenase and xanthine oxidase from mouse tissues. *Comp. Biochem. Physiol.* **61B:** 339-346.

Huang D., and Ichikawa Y. (1994). Two different enzymes are primarily responsible for retinoic acid synthesis in rabbit liver cytosol. *Biochem. Biophys. Res. Commun.* **205:** 1278-1283.

Huang D. Y., Furukawa A., and Ichikawa Y. (1999). Molecular cloning of retinal oxidase aldehyde oxidase cDNAs from rabbit and mouse livers and functional expression of recombinant mouse retinal oxidase cDNA in *Escherichia coli.* *Arch. Biochem. Biophys.* **364:** 264-272.

Ichida K., Amaya Y., Kamatani N., Nishino T., Hosoya T., and Sakai O. (1997). Identification of two mutations in human xanthine dehydrogenase gene responsible for classical type I xanthinuria. *J. Clin. Invest.* **99:** 2391-2397.

Ichida K., Amaya Y., Noda K., Minoshima S., Hosoya T., Sakai O., Shimizu N., and Nishino T. (1993). Cloning of the cDNA-encoding human xanthine dehydrogenase (oxidase) - structural-analysis of the protein and chromosomal location of the gene. *Gene* **133:** 279-284.

Ichida K., Matsumura T., Sakuma R., Hosoya T., and Nishino T. (2001). Mutation of human molybdenum cofactor sulfurase gene is responsible for classical xanthinuria type II. *Biochem. Biophys. Res. Commun.* **282:** 1194-1200.

Iwasaki T., Okamoto K., Nishino T., Mizushima J., and Hori H. (2000). Sequence motif-specific assignment of two [2Fe-2S] clusters in rat xanthine oxidoreductase studied by site-directed mutagenesis. *J. Biochem. (Tokyo)* **127:** 771-778.

Johnson C., Stubley-Beedham C., and Stell S. G. P. (1984). Elevation of molybdenum hydroxylase levels in rabbit liver after ingestion of pthalazine or its hydroxylated matabolite. *Biochem. Pharmacol.* **33:** 3699-3705.

Kalow W., and Tang B. K. (1991). Use of Caffeine Metabolite Ratios to Explore Cyp1a2 and Xanthine-Oxidase Activities. *Clin. Pharmacol. Ther.* **50:** 508-519.

Kawashima K., Hosoi K., Naruke T., Shiba T., Kitamura M., and Watabe T. (1999). Aldehyde oxidase-dependent marked species difference in hepatic metabolism of the sedative-hypnotic, Zaleplon, between monkeys and rats. *Drug Metab. Dispos.* **27:** 422-428.

Kitamura S., Nakatani K., Sugihara K., and Ohta S. (1999a). Strain differences of the ability to hydroxylate methotrexate in rats. *Comp. Biochem. Physiol. C* **122:** 331-336.

Kitamura S., Sugihara K., Nakatani K., Ohta S., Oh-Hara T., Ninomiya S., Green C. E., and Tyson C. A. (1999b). Variation of hepatic methotrexate 7-hydroxylase activity in animals and humans. *IUBMB Life* **48:** 607-611.

Kitchen B. J., Moser A., Lowe E., Balis F. M., Widemann B., Anderson L., Strong J., Blaney S. M., Berg S. L., O'Brien M., and Adamson P. C. (1999). Thioguanine administered as a continuous intravenous infusion to pediatric patients is metabolized to the novel metabolite 8- hydroxy-thioguanine. *J. Pharmacol. Exp. Ther.* **291:** 870-874.

Komoto N., Yukuhiro K., and Tamura T. (1999). Structure and expression of tandemly duplicated xanthine dehydrogenase genes of the silkworm (*Bombyx mori*). *Insect Mol. Biol.* **8:** 73-83.

Krenitsky T. A., Neil S. M., Elion G. B., and Hitchings G. H. (1972). A comparison of the specificities of xanthine oxidase and aldehyde oxidase. *Arch. Biochem. Biophys.* **150:** 585-599.

Krenitsky T. A., Spector T., and Hall W. W. (1986). Xanthine oxidase from human liver: Purification and characterization. *Arch. Biochem. Biophys.* **247:** 108-119.

Kuilenburg A., B, P., Dobritzsch D., Meinsma R., Haasjes J., Waterham H. R., Nowaczyk M. J. M., Aukett A., Duley J. A., Ward K. P., Lindqvist Y., and Gennip A. H. (2002). Novel disease-causing mutations in the dihydropyrimidine dehydrogenase gene interpreted by analysis of the three-dimentional protein structure. *Biochem. J.* **364:** 157-163.

Kurosaki M., Zanotta S., Calzi M. L., Garattini E., and Terao M. (1996). Expression of xanthine oxidoreductase in mouse mammary epithelium during pregnancy and lactation: Regulation of gene expression by glucocorticoids and prolactin. *Biochem. J.* **319:** 801-810.

Kurth J., and Kubicel A. (1984). Methode zur photometriscen bestimming der aktivitat von aldehyoxydase. *Biomed. Biochim. Acta* **11:** 1223-1226.

Lagziel A., Morad T., Usher S., Mani A., Levartovsky D., Ichida K., and Perez H. (2001). Identification of novel SNPs in the coding and non coding regions of the xanthine dehydrogenase gene. *HGM2001 Poster Abstract* **Number 178.**

Leimkuhler S., Angermuller S., Schwarz G., Mendel R. R., and Klipp W. (1999). Activity of the molybdopterin-containing xanthine dehydrogenase of

Rhodobacter capsulatus can be restored by high molybdenum concentrations in a moeA mutant defective in molybdenum cofactor biosynthesis. *J. Bacteriol.* **181:** 5930-5939.

Leimkuhler S., Kern M., Solomon P. S., McEwan A. G., Schwarz G., Mendel R. R., and Klipp W. (1998). Xanthine dehydrogenase from the phototrophic purple bacterium *Rhodobacter capsulatus* is more similar to its eukaryotic counterparts than to prokaryotic molybdenum enzymes. *Mol. Microbiol.* **27:** 853-869.

Levartovsky D., Lagziel A., Sperling O., Liberman U., Yaron M., Hosoya T., Ichida K., and Peretz H. (2000). XDH gene mutation is the underlying cause of classical xanthinuria: A second report. *Kidney Int.* **57:** 2215-2220.

Levy G. N., Martell K. J., Deleon J. H., and Weber W. W. (1992). Metabolic, molecular-genetic and toxicological aspects of the acetylation polymorphism in inbred mice. *Pharmacogenetics* **2:** 197-206.

Li Q., Murphree S. S., Willer S. S., Bolli R., and French B. A. (1998). Gene therapy with bilirubin-UDP-glucuronosyltransferase in the Gunn rat model of Crigler-Najjar syndrome type I. *Hum. Gene Ther.* **1:** 497-505.

Lowry O. H., Rosebrough N. J., Farr A. L., and Randall R. J. (1951). Protein measurement with the Folin phenol reagent. *J. Biol. Chem.* **193:** 539-559.

Maniatis T., Fritsch E. F., and Sambook J. (1982). *In* "Molecular cloning: A laboratory manual" (C. Nolan, Ed.), Cold Spring Harbour Laboratory, New York.

Martelin E., Palvimo J. J., Lapatto R., and Raivio K. O. (2000). Nuclear factor Y activates the human xanthine oxidoreductase gene promoter. *FEBS Lett.* **480:** 84-88.

Marti R., Varela E., Pascual C., and Segura R. M. (2001). Determination of xanthine oxidoreductase forms: influence of reaction conditions. *Clin. Chim. Acta* **303:** 117-125.

McCord J. M. (1985). Oxygen-derived free radicals in postischemic tissue injury. *New Eng. J. Med.* **312:** 159-163.

McManaman J. L., Neville M. C., and Wright R. M. (1999). Mouse mammary gland xanthine oxidoreductase: Purification, characterization, and regulation. *Arch. Biochem. Biophys.* **371:** 308-316.

Mendel R. R., and Schwarz G. (1999). Molybdoenzymes and molybdenum cofactor in plants. *Crit. Rev. Plant Sci.* **18:** 33-69.

Min X. J., Okada K., Brockmann B., Koshiba T., and Kamiya Y. (2000). Molecular cloning and expression patterns of three putative functional aldehyde oxidase genes and isolation of two aldehyde oxidase pseudogenes in tomato. *Biochim. Biophys. Acta.* **1493:** 337-341.

Mira L., Maia L., Barreira L., and Manso C. F. (1995). Evidence for free-radical generation due to NADH oxidation by aldehyde oxidase during ethanol-metabolism. *Arch. Biochem. Biophys.* **318:** 53-58.

Montalbini P. (2000). Xanthine dehydrogenase from leaves of leguminous plants: Purification, characterization and properties of the enzyme. *J. Plant Physiol.* **156:** 3-16.

Moriwaki Y., Yamamoto T., Yamakita J., Takahashi S., and Higashino K. (1998). Comparative localization of aldehyde oxidase and xanthine oxidoreductase activity in rat tissues. *Histochem. J.* **30:** 69-74.

Oda T., Akaike T., Hamamoto T., Suzuki F., Hirano T., and Maeda H. (1989). Oxygen radicals in influenza-induced pathogenesis and treatment with pyran polymer-conjugated SOD. *Science* **244:** 974-976.

Otto D. M., Henderson C. J., Carrie D., Davey M., Gunderson T. E., Blomhoff R., Adams R. H., Tickle C., and Wolf C. R. (2003). Identification of novel roles of the cytochrome p450 system in early embryogenesis: effects on vasculogenesis ans retinoic acid homeostasis. *Mol. Cell. Biol* **17:** 6103-6116.

Pineau T., Costet P., Puel O., Pfohl-Leskowicz A., Lesca P., Alvinerie M., and Galtier P. (1998). Knockout animals in toxicology: assessment of toxin bioactivation pathways using mice deficient in xenobiotic metabolizing enzymes. *Toxicol. Lett.* **102-103:** 459-464.

Rajagopalan K. V. (1997). Xanthine dehydrogenase and aldehyde oxidase. *In* "Comprehensive Toxicology, Biotransformation" (P. Guengerich, Ed.), pp. 165-177, Elsevier Science Ltd, Oxford.

Rashidi M. R., Smith J. A., Clarke S. E., and Beedham C. (1997). In vitro oxidation of famciclovir and 6-deoxypenciclovir by aldehyde oxidase from human, guinea pig, rabbit, and rat liver. *Drug Metab. Dispos.* **25:** 805-813.

Reiss J. (2000). Genetics of molybdenum cofactor deficiency. *Hum. Genet.* **106:** 157-163.

Reiss J., and Johnson J. L. (2003). Mutations in the molybdenum cofactor biosynthetic genes *MOCS1, MOCS2* and *GEPH. Hum. Mutat.* **21:** 569-576.

Rhoden E., Pereira-Lima L., Lucas M., Mauri M., Rhoden C., Pereira-Lima J. C., Zettler C., Petteffi L., and Bello-Klein A. (2000). The effects of allopurinol in hepatic ischemia and reperfusion: Experimental study in rats. *Eur. Surg. Res.* **32:** 215-222.

Robertson I. G. C., Palmer B. D., Paxton J. W., and Bland T. J. (1993). Metabolism of the experimental antitumor agent acridine carboxamide in the mouse. *Drug Metab. Dispos.* **21:** 530-536.

Romao M. J., Archer M., Moura I., Moura J. J. G., Legall J., Engh R., Schneider M., Hof P., and Huber R. (1995). Crystal-structure of the xanthine oxidase-related aldehyde oxidoreductase from *D.-gigas*. *Science* **270:** 1170-1176.

Rytkonen E. M. K., Halila R., Laan M., Saksela M., Kallioniemi O. P., Palotie A., and Raivio K. O. (1995). The human gene for xanthine dehydrogenase (Xdh) is localized on chromosome band 2p22. *Cytogenet. Cell Genet.* **68:** 61-63.

Sakamoto N., Yamamoto T., Moriwaki Y., Teranishi T., Toyoda M., Onishi Y., Kuroda S., Sakaguchi K., Fujisawa T., Maeda M., and Hada T. (2001). Identification of a new point mutation in the human xanthine dehydrogenase gene responsible for a case of classical type I xanthinuria. *Hum. Genet.* **108:** 279-283.

Saksela M., and Raivio K. O. (1996). Cloning and expression in vitro of human xanthine dehydrogenase oxidase. *Biochem. J.* **315:** 235-239.

Sato A., Nishino T., Noda K., and Amaya Y. (1995). The structure of chicken liver xanthine dehydrogenase - cDNA cloning and the domain structure. *J. Biol. Chem.* **270:** 2818-2826.

Sauer P., and Frebort I. (2003). Molybdenum cofactor-containing oxidoreductase family in plants. *Biologia Plantarium* **46:** 481-490.

Saugstad O. D. (1996). Role of xanthine oxidase and its inhibitor in hypoxia: Reoxygenation injury. *Pediatrics* **98:** 103-107.

Schlemper B., Siegers D. J., Paxton J. W., and Robertson I. G. C. (1993). Rat hepatocyte-mediated metabolism of the experimental anti-tumour agent N-[2'-(dimethylamino)ethyl]acridine-4-carboxamide. *Xenobiotica* **23:** 361-371.

Schofield P. C., Robertson I. G. C., and Paxton J. W. (2000). Inter-species variation in the metabolism and inhibition of N- [(2 '-dimethylamino)ethyl]acridine-4-carboxamide (DACA) by aldehyde oxidase. *Biochem. Pharmacol.* **59:** 161-165.

Segal B. H., Sakamoto N., Patel M., Maemura K., Klein A. S., Holland S. M., and Bulkley G. B. (2000). Xanthine oxidase contributes to host defense against *Burkholderia cepacia* in the p47(phox-/-) mouse model of chronic granulomatous disease. *Infect. Immun.* **68:** 2374-2378.

Shaw S., and Jayatilleke E. (1990). The role of aldehyde oxidase in ethanol-induced hepatic lipid- peroxidation in the rat. *Biochem. J.* **268:** 579-583.

Simmonds H. A., Reiter S., and Nishino T. (1995). Hereditary xanthinuria. *In* "The Metabolic and Molecular Basis of Inherited Disease" (C. R. Scriver, A. L. Beaudet, W. S. Sly, and D. Valle, Eds.), pp. 1781-1797, McGraw-Hill, New York.

Stanulovic M., and Chaykin S. (1971a). Aldehyde oxidase: catalysis of the oxidation of N^1-methynicatinamide and pyridoxal. *Arch. Biochem. Biophys.* **145:** 27-34.

Stanulovic M., and Chaykin S. (1971b). Metabolic origins of the pyridones of N^1-methylnicotinamide in man and rat. *Arch. Biochem. Biophys.* **145:** 35-42.

Sugihara K., Kitamura S., and Tatsumi K. (1995). Strain differences of liver aldehyde oxidase activity in rats. *Biochem. Mol. Biol. Int.* **37:** 861-869.

Terao M., Cazzaniga G., Ghezzi P., Bianchi M., Falciani F., Perani P., and Garattini E. (1992). Molecular-cloning of a cDNA coding for mouse-liver xanthine dehydrogenase - regulation of its transcript by interferons *in vivo*. *Biochem. J.* **283:** 863-870.

Terao M., Kurosaki M., Demontis S., Zanotta S., and Garattini E. (1998). Isolation and characterization of the human aldehyde oxidase gene: conservation of intron/exon boundaries with the xanthine oxidoreductase gene indicates a common origin. *Biochem. J.* **332:** 383-393.

Terao M., Kurosaki M., Marini M., Vanoni M. A., Saltini G., Bonetto V., Bastone A., Federico C., Saccone S., Fanelli R., Salmona M., and Garattini E. (2001). Purification of the aldehyde oxidase homologue 1 (AOH1) protein and cloning of the AOH1 and aldehyde oxidase homologue 2 (AOH2) genes - Identification of a novel molybdo-flavoprotein gene cluster on mouse chromosome 1. *J. Biol. Chem.* **276:** 46347-46363.

Terao M., Kurosaki M., Saltini G., Demontis S., Marini M., Salmona M., and Garattini E. (2000). Cloning of the cDNAs coding for two novel molybdo-flavoproteins showing high similarity with aldehyde oxidase and xanthine oxidoreductase. *J. Biol. Chem.* **275:** 30690-30700.

Tomita S., Tsujita M., and Ichikawa Y. (1993). Retinal oxidase is identical to aldehyde oxidase. *FEBS Lett.* **336:** 272-274.

Truglio J. J., Theis K., Leimkuhler S., Rappa R., Rajagopalan K. V., and Kisker C. (2002). Crystal structures of the active and alloxanthine-inhibited forms of xanthine dehydrogenase from *Rhodobacter capsulatus*. *Structure* **10:** 115-125.

Tsuchida S., Yamada R., Ikemoto S., and Tagawa M. (2001). Molecular cloning of a cDNA coding for feline liver xanthine dehydrogenase. *J. Vet. Med. Sci.* **63:** 353-355.

Umezawa K., Akaike T., Fujii S., Suga M., Setoguchi K., Ozawa A., and Maeda H. (1997). Induction of nitric oxide synthesis and xanthine oxidase and their roles in the antimicrobial mechanism against Salmonella typhimurium infection in mice. *Infect. Immun.* **65:** 2932-2940.

Unkles S. E., Heck I. S., Appleyard V. C. L., and Kinghorn J. R. (1999). Eukaryotic molybdenum synthase. *J. Biol. Chem.* **274:** 19286-19293.

Van Scoik K., Johnson C. A., and Porter W. R. (1985). The pharmacology and metabolism of the thiopurine drugs 6-mercaptopurine and azathiopurine. *Drug, Metab. Rev.* **16:** 157-174.

Venter J. C., Adams M. D., Myers E. W., Li P. W., Mural R. J., Sutton G. G., Smith H. O., Yandell M., Evans C. A., Holt R. A., Gocayne J. D., Amanatides P., and *et a.* (2001). The sequence of the human genome. *Science* **291:** 1304-+.

Voet D., Voet J., and Pratt C. (1999). *In* "Fundamentals of Biochemistry" (C. Mills, B. Heaney, E. Bari, S. Russell, H. Newman, and E. Starr, Eds.), John Wiley and Sons, Inc, Chichester.

Vorbach C., Scriven A., and Capecchi M. R. (2002). The housekeeping gene xanthine oxidoreductase is necessary for milk fat droplet enveloping and secretion: gene sharing in the lactating in the lactating mammary gland. *Gene. Dev.* **16:** 3223-3235.

Watanabe T., Ihara N., Itoh T., Fujita T., and Sugimoto Y. (2000). Accelerated publication - Deletion mutation in Drosophila ma-l homologueous, putative molybdopterin cofactor sulfurase gene is associated with bovine xanthinuria type II. *J. Biol. Chem.* **275:** 21789-21792.

Waud W. R., and Rajagopalan K. V. (1976). The mechanism of conversion of rat liver xanthine dehydrogenase from an NAD^+ form (type D) to an O_2 dependant form (type O). *Arch. Biochem. Biophys.* **172:** 365-379.

Wright R. M., Clayton D. K., Riley M. G., McManaman J. L., and Repine J. E. (1999). cDNA cloning, sequencing, and characterization of male and female rat liver aldehyde oxidase (rAOX1) - Differences in redox status may distinguish male and female forms of hepatic AOX. *J. Biol. Chem.* **274:** 3878-3886.

Wright R. M., and Repine J. E. (1997). The human molybdenum hydroxylase gene family: co-conspirators in metabolic free-radical generation and disease. *Biochem. Soc. Trans.* **25:** 799-805.

Wright R. M., Vaitaitis G. M., Wilson C. M., Repine T. B., Terada L. S., and Repine J. E. (1993). cDNA cloning, characterization, and tissue-specific expression of human xanthine dehydrogenase xanthine-oxidase. *Proc. Natl. Acad. Sci. U. S. A.* **90:** 10690-10694.

Wright R. M., Weigel L. K., VarellaGarcia M., Vaitaitis G., and Repine J. E. (1997). Molecular cloning, refined chromosomal mapping and structural analysis of the human gene encoding aldehyde oxidase (AOX1), a candidate for the ALS2 gene. *Redox Rep.* **3:** 135-144.

Wuebbens M. M., Liu M. T. W., Rajagopalan K. V., and Schindelin H. (2000). Insights into molybdenum cofactor deficiency provided by the crystal structure of the molybdenum cofactor biosynthesis protein MoaC. *Structure* **8:** 709-718.

Xiang Q., and Edmondson D. E. (1996). Purification and characterization of a prokaryotic xanthine dehydrogenase from *Comamonas acidovorans*. *Biochemistry* **35:** 5441-5450.

Xu P., Hueckstead T. P., Harrison R., and Hoidal J. R. (1994a). Molecular-cloning, tissue expression of human xanthine dehydrogenase. *Biochem. Biophys. Res. Commun.* **199:** 998-1004.

Xu P., Hueckstead T. P., Harrison R., and Hoidal J. R. (1995). Molecular-cloning, tissue expression of human xanthine dehydrogenase (Vol 199, Pg 998, 1994). *Biochem. Biophys. Res. Commun.* **215:** 429-429.

Xu P., Hueckstedt T. P., and Hoidal J. R. (1996). Molecular cloning and characterization of the human xanthine dehydrogenase gene (XDH). *Genomics* **34:** 173-180.

Xu P., Zhu X. L., Hueckstedt T. P., Brothman A. R., and Hoidal J. R. (1994b). Assignment of human xanthine dehydrogenase gene to chromosome 2p22. *Genomics* **23:** 289-291.

Yamamoto T., Moriwaki Y., Shibutani Y., Matsui K., Ueo T., Takahashi S., Tsutsumi Z., and Hada T. (2001). Human xanthine dehydrogenase cDNA sequence and protein in an atypical case of type I xanthinuria in comparison with normal subjects. *Clin. Chim. Acta* **304:** 153-158.

Yee S. B., and Pritsos C. A. (1997). Comparison of oxygen radical generation from the reductive activation of doxorubicin, streptonigrin, and menadione by xanthine oxidase and xanthine dehydrogenase. *Arch. Biochem. Biophys.* **347:** 235-241.

Yoshihara S., and Tatsumi K. (1997). Purification and characterization of hepatic aldehyde oxidase in male and female mice. *Arch. Biochem. Biophys.* **338:** 29-34.

Zamyatin A. A. (1972). Protein volume in solution. *Prog. Biophys. Mol. Biol* **24:** 107-123.

APPENDICES

APPENDIX 1

Example of a standard curve for the Lowry method of protein determination.

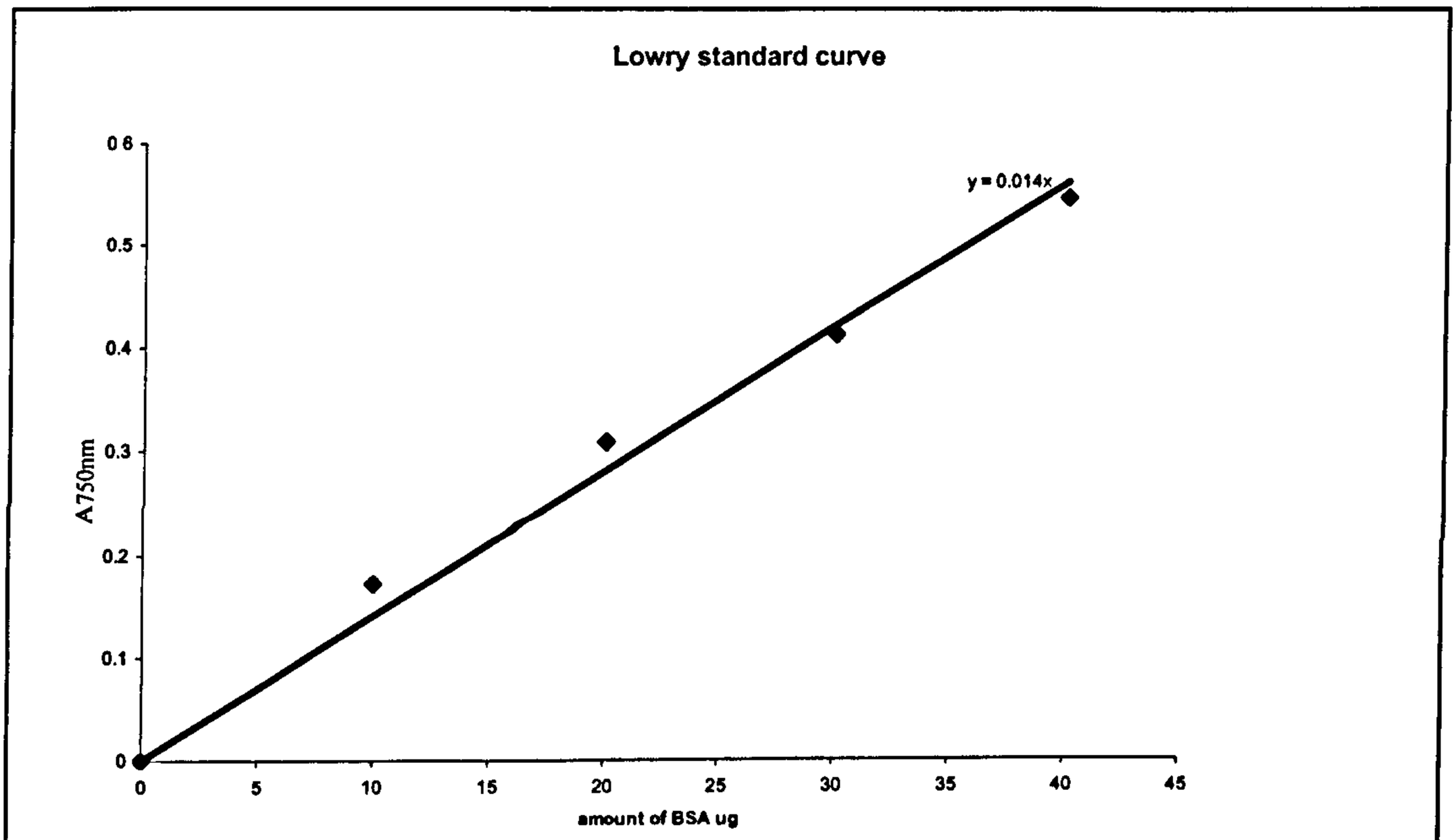

Example of a standard curve obtained using known amounts of bovine serum albumin for the calculation of the protein concentration in an unknown sample.

APPENDIX 2

Accession numbers for the sequences used in this thesis.

Protein/ nucleic acid sequence	Species	Accession numbers
AO	*A. thaliana*	AB005804
AO	bovine	X87251
AO	human	NM_001159
AO	mouse	NM_009676
AO	rabbit	AB009345
AO	rat female	NM_019363
AO	rat male	AF110478
AOH1	BAC (rat)	AC126841
AOH1	mouse	AAL36596
AOH2	mouse	AAL38126
AOR	*D. gigas*	A57429
XOR	*A. thaliana*	CAB45451
XOR	BACs (human)	AL121654 & AL121657
XOR	bovine	CAA67117
XOR	cat	AF286379
XOR	chicken	BAA02502
XOR	*D. melanogaster*	CAA6849
XOR	*E. nidulans*	A55875
XOR	human	U39487
XOR	mouse	CAA52997
XOR	rat	ACAA52997
XOR	*R. capsulatus*	1JRP_A
XOR	silkworm	BAA21640

APPENDIX 3

Table showing the genetic code.

First base											
Second base	T		C		A		G				
T	TTT	Phe	CTT	Leu	ATT	Ile	GTT	Val			
	TTC		CTC		ATC		GTC				
	TTA	Leu	CTA		ATA		GTA				
	TTG		CTG		ATG	Met	GTG				
C	TCT	Ser	CCT	Pro	ACT	Thr	GCT	Ala			
	TCC		CCC		ACC		GCC				
	TCA		CCA		ACA		GCA				
	TCG		CCG		ACG		GCG				
A	TAT	Tyr	CAT	His	AAT	Asn	GAT	Asp			
	TAC		CAC		AAC		GAC				
	TAA	STOP	CAA	Gln	AAA	Lys	GAA	Glu			
	TAG		CAG		AAG		GAG				
G	TGT	Cys	CGT	Arg	AGT	Ser	GGT	Gly			
	TGC		CGC		AGC		GGC				
	TGA	STOP	CGA		AGA	Arg	GGA				
	TGG	Trp	CGG		AGG		GGG				

APPENDIX 4

Single letter and triple letter codes for the amino acids.

Amino acid	Single letter code	Triple letter code
Alanine	A	Ala
Arginine	R	Arg
Asparagine	N	Asn
Aspartic acid	D	Asp
Cysteine	C	Cys
Glutamic acid	E	Glu
Glutamine	Q	Gln
Glycine	G	Gly
Histidine	H	His
Isoleucine	I	Ile
Leucine	L	Leu
Lysine	K	Lys
Methionine	M	Met
Phenylalanine	F	Phe
Proline	P	Pro
Serine	S	Ser
Threonine	T	Thr
Tryptophan	W	Trp
Tyrosine	Y	Tyr
Valine	V	Val

Appendix 5

Partial sequence obtained for rat AO intron 4.

CTGCTTGGAACTTGCTCTGTCCCAGGCTGGCCTTGATCTCAGAGATCTGC
TTGTTTTCGTCTCCTGGGAATAAAGGTGTGCACCACCTTGCCTGGGCCTA
AGCTTTTCATGGCTACTCTGTCTCAAAATCAGGATCAAAAATACGTGTCT
CTCAGCCTCAAGATCTGGATCACAGGGTGCGCCCTCCATTTCTGGATGGT
AGTTCATTCCAGAAATAGTCATGTTGACAACTGGGAATAACCATCAGAAA
TGATAAACTGATTCTTCAAGGGCTCAGAAACCAGTGTCTTAAAGTCAGGC
AGCTCAGAAGGCTCAAAAGTCAGACTGACCAGCCCAAAGGAGATGAGTTG
AAGGCTTTTGGGAGGTCTTCTCTCCAAATTCAGTGAATGCAAACATGTCC
TGTGGAAGTTGCTTTGATGCTTCAGGCCTGGCCTTCTAACCTTGCTGTGC
TTTCCAG**GAGAGGATCGCCAAGT**

The partial exon 5 sequence is in bold. Intron 4 is in normal type font. The sequence was obtained by sequencing the PCR products from RAO4/5F and RAO4/5R using the reverse primer and then reverse complemented using Genejockey™.